

CHAPTER 4

RESULTS AND DISCUSSION

1. Sample sources

Specimens were collected in the Northern Thailand with a primary focus in Chiang Mai Province since 2009. A total of Thai powdery mildew fungi, in tribe Phyllactinieae could be found only 30% of all (Fig. 21). All 27 specimens of powdery mildew fungi in tribe Phyllactinieae were found and classified to be in tribe Phyllactinieae (Table. 4). In figure 22 show proportion of powdery mildew fungi in tribe Phyllactinieae, the pie chart shows the powdery mildews mostly produce only anamorphic feature, lack of sexual morphology with 74%, of which 48% belong to genus *Oidiopsis* and 26% belong to genus *Ovulariopsis*. Only, 26% of powdery mildews had the connection of anamorph to their telemorph that have been found only in *Phyllactinia*.

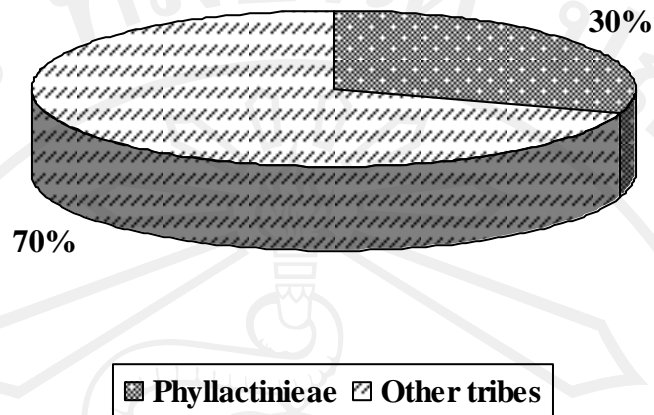


Figure 21 The proportion of powdery mildew fungi found in this study.

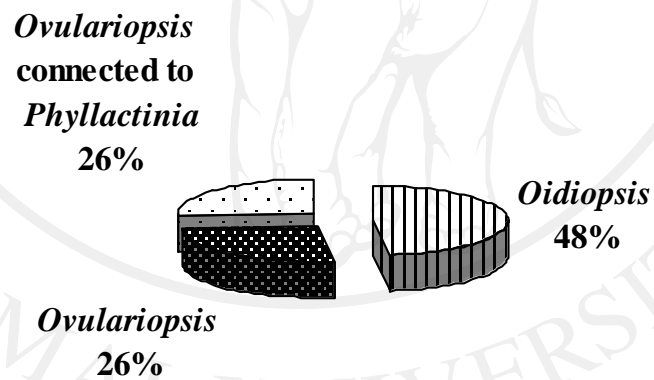


Figure 22 The percentage of Phyllactinieae genera found in this study.

Table 5 Isolates of Phyllactiniaceae from Thailand included for sequence analysis and morphological comparison.

Host Plants	Family Name	Common Name	Location	Voucher collection
<i>Oidiopsis</i>				
<i>Capsicum annuum</i> var. <i>grossum</i>	Solanaceae	Sweet Chilli	Chiang Mai (Mae On, Mae rim, Meaung)	MUMH5086,5096, 5097,5114
<i>Capsicum annuum</i> var. <i>minimum</i>	Solanaceae		Chiang Mai (Meaung)	MUMH3329
<i>Capsicum frutescens</i>	Solanaceae	Bird Chilli	Chiang Mai (Hangdong)	MUMH3346,5083
<i>Capsicum frutescens</i> × <i>C. chinense</i>	Solanaceae	Bhut Jologia	Chiang Mai (Meaung)	MUMH5106
<i>Capsicum</i> spp.	Solanaceae	Darby	Chiang Mai (Mae rim)	MUMH5119
<i>Capsicum</i> spp.	Solanaceae	Maxican Chilli	Lumphon (Lee)	MUMH5104
<i>Euphorbia heterophylla</i>	Euphorbiaceae	Mexican Fire Plant	Chiang Mai (Meaung), Prachaup Khiri Khan	MUMH5100
<i>Euphorbia pulcherrima</i>	Euphorbiaceae	Christmas	Chiang mai (Doi Inthanon)	CMU38
<i>Galphimia glauca</i>	Malpighiaceae	Gold shower	Chiang Mai (Maejoe)	CMU-MJ4
<i>Oxalis triangularis</i>	Oxalidaceae	Purple Shamrock	Chiang Mai (Chiang Dao)	CMU-HL1
<i>Sesamum indicum</i>	Pedaliaceae	Sesame	Chiang Mai (Meaung)	CMU16

Table 5 Isolates of Phyllactinieae from Thailand included for sequence analysis and morphological comparison. (continued)

Host Plants	Family Name	Common Name	Location	Voucher collection
<i>Oidiopsis</i>				
<i>Solanum aculeatissimum</i>	Solanaceae	Cockroach berry	Chiang Mai (Mae Kangluang)	MUMH5101,5102
<i>Solanum torvum</i>	Solanaceae	Pea Eggplant	Chiang Mai (Mae rim), Lumpang, Mae Hong Sorn (Pai)	MUMH5091,5092
<i>Ovulariopsis</i>				
<i>Alangium kurzii</i>	Alangiaceae		Chiang Mai (Doi Suthep)	CMU5120
<i>Boehmeria siamensis</i>	Urticaceae		Chiang Mai (Doi Suthep)	CMU-02-10
<i>Broussonetia papyrifera</i>	Moraceae		Chiang Mai (Meaung)	MUMH3339
<i>Cassia fistula</i>	Caesalpiniaceae (Leguminosae)	Golden Shower	Chiang Mai (Meaung)	MUMH5084,5088, 5093,5094,5107
<i>Dalbergia cana</i>	Caesalpiniaceae		Chiang Mai (Mae rim)	CMU-BG9
<i>Dalbergia lanceolaria</i>	Caesalpiniaceae		Chiang Mai (Meaung)	MUMH5087
<i>Ehretia laevis</i>	Boraginaceae		Chiang Mai (Mae rim)	MUMH5095
<i>Euphorbia heterophylla</i>	Euphorbiaceae	Mexican Fire Plant	Chiang Mai (Meaung)	CMU38
<i>Gmelina arborea</i>	Verbenaceae	Beechwood	Chiang Mai (Doi Suthep)	MUMH5117

Table 5 Isolates of Phyllactinieae from Thailand included for sequence analysis and morphological comparison. (continued)

Host Plants	Family Name	Common Name	Location	Voucher collection
<i>Ovulariopsis</i>				
<i>Lagerstroma macrocarpa</i>	Lythraceae	Queen's flower	Chiang Mai (Meaung)	MUMH335,5116
<i>Morus alba</i>	Moraceae	Mulberry	Chiang Mai (Meaung)	MUMH5089,5090, 5098,5099,5103,5105 ,5111,5115
<i>Pyrus pyrifolia</i>	Rosaceae		Chiang Mai (Mae rim)	MUMH5109
<i>Senna siamea</i>	Fabaceae		Chiang Mai (Meaung)	MUMH3331
<i>Terminalia bellirica</i>	Combretaceae		Chiang Mai (Meaung)	MUMH3337

2. Taxonomic implication

According to study the powdery mildew fungi in tribe Phyllactinieae in Thailand, 26 plants species (including varieties) covering 14 families were infected by this fungal group. All of which 14 plants families, 5 families represented in genus *Oidiopsis*: Euphorbiaceae, Malpighiaceae, Oxalidaceae, Pedaliaceae, Solanaceae, and 10 families represented in genus *Ovulariopsis*: Alangiaceae, Boraginaceae, Combretaceae, Euphorbiaceae, Fabaceae, Lythraceae, Moraceae, Rosaceae, Urticaceae, Verbenaceae. For taxonomic classification, key to genera was proposed to identify the genera of this fungal group as following below:

Key to genera of the Phyllactinieae

- 1 conidiophores and conidia pigmented; mycelium with special aerial hyphae, rigid, thickened, simple or dichotomously branched..... ***Queirozia***
- 1* conidiophores and conidia colorless; mycelium mostly without special aerial hyphae.....2
- 2 conidiophores always arising from superficial hyphae; foot-cells straight, sometimes spirally twisted; conidia uniform or dimorphic; anamorph belonging to *Ovulariopsis*; usually parasitic on trees and shrubs.....3
- 2* conidiophores mostly arising from internal hyphae, occasionally formed external hyphae, emerging through stomata; conidia usually dimorphic, with distinct differences in the shape of primary and secondary conidia; chasmothecia with myceloid appendages; asci usually 2-spored; anamorph belonging to *Oidiopsis*; usually parasitic on herbaceous plants.....***Leveillula***
- 3 Chasmothecia with acicular appendages, bulbous swelling at the base with obtuse to subacute apex; with penicillate cells in the apical portion that become mucilaginous; asci 2–4(–5)-spored..... ***Phyllactinia***
- 3* Chasmothecia with numerous appendages, attached around the equatorial zone or somewhat in the upper half; asci 2–5-spored..... ***Pleochaeta***

Descriptions and illustrations of powdery mildews in tribe Phyllactinieae

1. Descriptions and photographic figures of *Leveillula* (*Oidiopsis*)

1.1 *Oidiopsis sicula* on *Capsicum annuum* var. *grossum*, Solanaceae

Mycelium internal and external, superficial mycelium on stems, especial leaves, hypophyllous, mostly persistent, thin to dense, white, patches or covering the entire leaves; *hyphae* substraight to wavy; *hyphal appressoria* nipple-shaped, lobed to multilobed, coralloid; *conidiophores* emerging through stomata, erect, straight, (51–)100–276(–338) × (5–)8–12(–16) μm; basal septum (2–)11–24(–34) μm displaced from the branching point of the mycelium; *mother cells* forming conidia singly, (28.06–)30.5–122(–134.2) × 4.88–6.1(–7.32) μm; *foot-cells* usually straight, with a basal septum near branching point of mycelium up to away from it, (41–)49–140(–202) × 4–6(–7) μm; *conidia* dimorphic, without conspicuous fibrosin bodies, contain oil drop, *primary conidia* lanceolate, in the upper half narrowed towards the apex, 60–76(–83) × 13–17(–21) μm, mostly widest in the lower half, *secondary conidia* ellipsoid to cylindrical, usually widest in the upper half, (46–)52–69(–78) × (12–)13–17 μm; *conidial germination* formed *Ovulariopsis* type; *chasmothecia* can not be found (Fig. 23 and 24).

Specimens examined: on leaves of *Capsicum annuum* var. *grossum* MUMH5086, 5096, 5097, 5114



Figure 23 *Oidiopsis sicula* on leaves of *Capsicum annuum* var. *grossum*; (A) mycelia colonized on lower side of leaf (B) conidia (C) conidiophores and conidia (D) appressoria and (E) conidial germination. (Bar 30 μm)

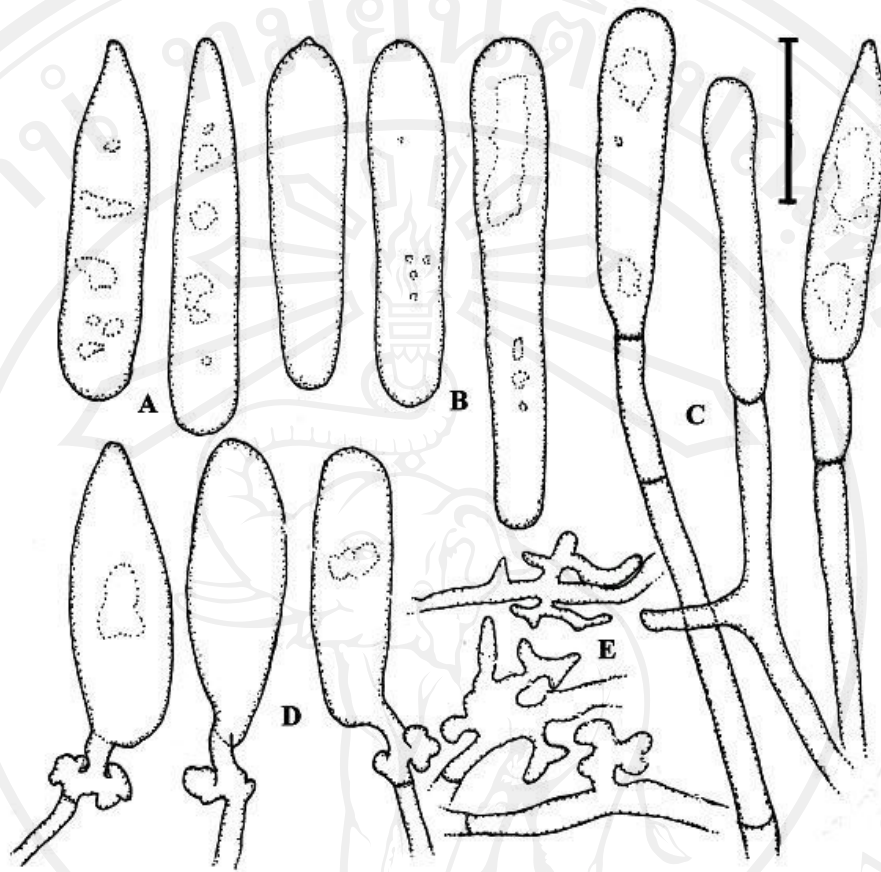


Figure 24 Illustration of *Oidiopsis sicula* on leaves of *Capsicum annuum* var. *grossum*; (A) primary conidia (B) secondary conidia (C) conidiophores and conidia (D) conidia with germ tubes of the pseudoidium pattern and (E) mycelia with appressoria. (Bar 30 μ m)

1.2 *Oidiopsis sicula* on *Capsicum annuum* var. *minimum*, Solanaceae

Mycelium superficial mycelium, hypophyllous, white, dense patches or covering the entire lower leaves surface; *hyphae* substraight to wavy; *hyphal appressoria* variable in shaped, nipple-shaped to elongated; *conidiophores* arising from the internal mycelium through stomata, rarely arising from the external mycelium, erect, straight, (76.86–)102.48–283.04(–474.58) μm ; *mother cells* forming conidia singly, (39.04–)48.8–131.76(–156.16) \times 3.66–7.32 μm ; *foot-cells* straight, (31.72–)61–134.2(–143.96) \times 4.88–6.1(–7.32) μm with a basal septum (4.88–)9.76–15.86(–24.4) μm displaced from the branching point of the mycelium; *conidia* dimorphic, without conspicuous fibrosin bodies, contain oil drop, *primary conidia* lanceolate, in the upper half narrowed towards the apex, (61–)63.44–75.64(–92.72) \times (12.2–)14.64–18.3(–19.52) μm , *secondary conidia* ellipsoid to cylindric, (51.24–)53.68–73.2(–80.52) \times (10.98–)13.42–17.08(–18.3) μm ; *conidial germination* formed *Ovulariopsis* type; *chasmothecia* can not be found (Fig. 25 and 26).

Specimens examined: on leaves of *Capsicum annuum* var. *minimum* MUMH3329

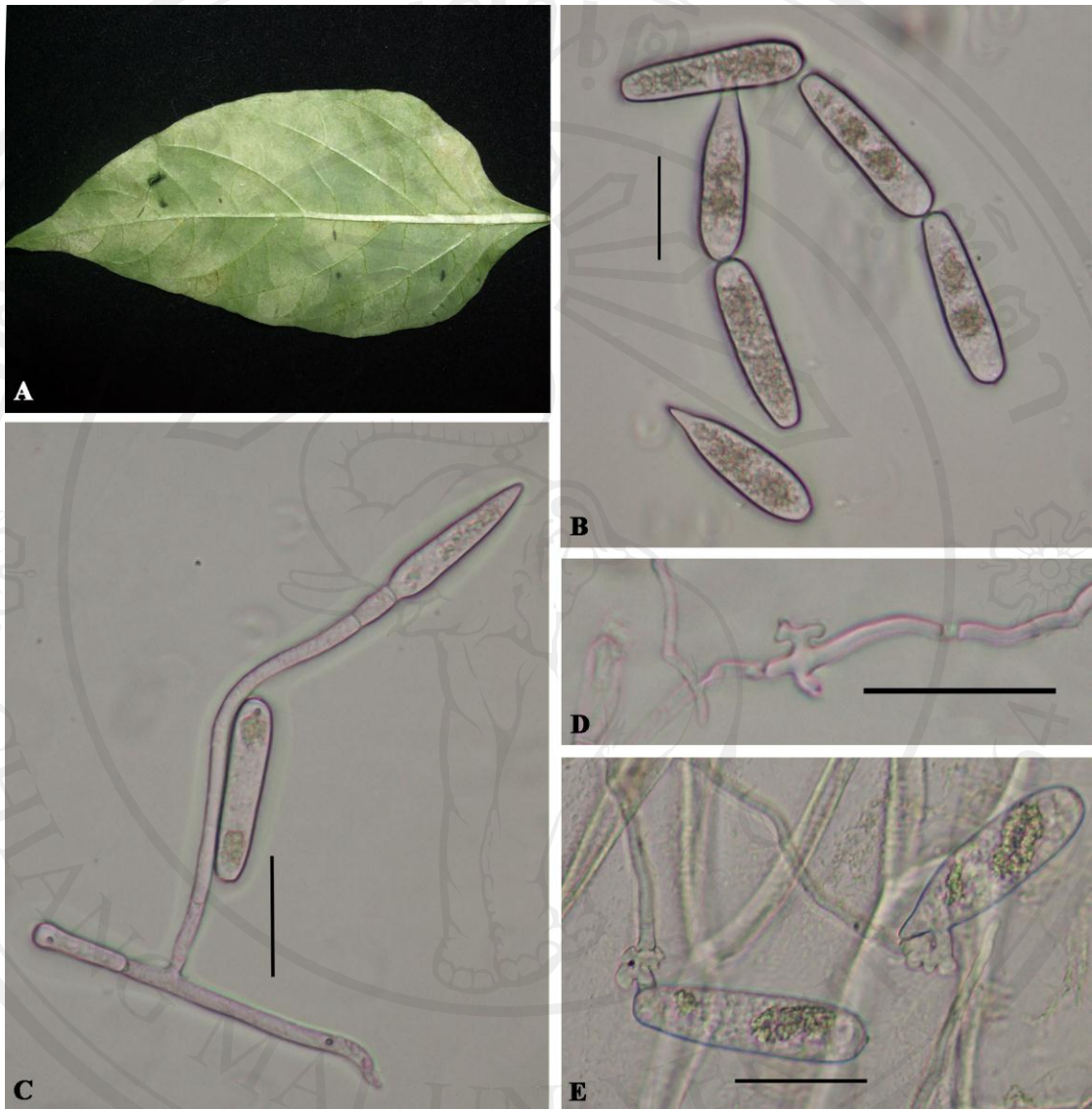


Figure 25 *Oidiopsis sicula* on leaves of *Capsicum annuum* var. *minimum*; (A) mycelia colonized on lower side of leaf (B) conidia (C) conidiophores and conidia (D) appressoria and (E) conidial germination. (Bar 30 μm)

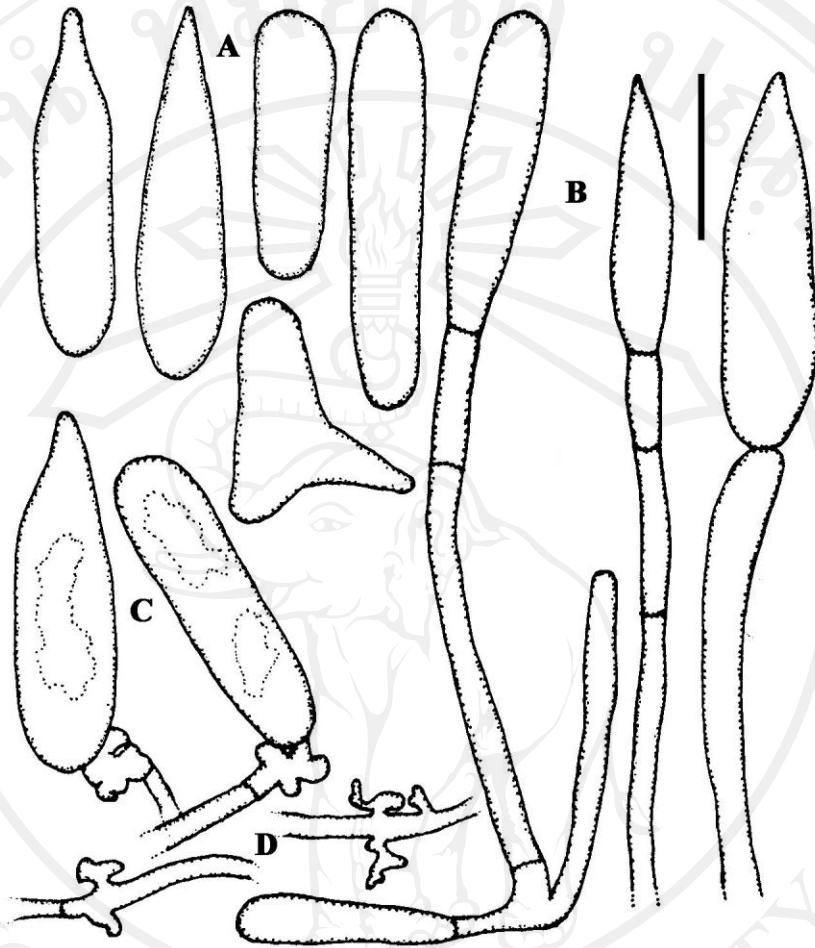


Figure 26 Illustration of *Oidiopsis sicula* on leaves of *Capsicum annuum* var. *minimum*; (A) conidia (B) conidiophores and conidia (C) conidia with germ tubes of the *Pseudoidium* and (D) mycelia with appressorium. (Bar 30 μm)

1.3 *Oidiopsis sicula* on *Capsicum frutescens*, Solanaceae

Mycelium internal and external, superficial mycelium on stems, mostly leaves, hypophyllous, mostly persistent, thin to dense, white, patches or covering the entire leaves; *hyphae* substraight to wavy; *hyphal appressoria* nipple-shaped, lobed to multilobed, coralloid; *conidiophores* emerging through stomata, erect, straight, (105–)178–273(–310) × (6–)8–15 μm; basal septum (0–)4.88–30.5(–36.6) μm displaced from the branching point of the mycelium; *mother cells* forming conidia singly, (46–)49–83(–151) × 5–6 μm; *foot-cells* usually straight, with a basal septum near branching point of mycelium up to away from it, (56–)90–149(–174) × 5–7 μm; *conidia* dimorphic, without conspicuous fibrosin bodies, contain oil drop, *primary conidia* lanceolate, apically attenuated, (58–)63–80(–88) × (15–)16–20 μm, *secondary conidia* ellipsoid to cylindric, usually widest in the upper half, (49–)54–71(–76) × (13–)15–20 μm; *conidial germination* formed *Ovulariopsis* type; *chasmothecia* can not be found (Fig. 27 and 28).

Specimens examined: on leaves of *Capsicum frutescens* MUMH3346, 5083

1.4 *Oidiopsis sicula* on *Capsicum frutescens* × *Capsicum chinense*, Solanaeae

Mycelium internal and external, superficial mycelium on leaves, hypophyllous, mostly persistent, thin to dense, white, patches; *hyphae* substraight to wavy; *hyphal appressoria* nipple-shaped, lobed to multilobed, coralloid; *conidiophores* emerging through stomata, erect, straight, (119–)144–195(–278) × (7–)8–14(–17) μm; basal septum (8.54–)12–15 μm displaced from the branching point of the mycelium; *mother cells* forming conidia singly, (22–)88–105(–115) × (5–)6–7 μm; *foot-cells* usually straight, with a basal septum near branching point of mycelium up to away from it, (39–)71–107(–149) × (5–)6–7 μm, forming conidia singly; *conidia* dimorphic, without conspicuous fibrosin bodies, contain oil drop, *primary conidia* lanceolate, in the upper half narrowed towards the apex, (54–)59–71(–73) × (12–)15–18 μm, mostly widest in the lower half, *secondary conidia* ellipsoid to cylindric, usually widest in the upper half, (46–)56–72(–73) × (13–)15–17(–18) μm; *conidial germination* formed *Ovulariopsis* type; *chasmothecia* can not be found (Fig. 29 and 30).

Specimens examined: on leaves of *Capsicum frutescens* × *Capsicum chinense* MUMH5106



Figure 27 *Oidiopsis sicula* on leaves of *Capsicum frutescens*; (A) mycelia colonized on lower side of leaf (B) conidia (C) conidiophores and conidia (D) appressoria and (E) conidial germination. (Bar 30 μ m)

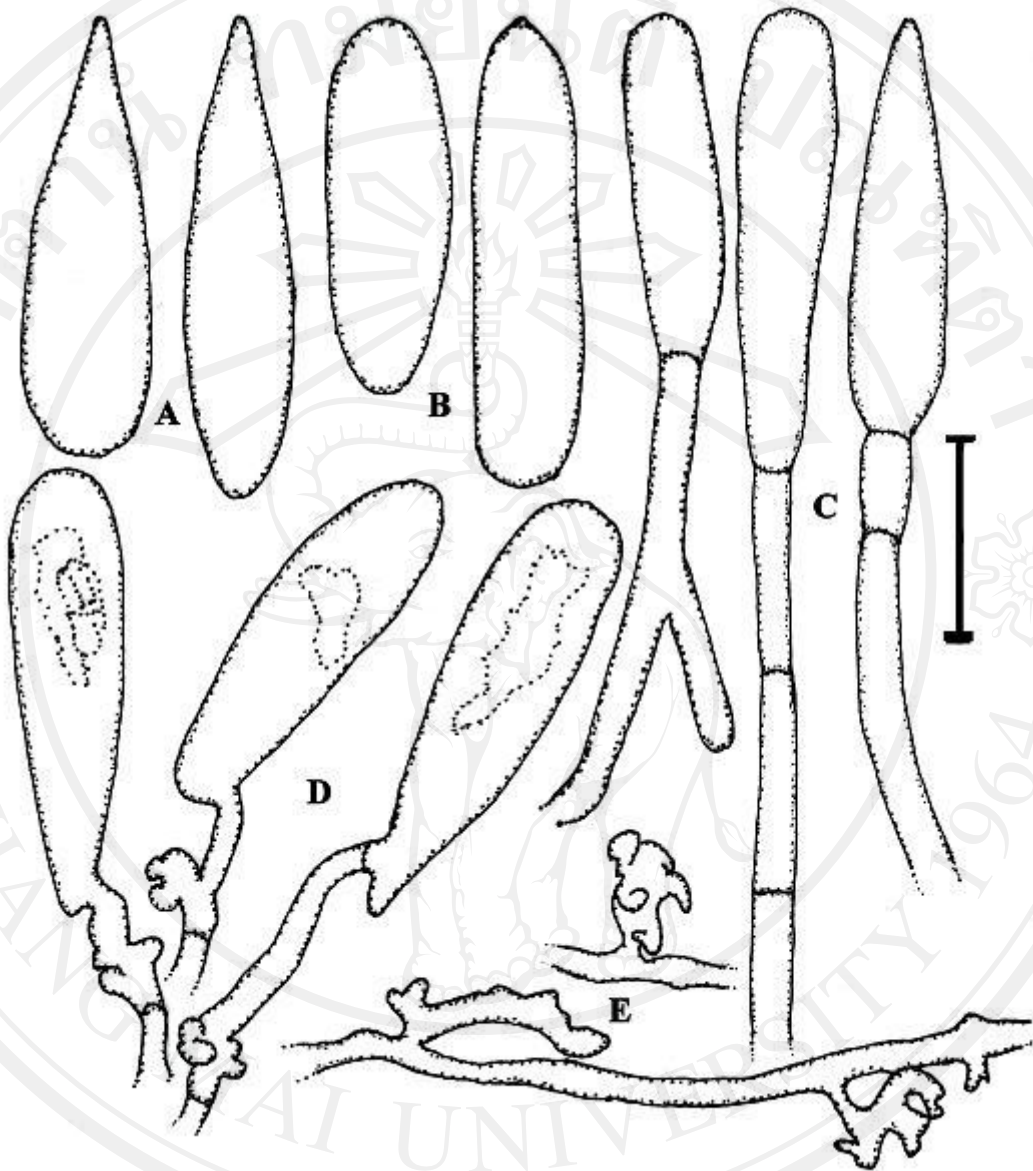


Figure 28 Illustration of *Oidiopsis sicula* on leaves of *Capsicum frutescens*; (A) primary conidia (B) secondary conidia (C) conidiophores and conidia (D) conidia with germ tubes of the *Ovulariopsis* pattern and (E) mycelia with appressoria. (Bar 30 μ m)

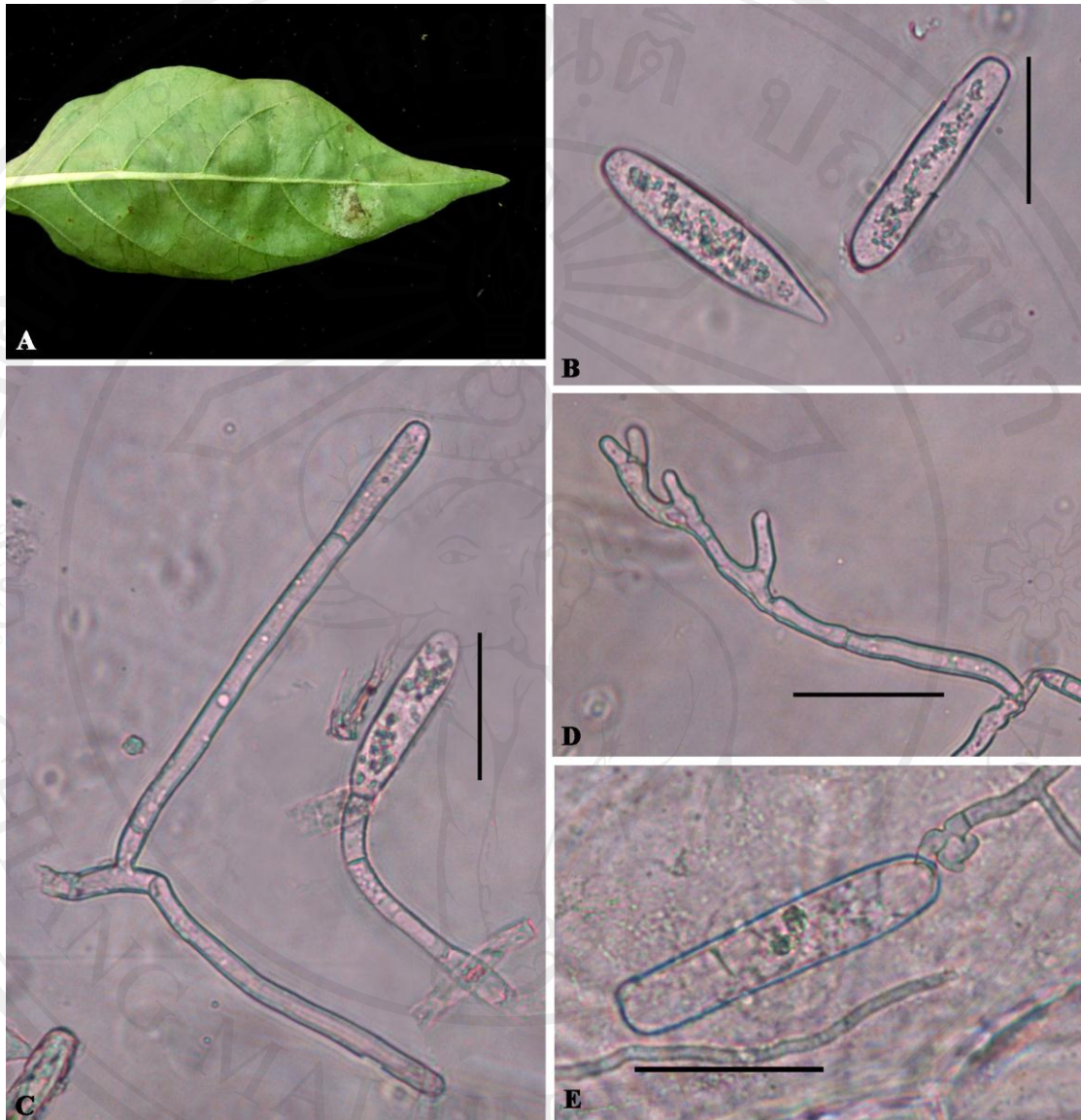


Figure 29 *Oidiopsis sicula* on leaves of *Capsicum frutescens* × *Capsicum chinense*; (A) mycelia colonized on lower side of leaf (B) conidia (C) conidiophores and conidia (D) appressoria and (E) conidial germination. (Bar 30 μm)

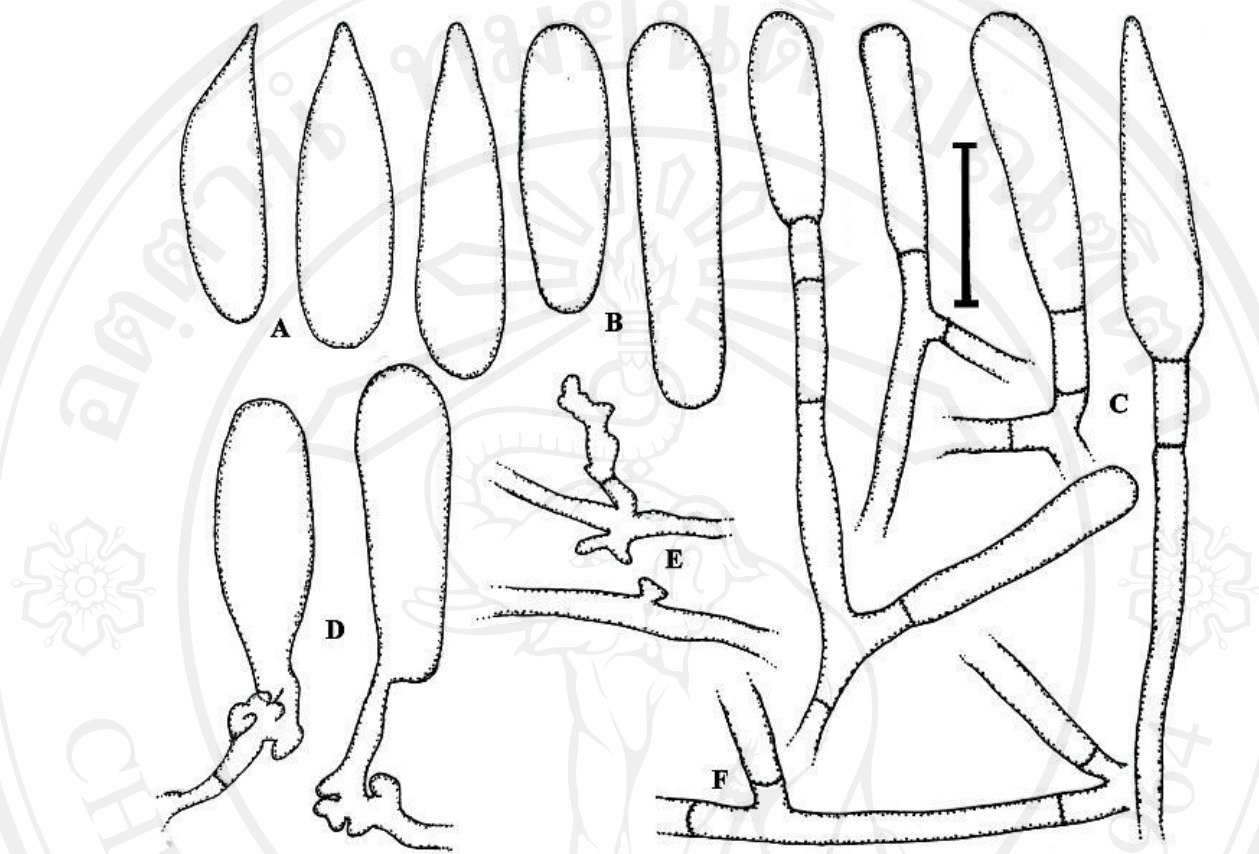


Figure 30 Illustration of *Oidiopsis sicula* on leaves of *Capsicum frutescens* × *Capsicum chinense*; (A) primary conidia (B) secondary conidia (C) conidiophores and conidia (D) conidia with germ tubes of the pseudoidium pattern (E) mycelia with appressoria and (F) mother cells that originate of conidiophore. (Bar 30 μm)

1.5 *Oidiopsis sicula* on *Capsicum* sp. (Darby chilli), Solanaceae

Mycelium internal and external, superficial mycelium on leaves, hypophyllous, mostly persistent, thin to dense, white, patches; *hyphae* substraight to wavy; *hyphal appressoria* nipple-shaped, lobed to multilobed, coralloid; *conidiophores* emerging through stomata, erect, straight, $(36-110-251(-301) \times (7-8-12 \mu\text{m})$; basal septum $0-19.52(-24.4) \mu\text{m}$ displaced from the branching point of the mycelium; *mother cells* forming conidia singly, $(30-35-89(-100) \times 5-7 \mu\text{m}$; *foot-cells* usually straight, with a basal septum near branching point of mycelium up to away from it, $(44-76-124(-177) \times 5-7 \mu\text{m}$, forming conidia singly; *conidia* dimorphic, without conspicuous fibrosin bodies, contain oil drop, *primary conidia* lanceolate, in the upper half narrowed towards the apex, $(47-59-73(-74) \times 14-20 \mu\text{m}$, mostly widest in the lower half, *secondary conidia* ellipsoid to cylindrical, usually widest in the upper half, $(44-49-60(-68) \times (14-16-21(-22) \mu\text{m}$; *conidial germination* formed *Ovulariopsis* type; *chasmothecia* can not be found (Fig. 31 and 32).

Specimens examined: on leaves of *Capsicum* sp. (Darby chilli) MUMH5119

1.6 *Oidiopsis sicula* on *Capsicum* sp. (Maxican chilli), Solanaceae

Mycelium internal and external, superficial mycelium on leaves, hypophyllous, mostly persistent, thin to dense, white, patches; *hyphae* substraight to wavy; *hyphal appressoria* nipple-shaped, lobed to multilobed, coralloid; *conidiophores* emerging through stomata, erect, straight, $(66-133-266(-281) \times (10-12-17 \mu\text{m})$; basal septum $(2-5-20(-24) \mu\text{m}$ displaced from the branching point of the mycelium; *mother cells* forming conidia singly, $(24-34-84(-107) \times 4-6 \mu\text{m}$; *foot-cells* usually straight, with a basal septum near branching point of mycelium up to away from it, $(17-48-137(-234) \times (3.66-5-6(-7) \mu\text{m}$, forming conidia singly; *conidia* dimorphic, without conspicuous fibrosin bodies, contain oil drop, *primary conidia* lanceolate, in the upper half narrowed towards the apex, $(61-63-76(-78) \times (13-15-19(-21) \mu\text{m}$, mostly widest in the lower half, *secondary conidia* ellipsoid to cylindrical, usually widest in the upper half, $(46-58-73(-78) \times (13-15-17(-20) \mu\text{m}$; *conidial germination* formed *Ovulariopsis* type; *chasmothecia* can not be found (Fig. 33 and 34).

Specimens examined: on leaves of *Capsicum* sp. (Maxican chilli) MUMH5104



Figure 31 *Oidiopsis sicula* on leaves of *Capsicum* sp. (Darby chilli); (A) mycelia colonized on lower side of leaf (B) conidia (C) conidiophores and conidia (D) appressoria and (E) conidial germination. (Bar 30 μm)

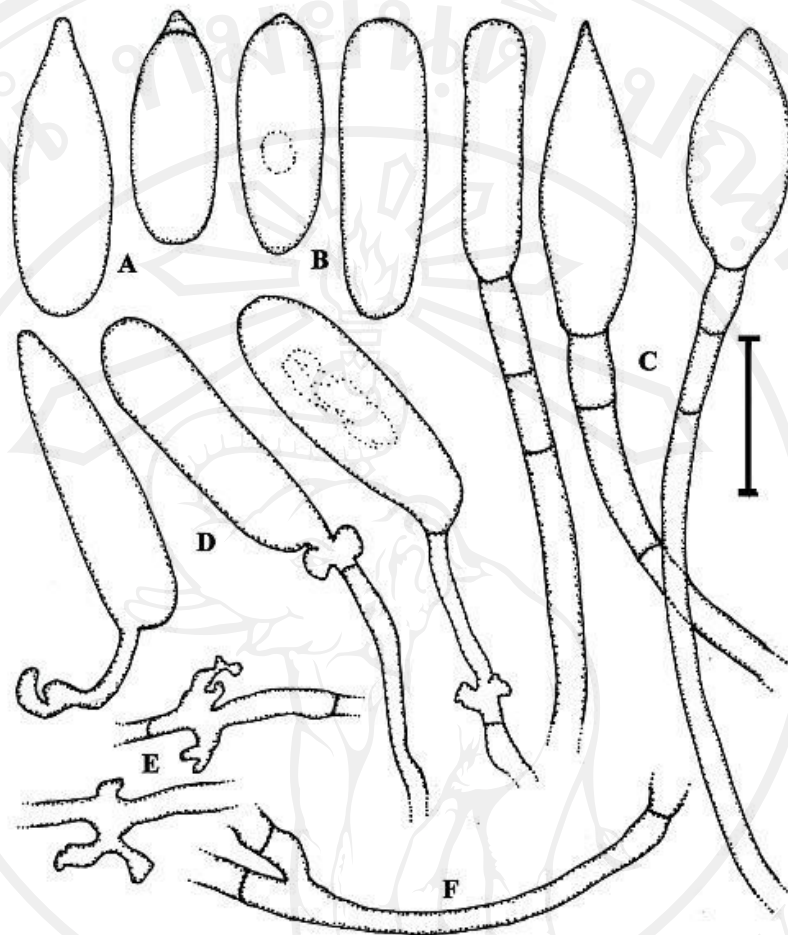


Figure 32 Illustration of *Oidiopsis sicula* on leaves of *Capsicum* sp. (Darby chilli); (A) primary conidia (B) secondary conidia (C) conidiophores and conidia (D) conidia with germ tubes of the pseudoidium pattern (E) mycelia with appressoria and (F) mother cells that originate of conidiophore (Bar 30 μ m)



Figure 33 *Oidiopsis sicula* on leaves of *Capsicum* sp. (Maxican chilli); (A) mycelia colonized on lower side of leaf (B) conidia (C) conidiophores and conidia (D) appressoria and (E) conidial germination. (Bar 30 μm)

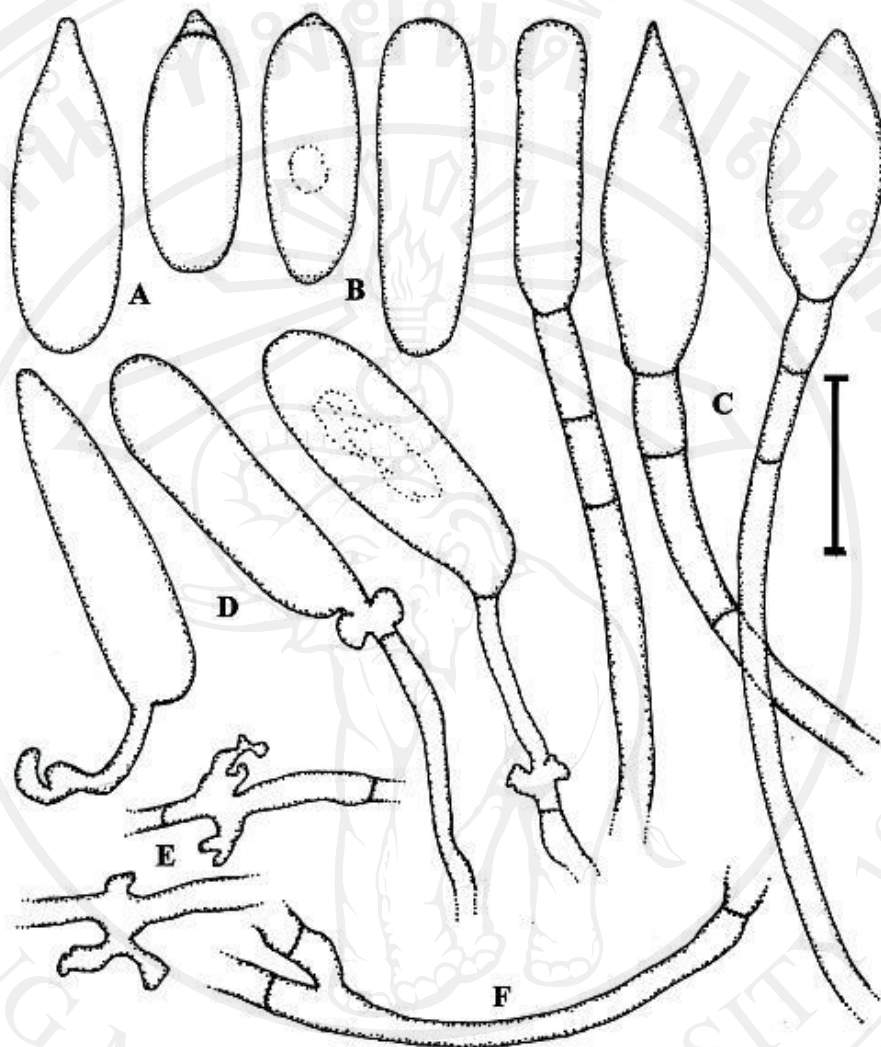


Figure 34 Illustration of *Oidiopsis sicula* on leaves of *Capsicum* sp. (Maxican chilli); (A) primary conidia (B) secondary conidia (C) conidiophores and conidia (D) conidia with germ tubes of the pseudoidium pattern (E) mycelia with appressoria and (F) mother cells that originate of conidiophore. (Bar 30 μ m)

Note: The teleomorphic state of powdery mildews on chilli species has not been discovered in Thailand. The size of morphological characteristics of powdery mildew on each chilli species in this study showed in Table 5. The morphological examination showed no significance differences among 5 *Oidiopsis* found on *Capsicum* spp. The morphological characteristics of this species were discussed by Palti (1988) in detail. The anamorphic features of Thailand collection were agreement with the previous records of this species that was identified as *Leveillula taurica* (Braun, 1987; Palti, 1988 and Braun and Cook, 2012). In addition, Goldberg (2004) demonstrated that the powdery mildew on chilli plants caused by *Oidiopsis sicula* that a conidial state of *Leveillula taurica*. *Leveillula taurica* is well known as a fungal parasitic plant on various hosts including *Capsicum* spp. Khodaparast *et al.* (2001) determined the nucleotide sequences of the rDNA ITS regions for 13 *Leveillula* species on 50 host plant species and reported that the morphology of primary conidia mostly provides a good criterion to identify *Leveillula* species. And, his study also demonstrated that *Leveillula taurica* is a species complex composed of several biological species. The present phylogenetic result also supported the morphological examination. Therefore, based on the morphological and molecular characteristics of powdery mildew on *Capsicum* spp. in this study can be identified as *Leveillula taurica*.

Table 6 Morphological characteristics of powdery mildew fungi on chilli species.

Host	Size of morphological characteristics (μm)				
	conidiophores	mother cells	foot cells	primary conidia	secondary conidia
<i>Capsicum</i>	(51-)100-276	(28-)30-122	(41-)49-	60-76(-83)×	(46-)52-69
<i>annuum</i> var.	(-338) × (5-)8-	(-134) × 5-	140(-202) ×	13-17(-21)	(-78) × (12-
<i>grossumum</i> (MUMH5096)	12(-16)	6(-7)	5-6(-7))13-17
<i>Capsicum</i> sp.	(66-)133-266	(24-)34-84	(17-)48-137	(61-)63-76	(46-)58-73
(Maxican chilli) MUMH5104)	(-281) × (10-)12-17	(-107)×5-6	(-234) × (4-)5-6(-7)	(-78) × (13-)15-19(-21)	(-78) × (13-)15-17(-19)
<i>Capsicum</i> <i>frutescens</i> (MUMH5083)	(105-)178- 273(-310) × (6-)8-15	(46-)49-83 (-151) × 5-6	(56-)90- 149(-174) × 5-7	(58-)63-80 (-88) × (15-)16-20	(49-)54-71 (-76) × (13-)15-19
<i>Capsicum</i> sp. (Darby) chilli) (MUMH5119)	(37-)110-251 (-301) × (7-)8- 12.2	(30-)35-89 (-100) × 5-7	(44-)76- 124(-177) × 5-7	(47-)58-73 (-74) × 14-19	(41-)51-68 (-76) × (11-)13-18(-19)
<i>C. frutescens</i> ×	(119-)144-	(22-)88-	(39-)71-	(54-)58-71	(46-)5-72
<i>C. chinense</i> (Bhut Jologia) (MUMH5106)	195(-278) × (7-)8-15(-17)	105(-115) × (5-)6-7	107(-149) × (5-)6-7	(-73) × (12-)15-18	(-73) × (13-)15-17(-18)

1.7 *Oidiopsis sicula* on *Euphorbia heterophylla*, Euphorbiaceae

Mycelium hypophyllous, white, forming dense patches on the lower leaves surface; *hyphae* substraight to wavy; *hyphal appressoria* nipple-shaped to coral-like; *conidiophores* arising from the internal mycelium through stomata, rarely arising from the external mycelium, erect, straight, (118.34–)158.6–251.32(–300.12) × (8.54–)9.76–17.08 μm; *mother cells* forming conidia singly, (23.18–)32.94–76.86(–93.94) × 4.88–7.32(–8.54) μm; *foot-cells* straight, (48.8–)63.44–114.68(–141.52) × 4.88–6.1(–8.54) μm with a basal septum (4.88–)7.32–15.86(–17.08) μm displaced from the branching point of the mycelium; *conidia* dimorphic, without conspicuous fibrosin bodies, contain oil drop, *primary conidia* lanceolate, in the upper half narrowed towards the apex, (34.16–)45.14–59.78(–67.1) × (9.76–)13.42–18.3 μm, *secondary conidia* ellipsoid to cylindrical, (50.02–)54.9–71.98(–74.42) × 14.64–18.3(–19.52) μm; *conidial germination* formed *Ovulariopsis* type; *chasmothecia* absent.

Specimens examined: on leaves of *Euphorbia heterophylla* MUMH5100

Note: *Leveillula taurica* was reported as a powdery mildew fungus on *Euphorbia heterophylla* (Amino, 1986; Bappammal *et al.* 1995). *Leveillula taurica* is known on a wide range of hosts and taxonomically difficult to species. Khodaparast *et al.* (2001) attempt to solve the taxonomic problem by using molecular sequence analysis based on ITS regions to clarify identification of the genus *Leveillula* for 4 species: *L. chrozophorae*, *L. duriaei*, *L. elaeagni* and *L. taurica*. The result showed *Leveillula taurica* on *Euphorbia* from Iran has only one base difference from *L. taurica* on *Euphorbia heterophylla* collected in Thailand. Therefore, powdery mildew on *Euphorbia heterophylla* in this study can be identified as *Leveillula taurica* based on morphological and molecular characteristics that was matched with previously study (Braun, 1987; Braun and Cook, 2012). Lack of teleomorphic state was found in Thailand. Additionally, the phylogenetic analysis revealed that *Oidiopsis* sp. on *Euphorbia heterophylla* cluster together with *Leveillula taurica*.

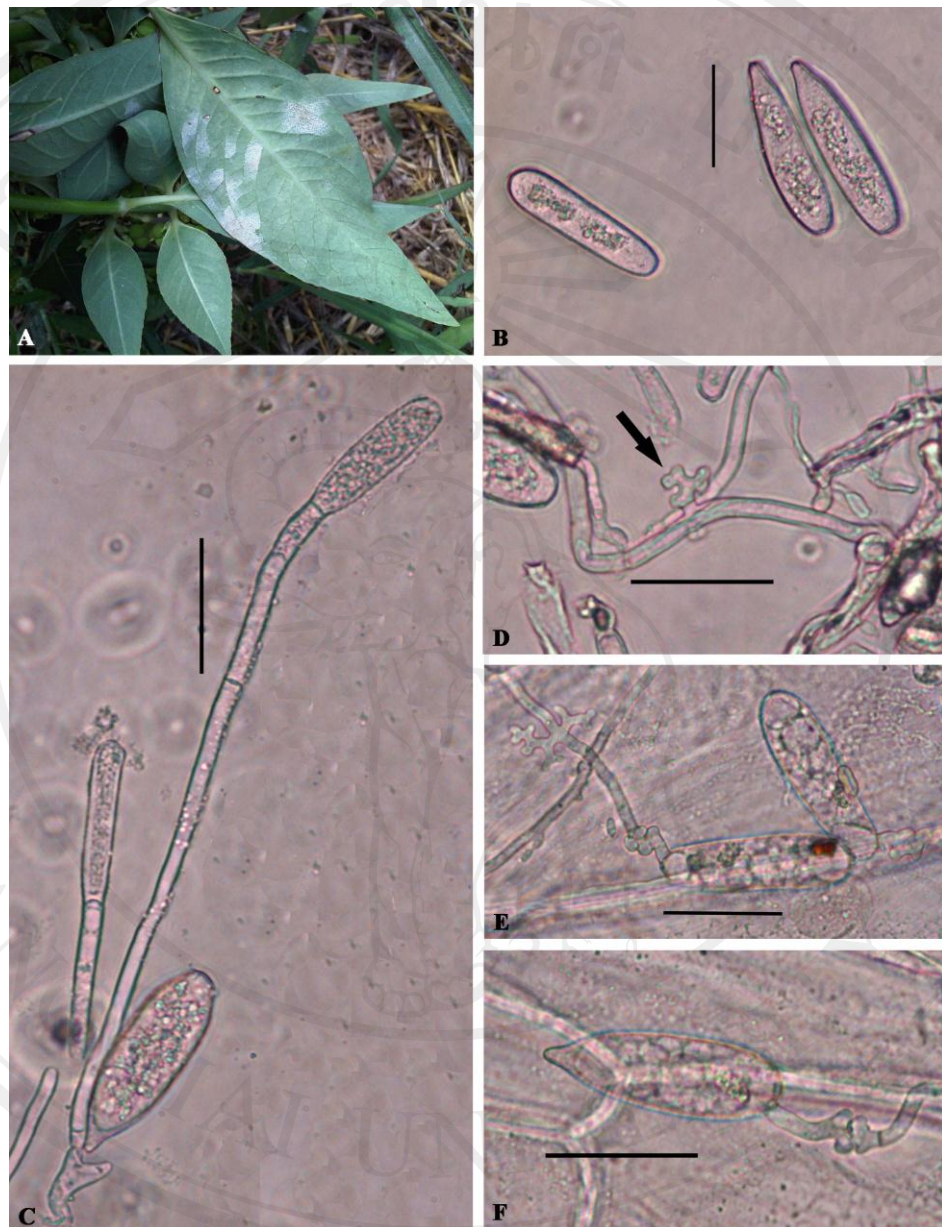


Figure 35 *Oidiopsis sicula* on leaves of *Euphorbia heterophylla*; (A) mycelia colonized on lower side of leaf (B) conidia (C) conidiophores and conidia (D) appressoria and (E and F) conidial germination. (Bar 30 μ m)

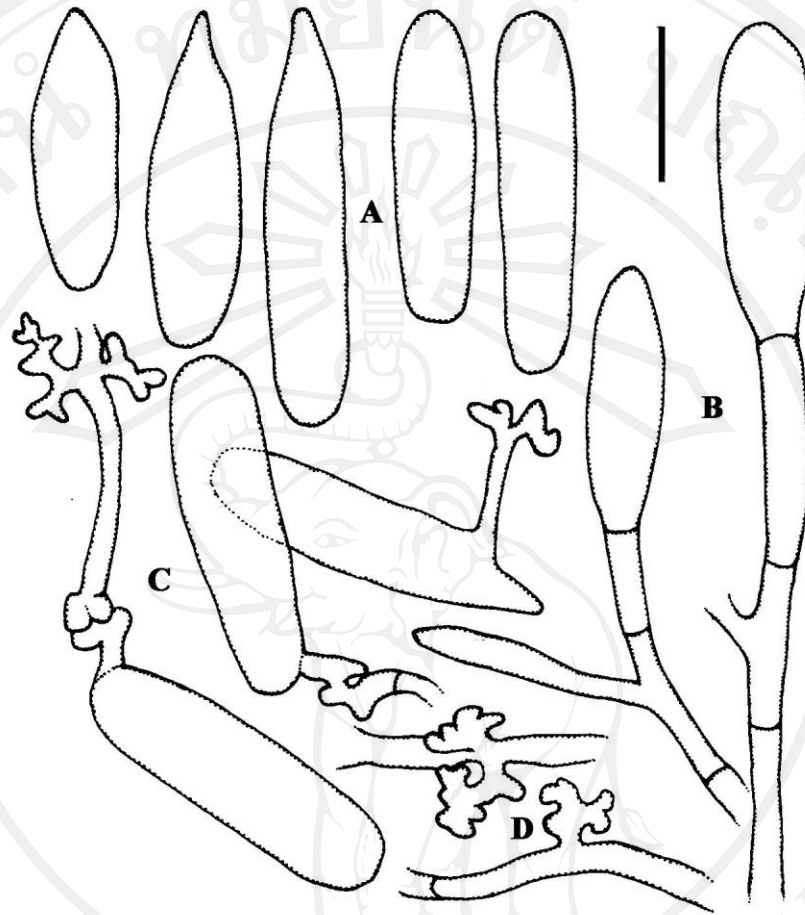


Figure 36 Illustration of *Oidiopsis sicula* on leaves of *Euphorbia heterophylla*; (A) conidia (B) conidiophores and conidia (C) conidia with germ tubes of the *Ovulariopsis* pattern and (D) mycelia with appressorium. (Bar 30 μ m)

1.8 *Oidiopsis* sp. on *Euphorbia pulcherrima*, Euphorbiaceae

Mycelium hypophyllus, white, thin patches, hyaline, internal and external, superficial mycelium on leaves; *hyphae* substraight to wavy; *apressoria* slightly nipple to nipple-shaped; *conidiophores* emerging through stomata, erect, straight, (118.34–158.6–251.32(–300.12) × (8.54–)9.76–17.08 μm; basal septum (4.88–)7.32–15.86(–17.08) μm displaced from the branching point of the mycelium; *mother cells* forming conidia singly, (23.18–)32.94–76.86(–93.94) × 4.88–7.32(–8.54) μm; *foot-cells* usually straight, with a basal septum near branching point of mycelium up to away from it, (48.8–)63.44–114.68(–141.52) × 4.88–6.1(–8.54) μm; *conidia* dimorphic, without conspicuous fibrosin bodies, contain oil drop, *primary conidia* lanceolate, apically attenuated, (34.16–)45.14–59.78(–67.1) × (9.76–)13.42–18.3 μm, *secondary conidia* ellipsoid to cylindrical, usually widest in the upper half, (50.02–)54.9–71.98(–74.42) × 14.64–18.3(–19.52) μm; *conidial germination* formed *Ovulariopsis* type; *chasmothecia* absent.

Specimens examined: on leaves of *Euphorbia pulcherrima* CMU38

Note: *Leveillula taurica* was reported on *Euphorbia* spp. (Arnaud, 1921). After that, Nour (1957) reported that *Euphorbia pulcherrima* is infected by *Leveillula clavata* in Africa (Kenya). In 2006, Paul and Thakur reported *Oidiopsis sicula* (*Leveillula taurica*) in India. Base on the features mentioned above, the characteristics of the fungus in this study are closely similar to those of the anamorph of *L. taurica* based on Braun (1987), Braun and Cook (2012) and Shin (2000), it might be identified as *Leveillula taurica*. In this study, chasmothecia can not be found. However, molecular analysis should be use for clarify the identification.

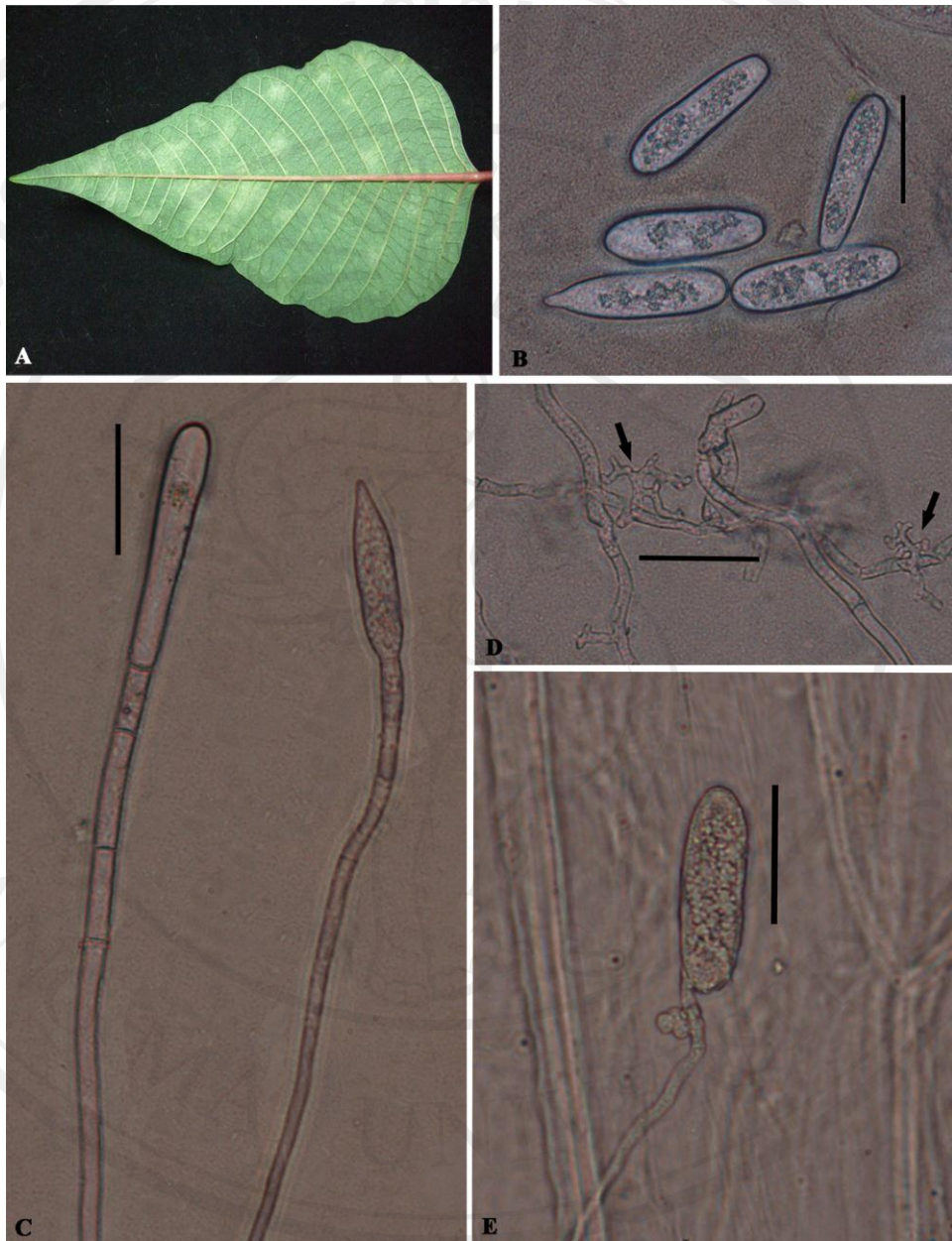


Figure 37 *Oidiopsis* sp. on leaves of *Euphorbia pulcherrima*; (A) mycelia colonized on lower side of leaf (B) conidia (C) conidiophores and conidia (D) appressoria and (E) conidial germination. (Bar 30 μm)

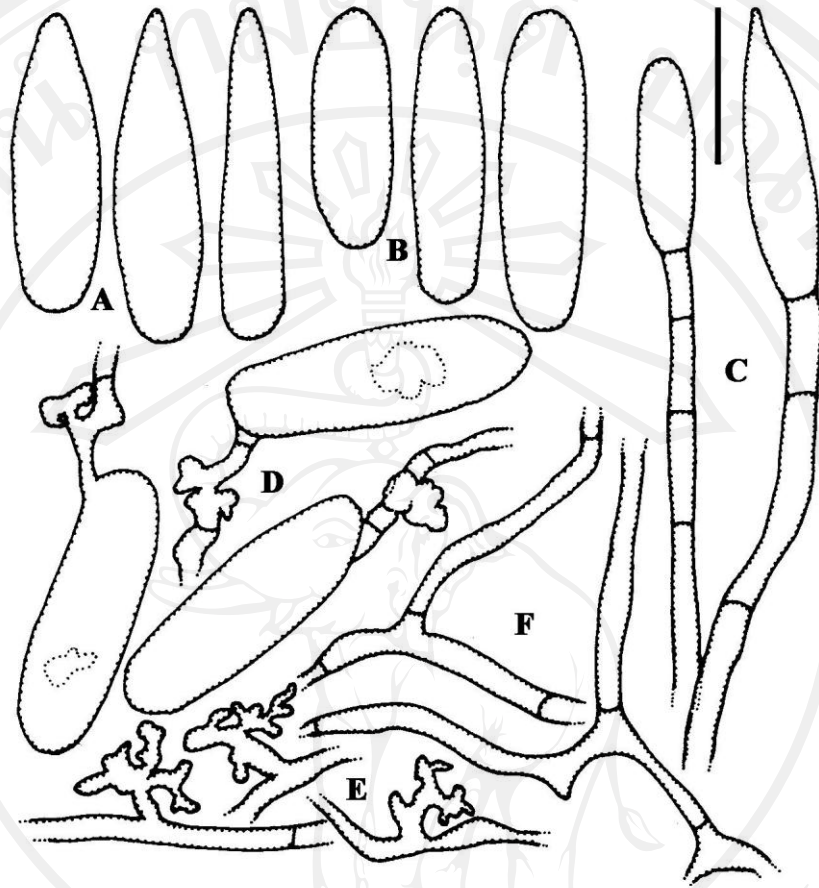


Fig. 38 Illustration of *Oidiopsis* sp. on leaves of *Euphorbia pulcherrima*; (A) primary conidia (B) secondary conidia (C) conidiophores and conidia (D) conidia with germ tubes of the *Ovulariopsis* pattern (E) mycelia with appressoria and (F) mother cells that originate of conidiophore. (Bar 30 μm)

1.9 *Oidiopsis* sp. on *Galphimia glauca*, Malpighiaceae

Mycelium white, thin to thick patches, hypophyllous, hyaline, superficial mycelium on leaves; *hyphae* substraight; *appressoria* slightly nipple to nipple-shaped; *conidiophores* emerging through stomata, erect, straight, (85.4–)148.84–241.56(–324.52) × (7.32–)9.76–15.86(–17.08) μm; basal septum (2.44–)4.88–20.74(–48.8) μm displaced from the branching point of the mycelium; *mother cells* forming conidia singly, (28.06–)31.72–95.16(–112.24) × 4.88–6.1 μm; *foot-cells* usually straight, with a basal septum near branching point of mycelium up to away from it, (26.84–)73.2–154.94(–225.7) × 4.88–6.1 μm; *conidia* dimorphic, without conspicuous fibrosin bodies, contain oil drop, *primary conidia* lanceolate, apically attenuated, (57.34–)63.44–75.64(–85.4) × (12.2–)14.64–17.08(–19.52) μm, *secondary conidia* ellipsoid to cylindrical, usually widest in the upper half, (48.8–)53.68–73.2(–75.64) × (12.2–)13.42–15.68(–18.3) μm; *conidial germination* formed *Ovulariopsis* type; *chasmothecia* absent.

Specimens examined: on leaves of *Galphimia glauca* CMU-MJ4

Note: Base on the features mentioned aboved, the characteristics of the fungus in this study are closely similar to those of the anamorph of *L. taurica* based on Braun (1987), Braun and Cook (2012) and Shin (2000), it might be identified as *Leveillula taurica*. In this study, chasmothecia can not be found. However, molecular analysis should be used for clarify the identification. This is the first report of *Oidiopsis* sp. on *Galphimia glauca*.

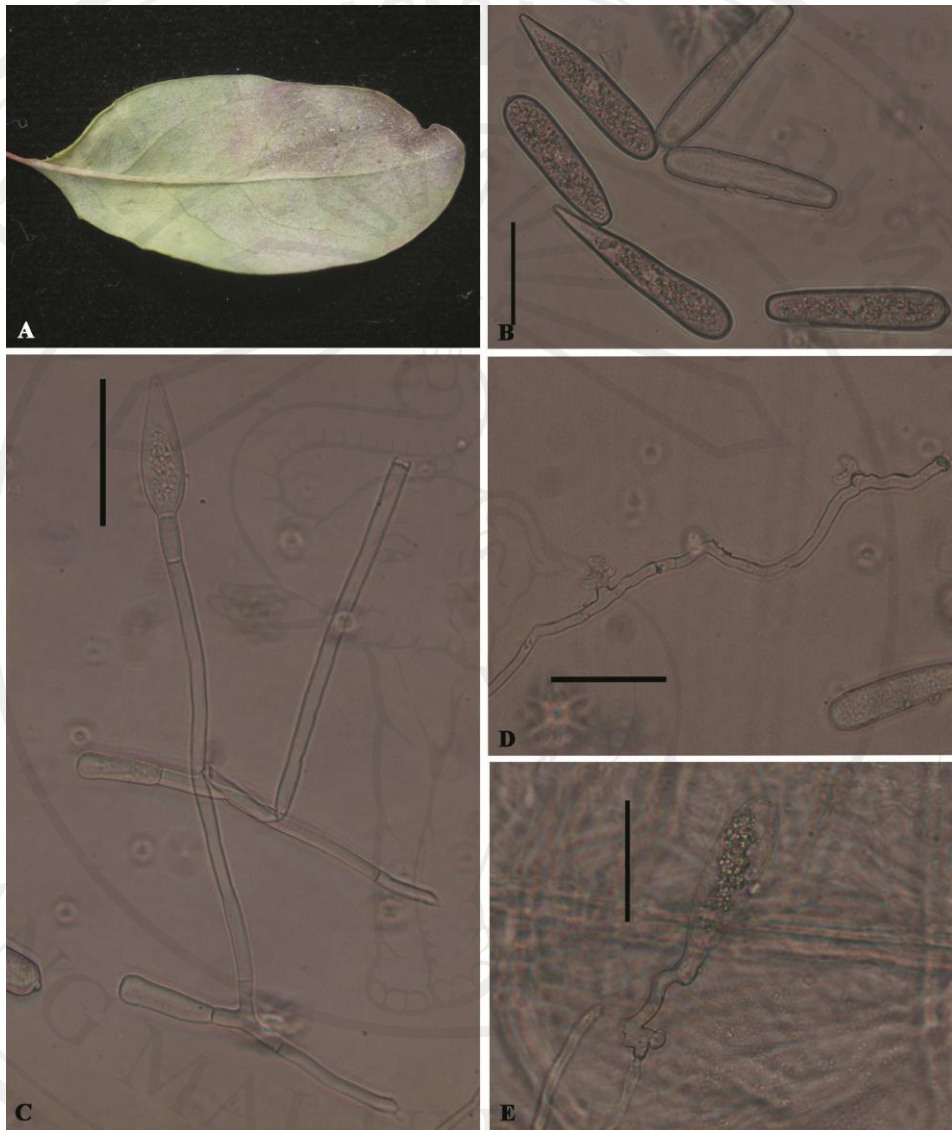


Figure 39 *Oidiopsis* sp. on leaves of *Galphimia glauca*; (A) mycelia colonized on lower side of leaf (B) conidia (C) conidiophores and conidia (D) appressoria and (E) conidial germination. (Bar 30 μ m)

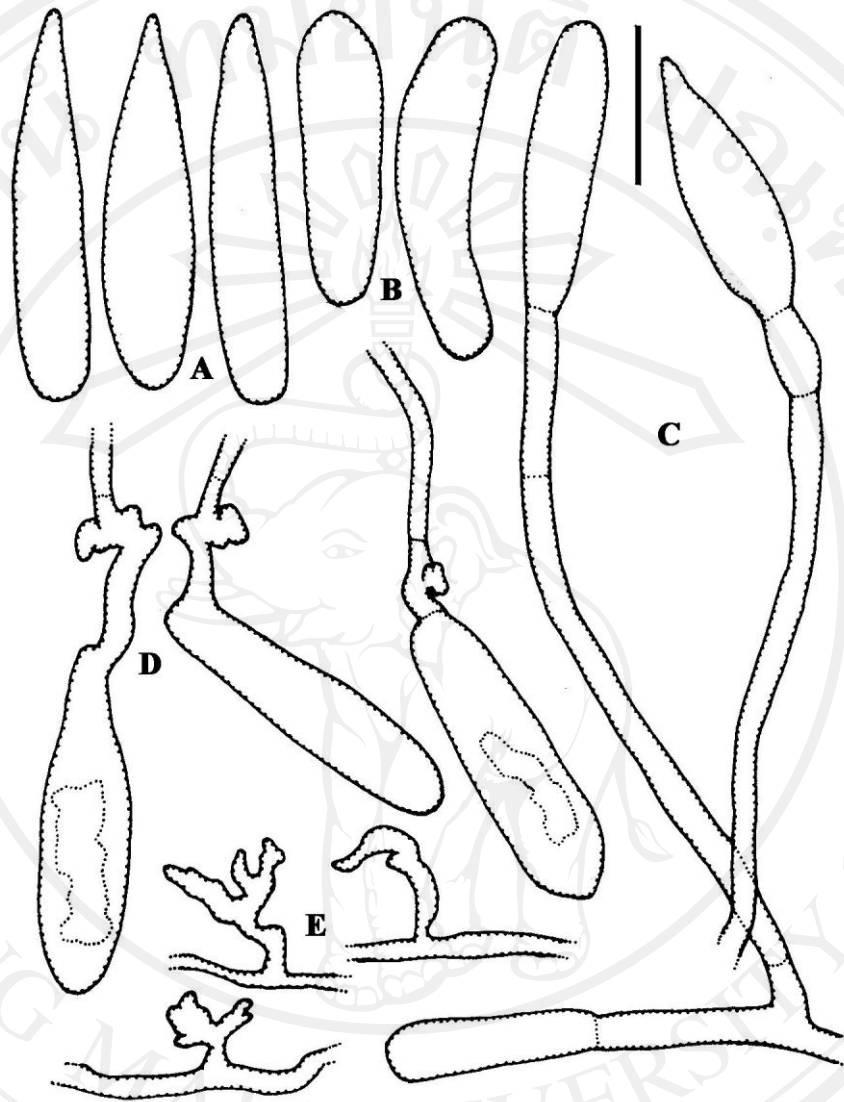


Figure 40 Illustration of *Oidiopsis* sp. on leaves of *Galphimia glauca*; (A) primary conidia (B) secondary conidia (C) conidiophores and conidia (D) conidia with germ tubes of the *Ovulariopsis* pattern and (E) mycelia with appressoria. (Bar 30 μ m)

1.10 *Oidiopsis* sp. on *Oxalis triangularis*, Oxalidaceae

Mycelium white, thin to thick patches, hypophyllous, hyaline, superficial mycelium on leaves; *hyphae* substraight to wavy; *appressoria* slightly nipple to nipple-shaped; *conidiophores* emerging through stomata, erect, straight, (152.5–)165.92–265.96(–353.8) × 9.76–14.64(–17.08) μm; basal septum (1.22–)3.66–7.32(–8.54) μm displaced from the branching point of the mycelium; *mother cells* forming conidia singly, (54.9–)85.4–92.72(–112.24) × 4.88–6.1(–7.32) μm; *foot-cells* usually straight, with a basal septum near branching point of mycelium up to away from it, (40.26–)46.36–157.38(–191.54) × (3.66–)4.88–6.1 μm; *conidia* dimorphic, without conspicuous fibrosin bodies, contain oil drop, *primary conidia* lanceolate, apically attenuated, (53.68–)58.56–71.98(–74.42) × 14.64–18.3(–19.52) μm, *secondary conidia* ellipsoid to cylindrical, usually widest in the upper half, (48.8–)52.46–67.1(–84.18) × (12.2–)13.42–18.3(–19.52) μm; *conidial germination* formed *Ovulariopsis* type; *chasmothecia* absent.

Specimens examined: on leaves of *Oxalis triangularis* CMU-HL1

Note: Berger (1938) reported that powdery mildew on *Oxalis triangularis* was caused by *Leveillula taurica* f. *oxalidis*, but lacking of valid publication of “f. *oxalidis*”. Later, *Leveillula taurica* on *Oxalis triangularis* has been reported in Mongolia by Zhi (2010). Base on symptom on host and the features mentioned above, the characteristics of the fungus in this study are closely similar to those of the anamorph of *L. oxalidicola* based on Braun and Cook (2012). Therefore, this fungus can be identified as *L. oxalidicola* or *Oidiopsis oxalidis* in its anamorph. However, molecular analysis should be used for clarify the identification. This is the first report of *Oidiopsis* sp. on *Oxalis triangularis* in Thailand.



Figure 41 *Oidiopsis* sp. on leaves of *Oxalis triangularis*; (A) mycelia colonized on lower side of leaf (B) conidia (C) conidiophores and conidia (D) and (E) conidial germination of secondary and primary conidia, respectively. (Bar 30 μm)

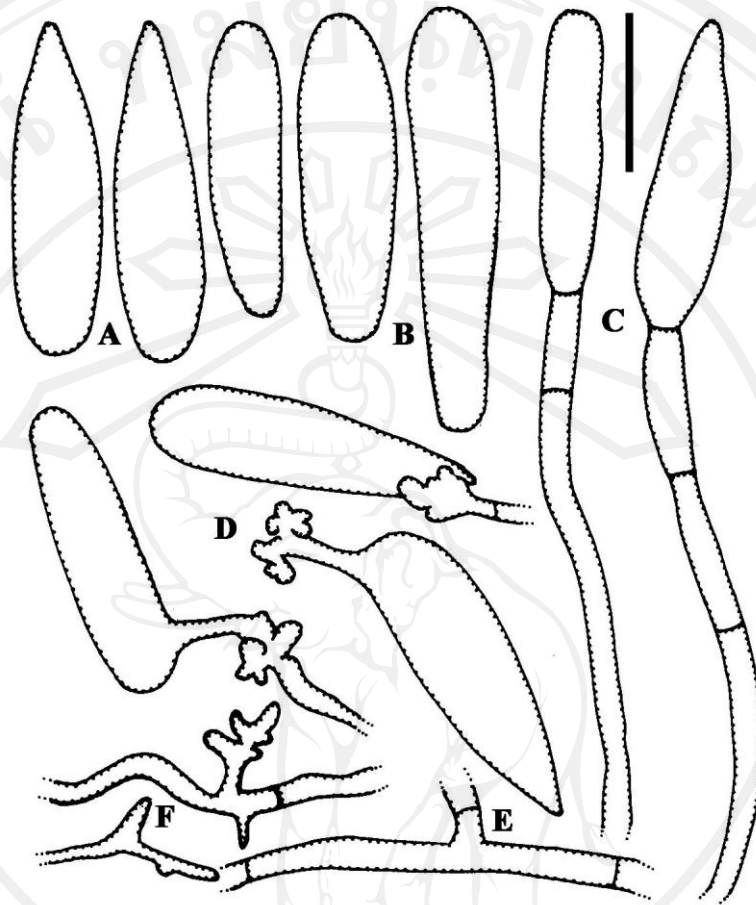


Figure 42 Illustration of *Oidiopsis* sp. on leaves of *Oxalis triangularis*; (A) primary conidia (B) secondary conidia (C) conidiophores and conidia (D) conidia with germ tubes of the *Ovulariopsis* pattern and (E) mycelia with appressoria. (Bar 30 μ m)

1.11 *Oidiopsis* sp. on *Sesamum indicum*, Pedaliaceae

Mycelium amphigenous, mostly epiphyllous, white, forming dense patches; *hyphae* substraight to wavy; *hyphal appressoria* nipple-shaped to elongated; *conidiophores* arising from the internal mycelium through stomata, rarely arising from the external mycelium, erect, straight, (114.68–)148.84–209.84(–285.48) × (7.32–)10.98–14.64(–17.08) μm; *mother cells* forming conidia singly, (22–)29–38(–42) × 2–3 μm; *foot-cells* straight, (35.38–)63.44–113.46(–143.96) × 4.88–7.32(–8.54) μm with a basal septum 7.32–13.42(–17.08) μm displaced from the branching point of the mycelium; *conidia* dimorphic, without conspicuous fibrosin bodies, contain oil drop, *primary conidia* lanceolate, in the upper half narrowed towards the apex, (51.24–)56.12–69.54(–86.62) × (9.76–)10.98–17.08 μm, *secondary conidia* ellipsoid to cylindric, (46.36–)50.02–68.32 × (12.2–)13.42–17.08(–20.74) μm; *conidial germination* formed *Ovulariopsis* type; *chasmothecia* absent.

Specimens examined: on leaves of *Sesamum indicum* CMU16

Note: *Leveillula taurica* is well known on a wide range of hosts, and also neither morphological features nor molecular analyses are still unclear. *Sesamum indicum* was reported as a host of *Leveillula taurica* (Amino, 1986; Braun, 1995, Braun, 1987 and Braun and Cook, 2012). The anamorphic state of powdery mildew on *Sesamum indicum* in this study is morphologically most similar to anamorph of *Leveillula taurica* that was demonstrated in previously report (Braun, 1987; Braun and Cook, 2012). Therefore, based on morphology and host can be identified powdery mildew on *Sesamum indicum* as *Leveillula taurica* which proposed anamorphic state as *Oidiopsis sicula*. However, molecular analysis should be used for the identification. This is the first report of *Oidiopsis* sp. on *Sesamum indicum* in Thailand.

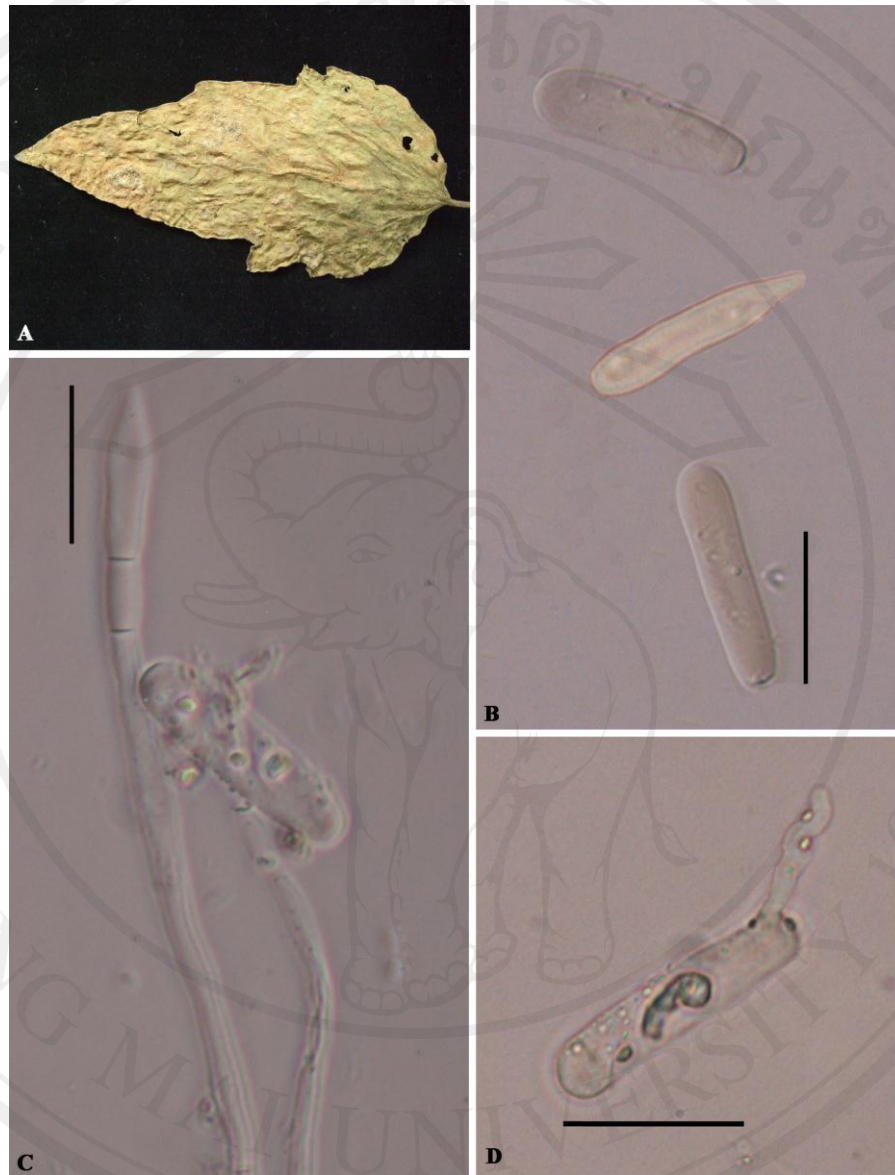


Figure 43 *Oidiopsis* sp. on leaves of *Sesamum indicum*; (A) mycelia colonized on upper side of leaf (B) conidia (C) conidiophores and conidia and (D) conidial germination. (Bar 30 µm)

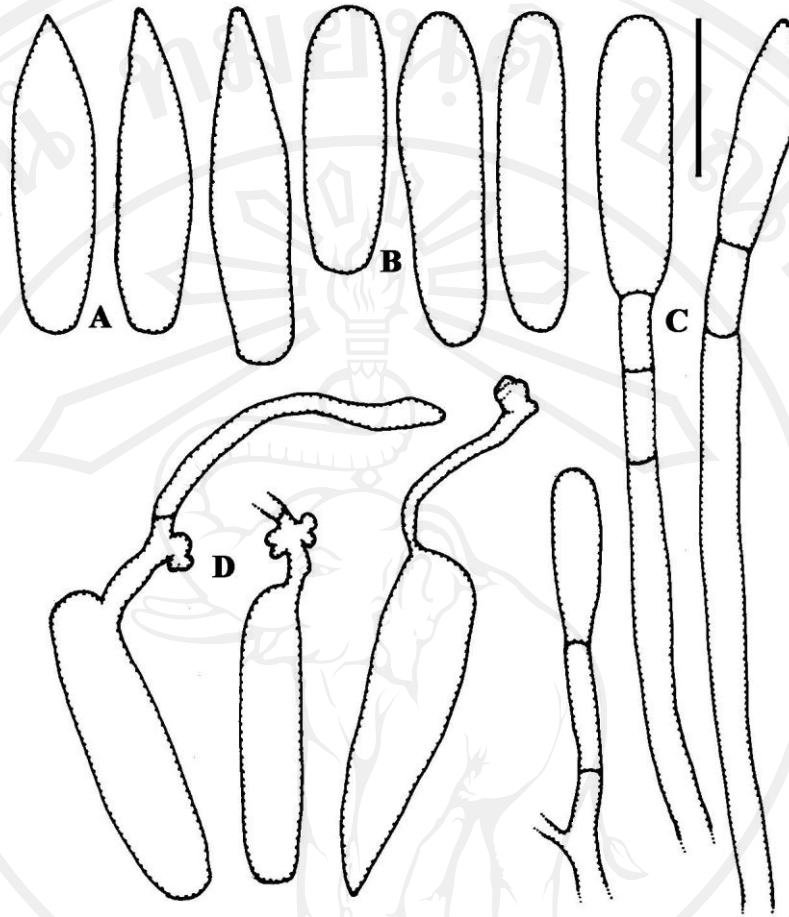


Figure 44 Illustration of *Oidiopsis* sp. on leaves of *Sesamum indicum*; (A) primary conidia (B) secondary conidia (C) conidiophores and conidia and (D) conidia with germ tubes of the *Ovulariopsis* pattern. (Bar 30 μ m)

1.12 *Oidiopsis sicula* on *Solanum aculeatissimum*, Solanaceae

Mycelium hypophyllous, white, forming dense patches on the lower leaves surface; *hyphae* substraight to wavy; *hyphal appressoria* nipple-shaped to coral-like; *conidiophores* arising from the internal mycelium through stomata, rarely arising from the external mycelium, erect, straight, (85.4–)119.56–290.36(–485.56) × (8.54–)12.2–14.64(–18.3) μm; *mother cells* forming conidia singly, (53.68–)61–114.68(–134.2) × (3.66–)4.88–7.32 μm; *foot-cells* straight, (31.72–)50.02–134.2(–143.96) × 4.88–7.32(–8.54) μm with a basal septum (3.66–)4.88–17.08(–24.4) μm displaced from the branching point of the mycelium; *conidia* dimorphic, without conspicuous fibrosin bodies, contain oil drop, *primary conidia* lanceolate, in the upper half narrow towards the apex, (43.92–)48.8–61(–74.42) × 17.08–21.96(–26.84) μm, *secondary conidia* ellipsoid to cylindrical, (43.92–)48.8–62.22(–65.88) × (14.64–)15.86–19.52(–20.74) μm; *conidial germination* formed *Ovulariopsis* type; *chasmothecia* absent.

Specimens examined: on leaves of *Solanum aculeatissimum* MUMH5101, 5102

Note: The genus *Solanum* was reported as a host of *Leveillula taurica* since 1986 by Amino. *Leveillula taurica* is a fungal pathogen of powdery mildew disease that well known on various host species. Base on symptom on host and the features mentioned above, the characteristics of the fungus in this study are closely similar to those of the anamorph of *L. taurica* (Braun, 1987; Braun and Cook, 2012). Therefore, this fungus can be identified as *L. taurica* or *Oidiopsis sicula* in its anamorph. Additionally, the phylogenetic analysis revealed that *Oidiopsis* sp. on *Solanum aculeatissimum* cluster together with *Leveillula taurica*. This is the first report of *Oidiopsis sicula* on *Solanum aculeatissimum*.

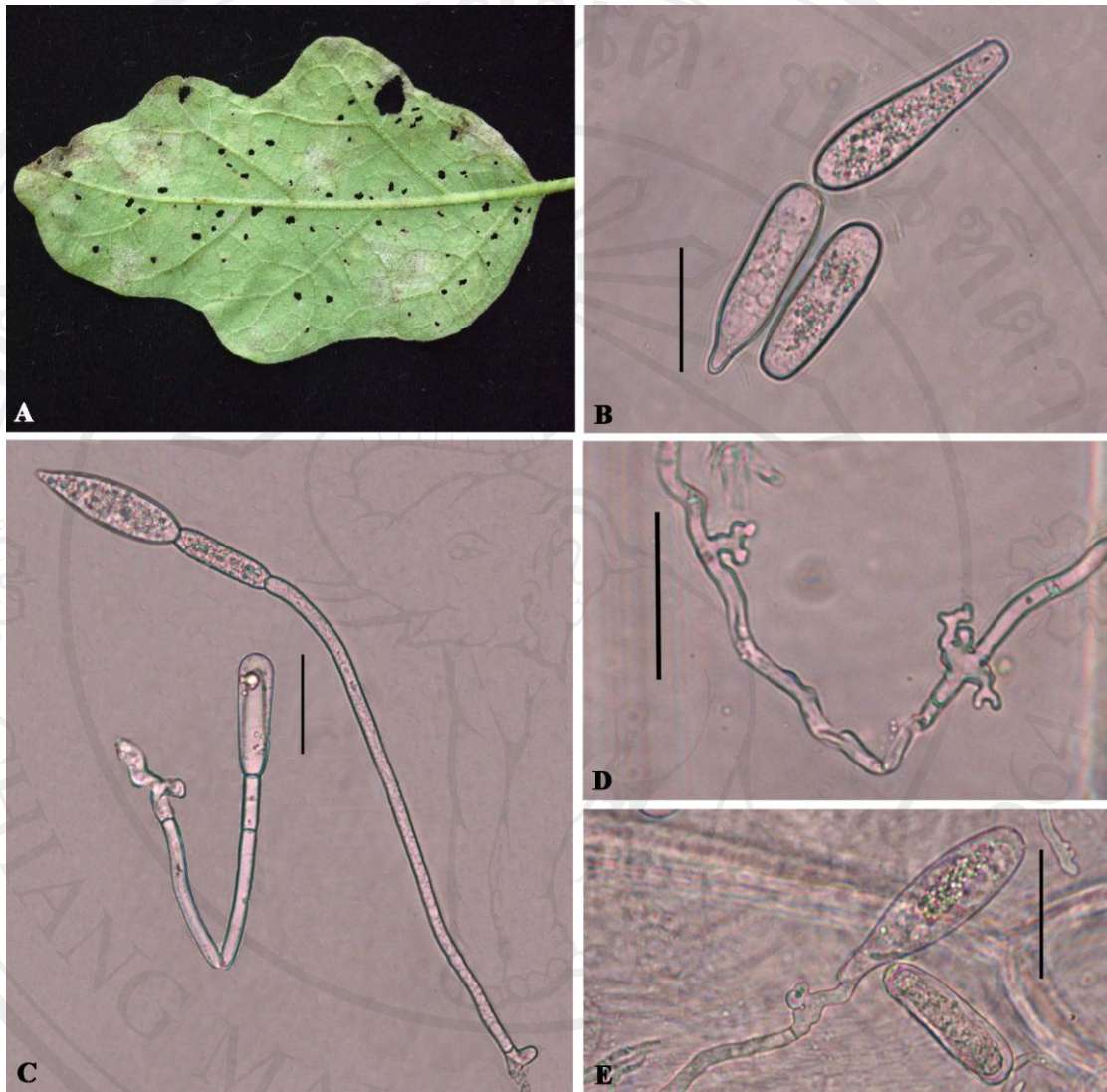


Figure 45 *Oidiopsis sicula* on leaves of *Solanum aculeatissimum*; (A) mycelia colonized on lower side of leaf (B) conidia (C) conidiophores and conidia (D) appressoria and (E) conidial germination. (Bar 30 μm)

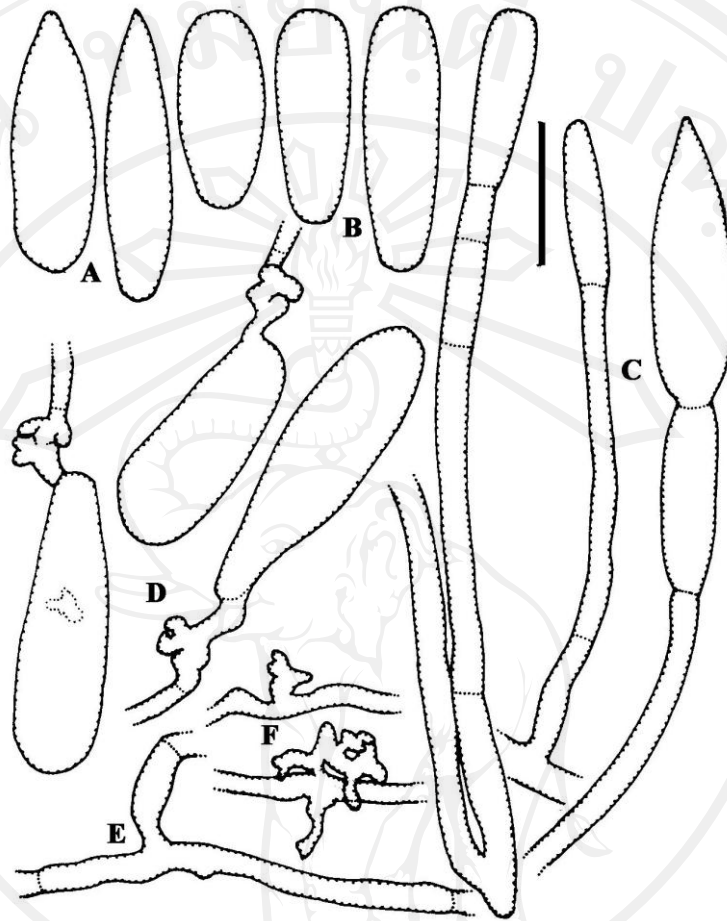


Figure 46 Illustration of *Oidiopsis sicula* on leaves of *Solanum aculeatissimum*; illustrated using a line drawing under a light microscope; (A) primary conidia (B) secondary conidia (C) conidiophores and conidia (D) conidia with germ tubes of *Ovulariopsis* pattern (E) mother cell that leading originated of conidiophore and (F) mycelia with appressorium. (Bar 30 μm)

1.13 *Oidiopsis sicula* on *Solanum torvum*, Solanaceae

Mycelium hypophyllous, white, forming dense patches on the lower leaves surface; *hyphae* substraight to wavy; *hyphal appressoria* nipple-shaped to coral-like; *conidiophores* arising from the internal mycelium through stomata, rarely arising from the external mycelium, erect, straight, (47.58–)131.76–280.6(–292.8) × (8.54–)9.76–14.64(–15.86) μm; *mother cells* forming conidia singly, (24.4–)42.7–109.8(–130.54) × 4.88–7.32 μm; *foot-cells* straight, (34.16–)43.92–104.92(–139.08) × (4.88–)6.1–7.32 μm with a basal septum (0–)3.66–21.96(–29.28) μm displaced from the branching point of the mycelium; *conidia* dimorphic, without conspicuous fibrosin bodies, contain oil drop, *primary conidia* lanceolate, in the upper half narrowed towards the apex, (56.12–)58.56–65.88(–70.76) × 15.86–18.3(–19.52) μm, *secondary conidia* ellipsoid to cylindric, (43.92–)52.46–64.66(–73.2) × 15.86–19.52 μm; *conidial germination* formed *Ovulariopsis* type; *chasmothecia* absent.

Specimens examined: on leaves of *Solanum torvum* MUMH5091, 5092

Note: *Leveillula taurica* is well known on a wide range of hosts. However, neither morphological features nor molecular analyses are still unclear. Khodaparast *et al.* (2001) determined the nucleotide sequences of the rDNA ITS regions for 13 *Leveillula* species on 50 host plant species and demonstrated that *Leveillula taurica* is a species complex composed of several biological species. *Solanum torvum* was reported as a host of *Leveillula taurica* (Amino, 1986; Bappammal *et al.*, 1995). The anamorphic state of powdery mildew fungus on *Solanum torvum* in this study is morphologically most similar to anamorph of *Leveillula taurica* that was demonstrated in previous report (Braun, 1987; Braun and Cook, 2012). The present phylogenetic result also supported the morphological examination. Therefore, based on the morphological and molecular characteristics of powdery mildew on *Solanum torvum* in this study can be identified as *Leveillula taurica*. This is the first report of *Oidiopsis sicula* on *Sesamum indicum* in Thailand.

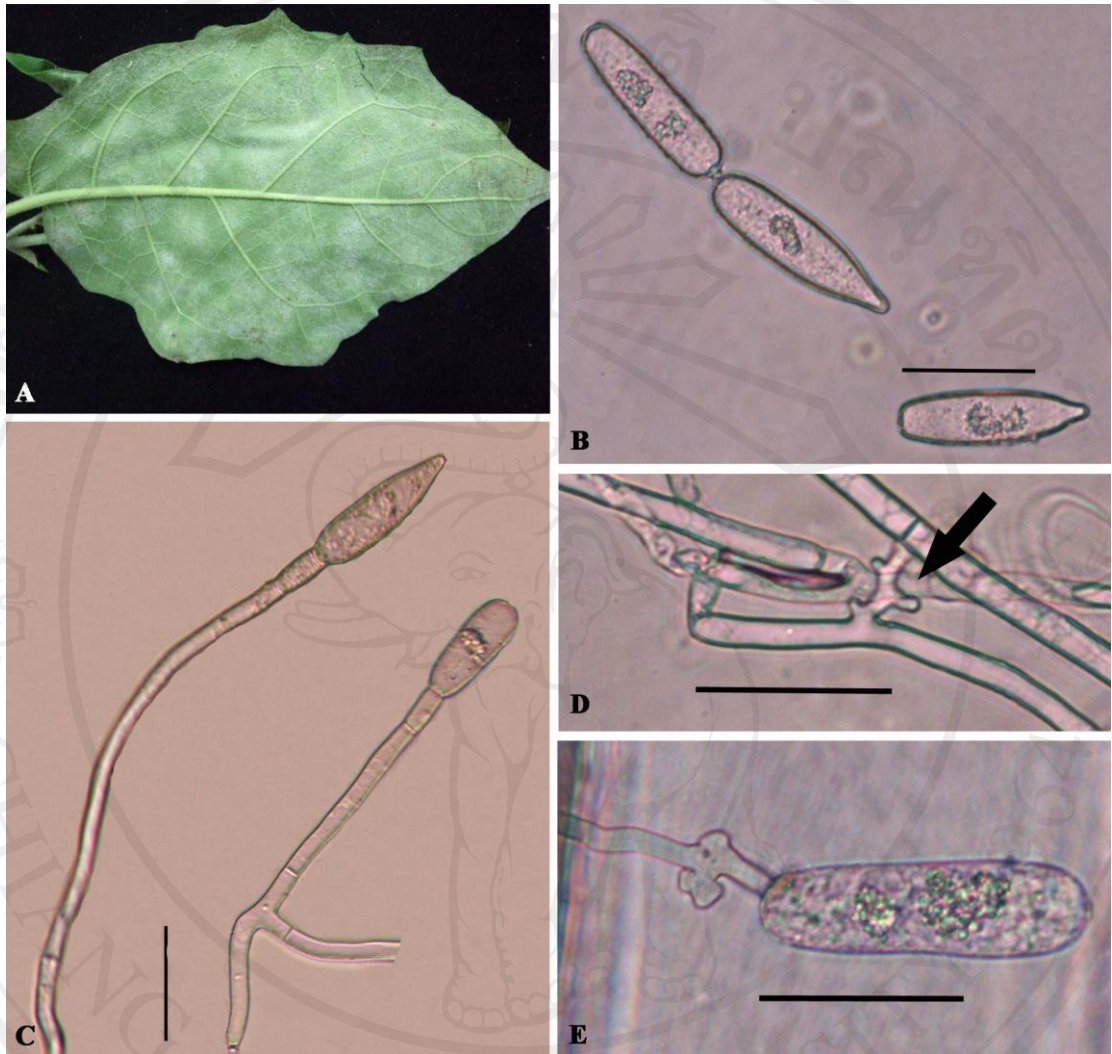


Figure 47 *Oidiopsis sicula* on leaves of *Solanum torvum*; (A) mycelia colonized on lower side of leaf (B) primary and secondary conidia (C) primary (leaf) and secondary (right) conidia attached singly on conidiophores (D) appressoria (arrow) and (E) conidial germination. (Bar 30 μ m)

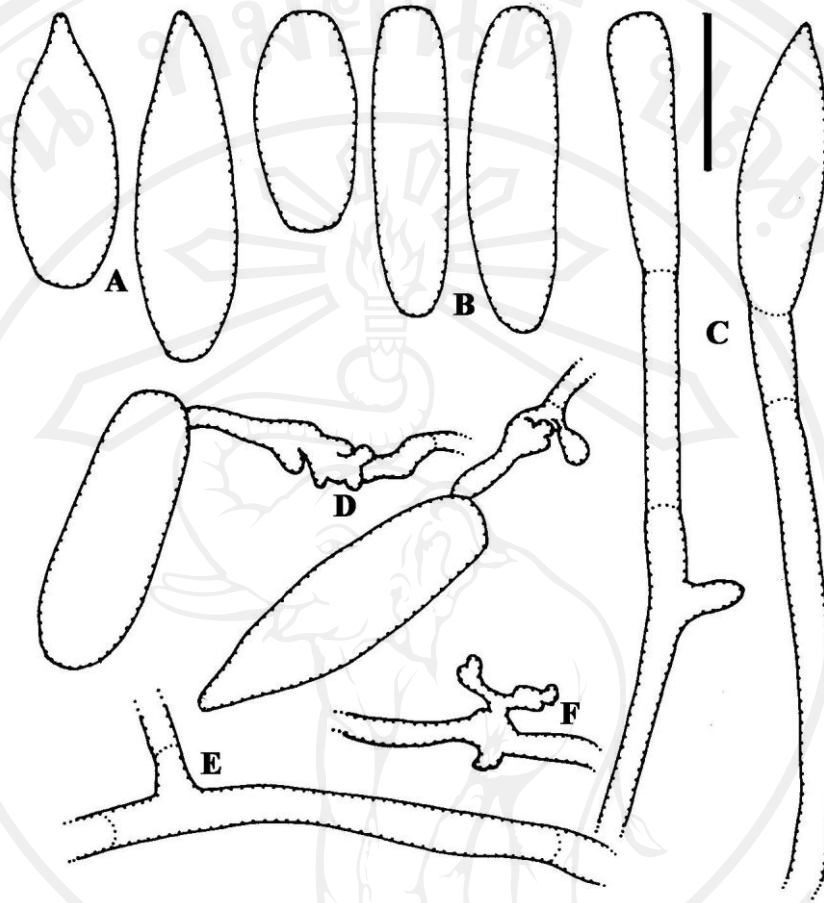


Figure 48 Illustration of *Oidiopsis sicula* on leaves of *Solanum torvum*; illustrated using a line drawing under a light microscope; (A) primary conidia (B) secondary conidia (C) conidiophores and conidia (D) conidia with germ tubes of the *Ovulariopsis* pattern (E) mother cell that leading originated of conidiophore and (F) mycelia with appressorium. (Bar 30 μm)

2. Descriptions and photographic figures of *Phyllactinia* (*Ovulariopsis*)

2.1 *Ovulariopsis* sp. on *Alangium kurzii*, Alangiaceae

Mycelium hypophyllus, white, thin to dense patches, hyaline; *apressoria* slightly nipple to nipple-shaped; *conidiophores* arising from upper part of ectophytic hyphae, erect or slightly bent, long, (319.64–)336.72–578.28(–644.16) μm ; *mother cell* forming conidia singly; straight in *foot-cells*, (80.52–)90.28–129.32(–136.64) \times (4.88–)6.1–7.32(–8.54) μm , with a basal septum at (7.32–)12.2–14.64(–19.52) μm away from the branching point of mycelium; *conidia* clavate, non-papillate, (40.26–)51.24–69.54(–87.84) \times (18.3–)21.96–29.28 μm , hyaline without conspicuous fibrosin-bodies and *conidial germination* formed *Ovulariopsis* type.

Specimens examined: on leaves of *Alangium kurzii* CMU5120

Note: *Alangium kurzii* has been recorded to be infected with *Phyllactinia alangii* (Amino, 1986). Braun and Cook (2012) reported *Alangium kurzii* on *Alangium kurzii* and also other *Alangium* species; *A. chinense*, *A. platanifolium* in Asia (China and Japan). But, the anamorphic features were demonstrated just a few detail in their report. The anamorphic state of powdery mildew on *Alangium kurzii* in this study is morphologically most similar to anamorph of *Phyllactinia alangii* that was demonstrated in previously report (Braun and Cook, 2012). Therefore, based on the morphological characteristics and host plant of powdery mildew on *Alangium kurzii* in this study can be identified as *Phyllactinia alangii*. However, molecular analysis should be used for clarify the identification. This is the first report of *Ovulariopsis* sp. on *Alangium kurzii* in Thailand.



Figure 49 *Ovulariopsis* sp. on leaves of *Alangium kurzii* Craib; (A) mycelia colonized on lower side of leaf (B) conidia (C) conidiophores and conidia (D) appressoria and (E) conidial germination. (Bar 30 μ m)

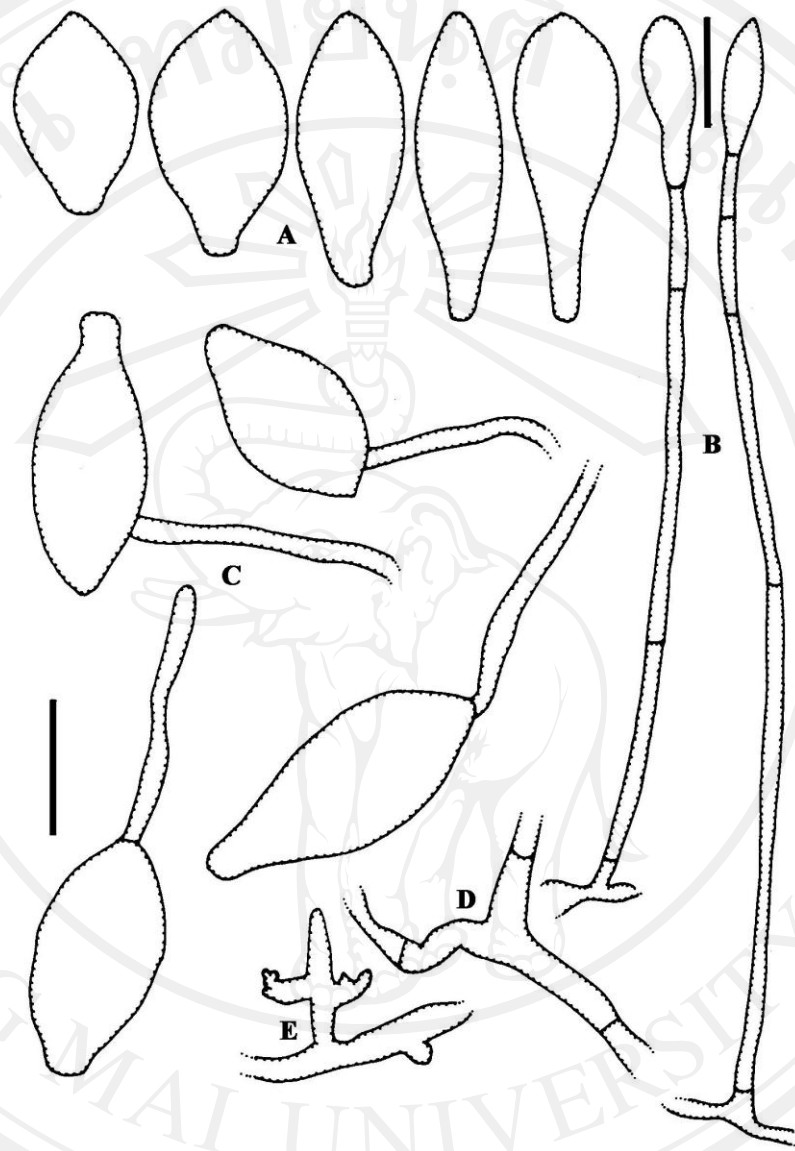


Figure 50 Illustration of *Ovulariopsis* sp. on leaves of *Alangium kurzii* Craib; (A) conidia (B) conidiophores and conidia (C) conidia with germ tubes of the *Ovulariopsis* pattern (D) mother cells that originate of conidiophore and (E) mycelia with appressoria. (Bar 30 μm in A, C-E and Bar 50 μm in B)

2.2 *Ovulariopsis* sp. on *Boehmeria siamensis*, Urticaceae

Mycelium hypophyllus, white, thin to thick patches, hyaline; *appressoria* variable in morphology, nipple to elongate shaped, rarely lobed; *conidiophores* arising from upper part of ectophytic hyphae, erect or slightly bent, long, (117.12–)179.34–239.12(–265.96) × (8.54–)9.76–23.18(–26.84) μm, composed of 2–5 cells of variable length, position non-central; *mother cell* forming conidia singly, (41.48–)53.68–75.64(–86.62) × 4.88–6.1(–7.32) μm, straight in *foot-cells*, (34.16–)65.88–97.6(–109.8) × 4.88–7.32 μm, with a basal septum at (0–)7.32–21.96(–39.04) μm away from the branching point of mycelium; *conidia* clavate, non-papillate, (46.36–)58.56–74.42(–82.96) × 14.64–25.62(–29.28) μm, hyaline without conspicuous fibrosin-bodies and *conidial germination* produced germ tubes on the apically side or at the end of spore, lobed appressorium, formed *Ovulariopsis* type.

Chasmothecia scattered to gregarious, (150–)160–180(–190) μm in diam, brown-blackish; *appendages* 4–8 in number, acicular with bulbous basal swelling, (135–)220–310(–335) × (35–)40–50 μm, apex subacute or subobtuse, hyaline; *Chasmothecia* proposed in immature stage; *asci* and *ascospores* can not observed; *penicillate cells* not clear to observation.

Specimens examined: on leaves of *Boehmeria siamensis* CMU-02–10

Note: This is first report of powdery mildew fungi on *Boehmeria siamensis* in Thailand and in the world. Based on teleomorphic features mentioned above, this fungus can be identified as genus *Phyllactinia* sp. which having acicular appendage with bulbous swelling at the base as a typical character for *Phyllactinia* teleomorph including its anamorphic features showed identical with *Ovulariopsis* that is the anamorphic state (Braun, 1987; Takamatsu *et al.*, 2008; Braun and Cook, 2012). However, molecular analysis should be used for identification in this species.

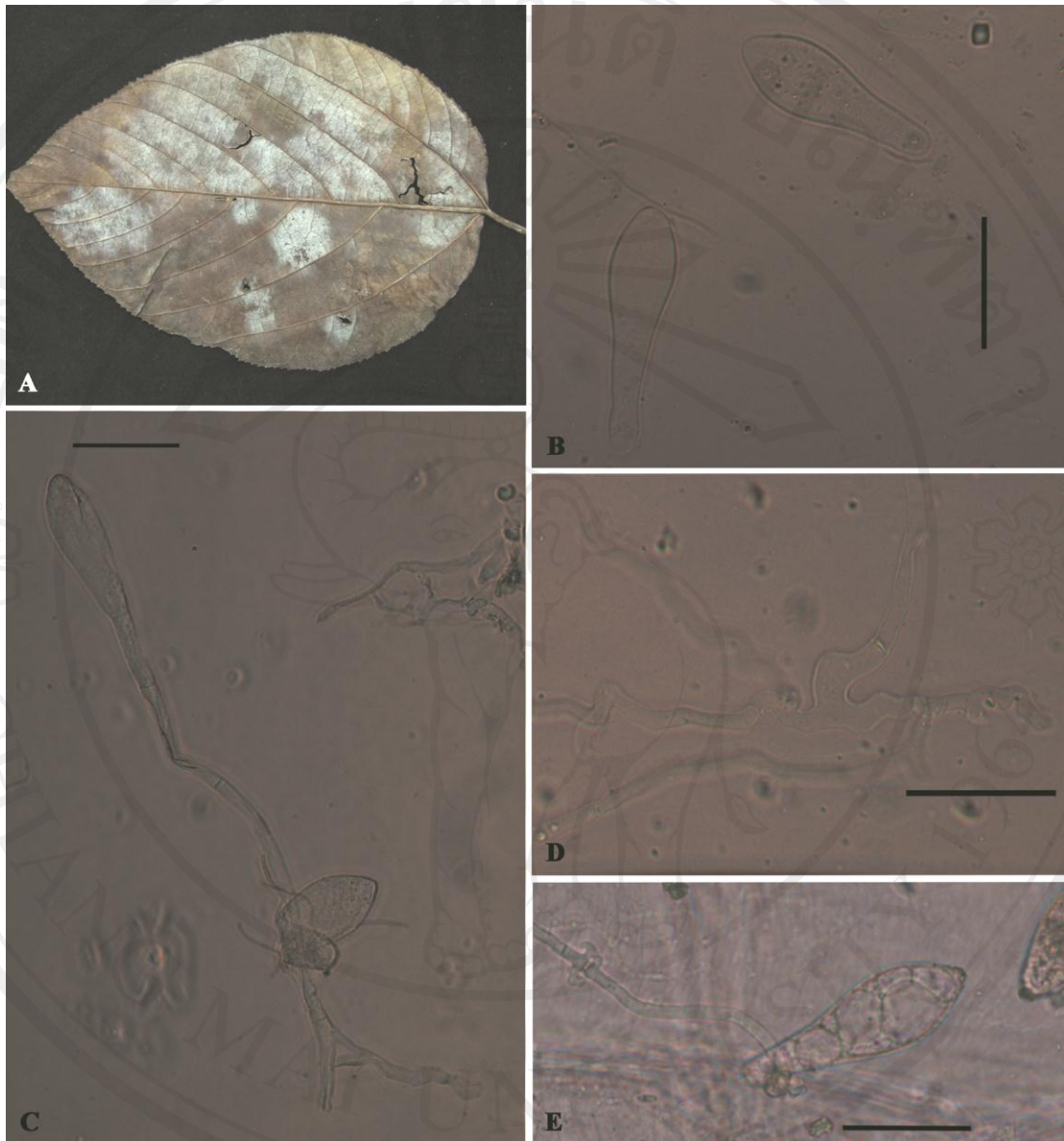


Figure 51 *Ovulariopsis* sp. on leaves of *Boehmeria siamensis*; (A) mycelia colonized on lower side of leaf (B) conidia (C) conidiophores and conidia (D) mother cell and (E) conidial germination. (Bar 30 μ m)

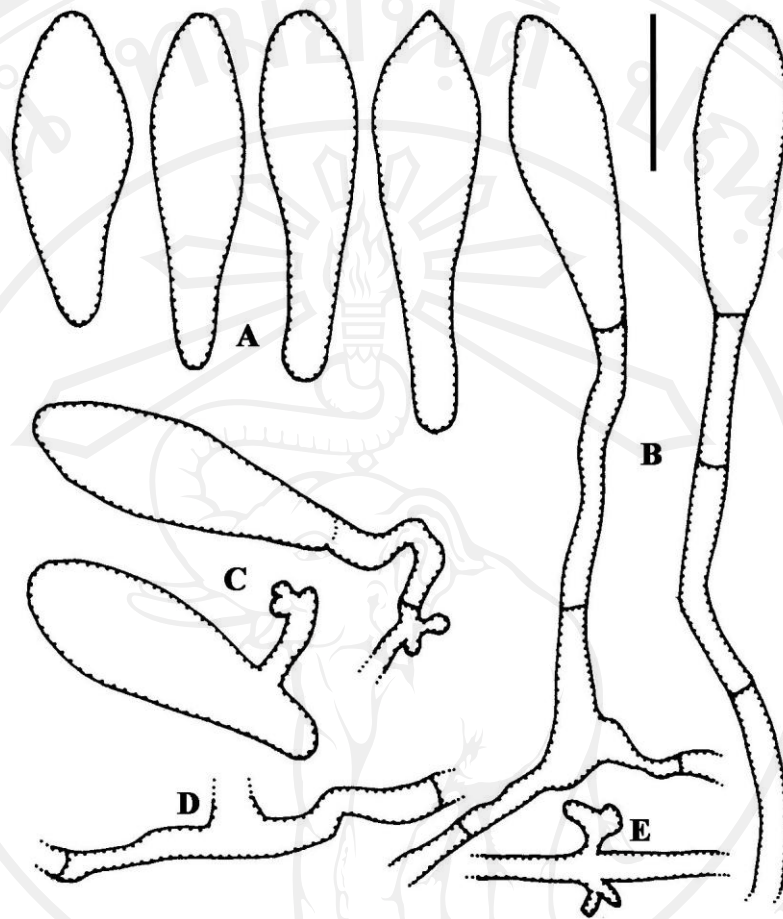


Figure 52 Illustration of *Ovulariopsis* sp. on leaves of *Boehmeria siamensis*; (A) conidia (B) conidiophores and conidia (C) conidia with germ tubes of *Ovulariopsis* pattern (D) mother cell and (E) mycelia with appressoria. (Bar 30 μm)



Figure 53 *Phyllactinia* sp. on leaves of *Boehmeria siamensis*; (A) chasmothecia scattered on the lower surface of leaves and (B) chasmothecia. (Bar 50 μm in B).

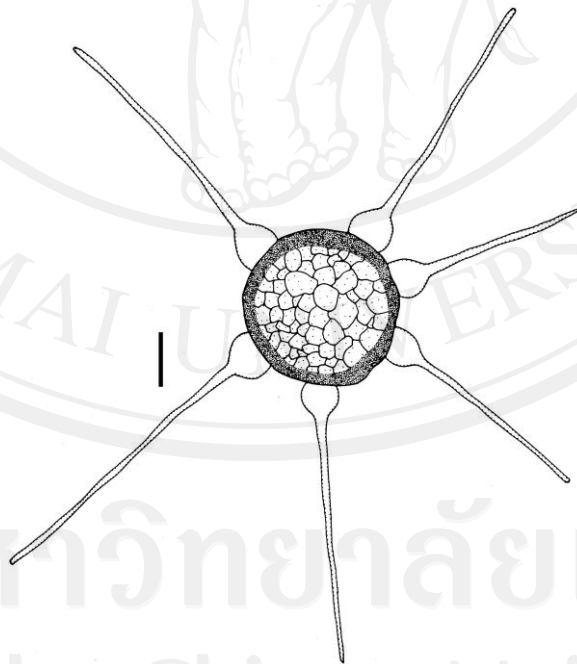


Figure 54 Illustration of *Phyllactinia* sp. on leaves of *Boehmeria siamensis*. (Bar 50 μm in A)

2.3 *Ovulariopsis* sp. on *Broussonetia papyrifera*, Moraceae

Mycelium hypophyllus, white, thin to dense patches or colonies covering the whole lower leaf surface, hyaline; *appressoria* slightly nipple to nipple-shaped; *conidiophores* arising from upper part of ectophytic hyphae, erect or slightly bent, long, (221–)260.8–504(–676) × (12.3–)20–27(–34) μm; *mother cell* forming conidia singly, (62–)74–123(–148) × 5–7 μm; straight in *foot-cells*, (34–)39–117(–169) × 6.5–9(–13) μm, with a basal septum upward from the branching point of mycelium; *conidia* clavate to broadly ellipsoid-ovoid, non-papillate, (50.02–)58.56–76.86(–82.96) × (17.08–)19.52–26.84(–29.28) μm, hyaline without conspicuous fibrosin-bodies and *conidial germination* formed *Ovulariopsis* type.

Specimens examined: on leaves of *Broussonetia papyrifera* MUMH3339

Note: *Broussonetia kaempferi*, *Broussonetia kazinoki* and *Broussonetia papyrifera* have been reported to be infected with *Phyllactinia moricola* (Amino, 1986). Shin (2000) reported *Phyllactinia moricola* on *Broussonetia kazinoki* that found both of anamorphic and teleomorphic state in Korea. And then, Braun (1987) proposed the powdery mildew on *Broussonetia* spp. and *Ficus tikoua* to be new species as *Phyllactinia broussonetiae-kaempferi* in Asia (China, including Taiwan, Japan). In this study, we found and demonstrated the anamorphic features of this genus. Furthermore, the present phylogenetic analysis based on ITS and 28S rDNA revealed that *Ovulariopsis* sp. on *Broussonetia papyrifera* from Thailand cluster together with *Phyllactinia guttata* on *Morus* and *Phyllactinia broussonetiae-kaempferi*. Therefore, *Ovulariopsis* sp. on *Broussonetia papyrifera* from Thailand showed closely relation with *Phyllactinia guttata* on *Morus* and *Phyllactinia broussonetiae-kaempferi*, but was identical with neither the fungi. So, some sequences of *Ovulariopsis* sp. on *Broussonetia papyrifera* need more to confirm the result.

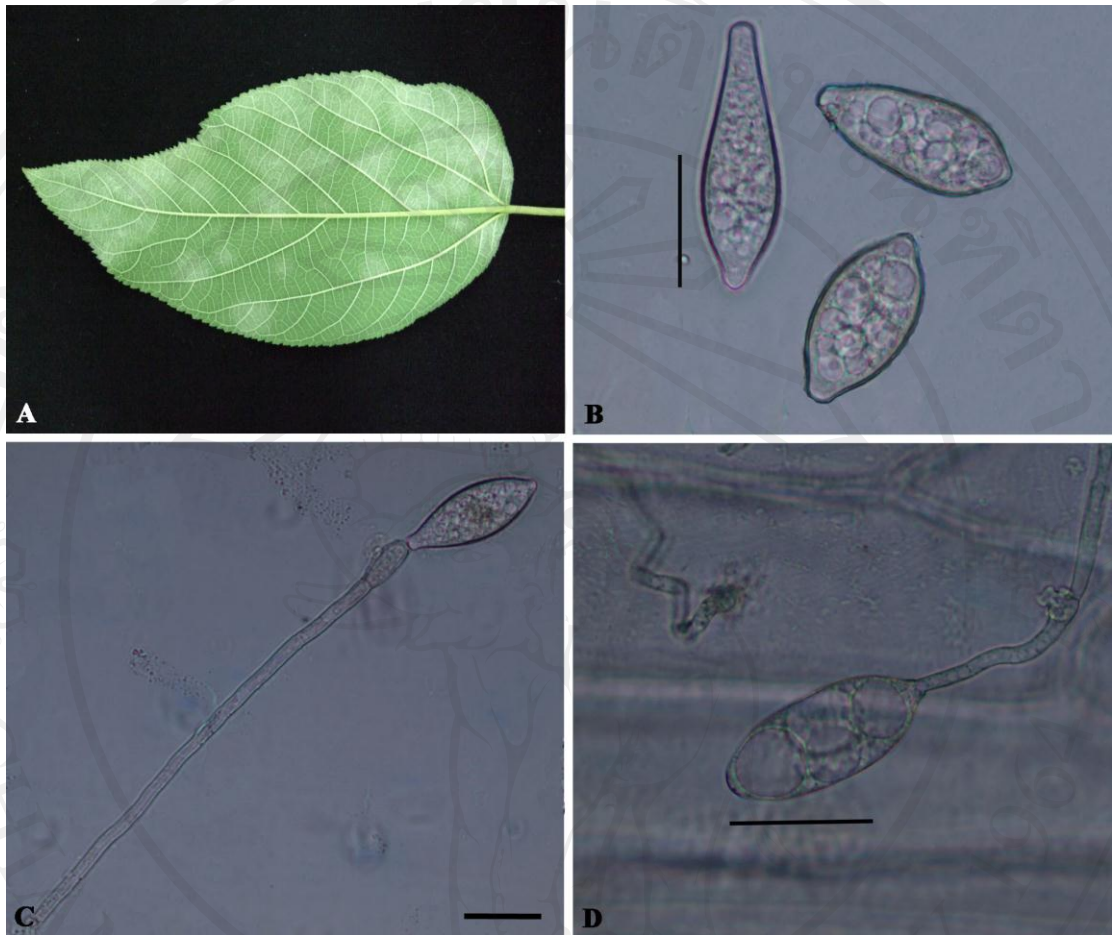


Figure 55 *Ovulariopsis* sp. on leaves of *Broussonetia papyrifera*; (A) mycelia colonized on lower side of leaf (B) conidia (C) conidiophores and conidia and (D) conidial germination. (Bar 30 μm)

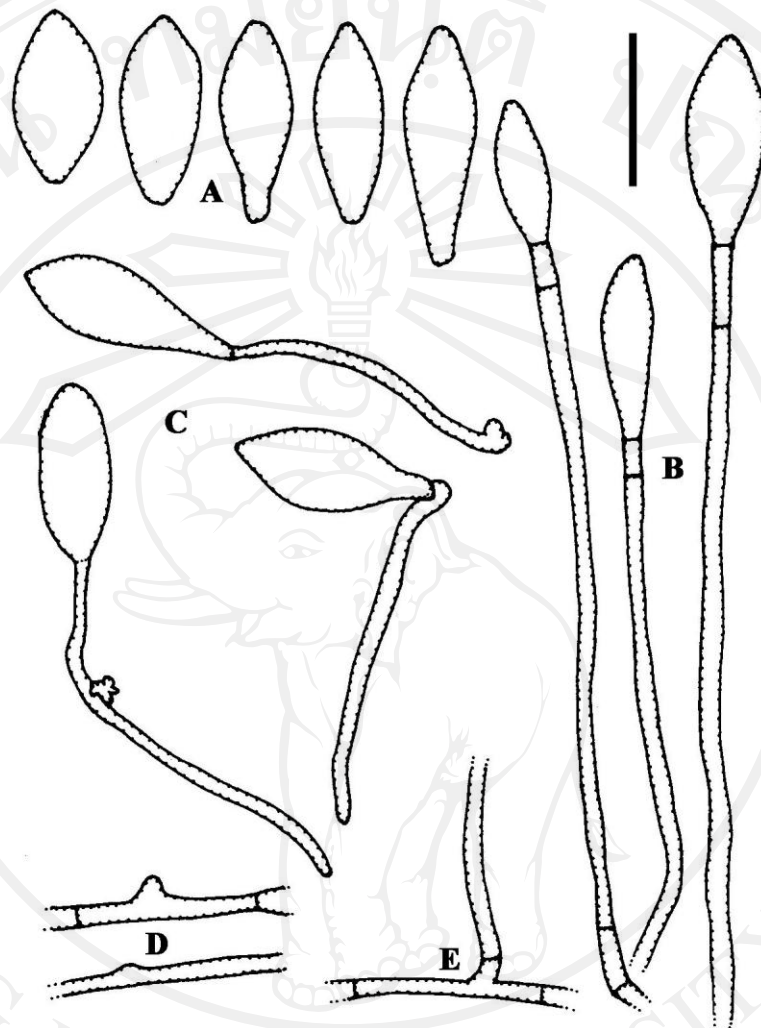


Figure 56 Illustration of *Ovulariopsis* sp. on leaves of *Broussonetia papyrifera*; (A) conidia (B) conidiophores and conidia (C) conidia with germ tubes of *Ovulariopsis* pattern (D) mycelia with appressoria and (E) mother cell. (Bar 30 μ m)

2.4 *Ovulariopsis* sp. on *Cassia fistula*, Caesalpinaceae (Leguminosae)

Mycelium hypophyllous, white, thin to dense, hyaline; *hyphal appressoria* nipple-shaped, rarely lobed to elongated; *conidiophores* arising from ectophytic hyphae, on upper surface of mother cells, position not central, rarely central, erect, straight or slightly bent, (41–)86–173(–200) × (7–)10–15(–17) μm; basal septum (2.44–)5–17(–22) μm displaced from the branching point of the mycelium; *mother cells* forming conidia singly, (24–)31–80(–89) × 4–6 μm; *foot-cells* straight with a basal septum near branching point of mycelium up to away from it, (28–)44–100(–151) × 3–6 μm; *conidia* cylindrical-ellipsoid, (32–)38–50(–54) × (10–)13–17(–20) μm, hyaline without conspicuous fibrosin-bodies, produced solitary on conidiophores; *conidial germination* germinate at the ends, long branch, sometime rarely lobed, formed *Ovulariopsis* type.

Chasmothecia scattered to gregarious, (126–)163–198(–210) μm, brown-blackish; *appendages* 5–13 in number, acicular with bulbous basal swelling, (67–)129–207(–305) × (20–)27–32(–34) μm, apex subacute or subobtuse, hyaline; *penicillate cells* in the upper part; *asci* numerous, sessile, (43–)49–63(–84) × (25–)27–32(–40) μm, 2-spored; *ascospores* ellipsoid-ovoid, rarely subglobose, (21–)24–40(–46) × (10–)13–16(–20) μm.

Specimens examined: on leaves of *Cassia fistula* MUMH5084, 5088, 5093, 5094, 5107

Note: Powdery mildew fungus on *Cassia fistula* was first described by Paul and Thakur (2006) in India as a new variety *P. bauhiniae* var. *cassia*, and later revised as *P. cassiae-fistulae* by Braun and Paul (2009). Kirschner and Chen (2008) demonstrated first record of this species on *Cassia fistula* in Taiwan (without teleomorphic stage) and reported detailed morphological characteristics of anamorphic stage. Anamorph of this fungus has a unique characteristic that is conspicuously distinct from all other species of *Phyllactinia*, but produced *Phyllactinia* teleomorph. Morphological observations showed conidiophore shorter than other *Ovulariopsis* species anamorph of *Phyllactinia* and showed production of cylindrical-ellipsoid conidia. This anamorphic feature is consistent with typical characteristic of *Oidium*, not *Ovulariopsis*. The present study, morphological features mentioned above has identical with powdery mildew on *Cassia fistula* in previously study (Braun, 1987). In this study, molecular analysis combined with morphological analysis was performed to clarify taxonomy of *Phyllactinia cassiae-fistulae*. The result indicated that *P. cassiae-fistulae* sequences on *C. fistula* formed an independent clade at the basal part of *Phyllactinia/Leveillula* clade with bootstrap support of 100%. Therefore, molecular phylogenetic analysis based on the 28S rDNA sequences supported the unique anamorphic morphology of *P. cassiae-fistulae*.

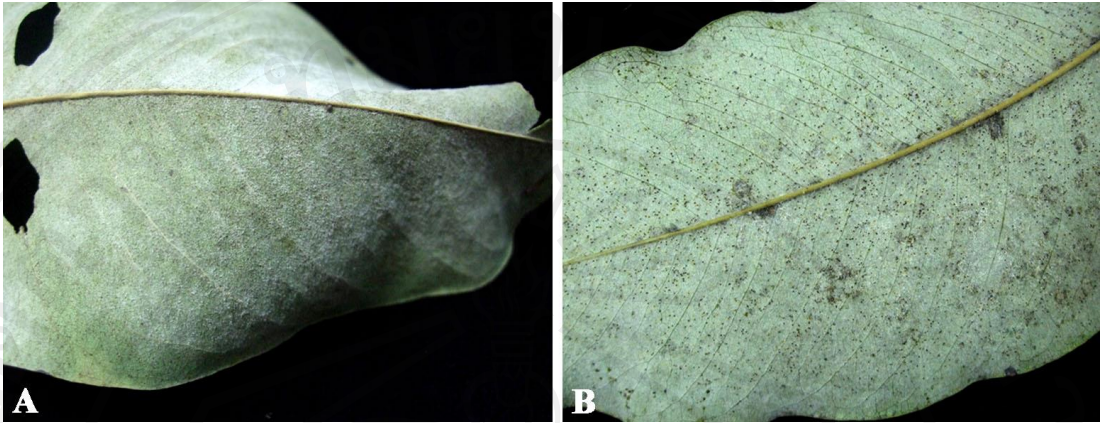


Figure 57 *Phyllactinia cassiae-fistulae* on *Cassia fistula* leaves; (A) white hypophyllous mycelia and (B) chasmothecia scattered on lower leaves.



Figure 58 Chasmothecia on the lower side of *Cassia fistula* leaves.

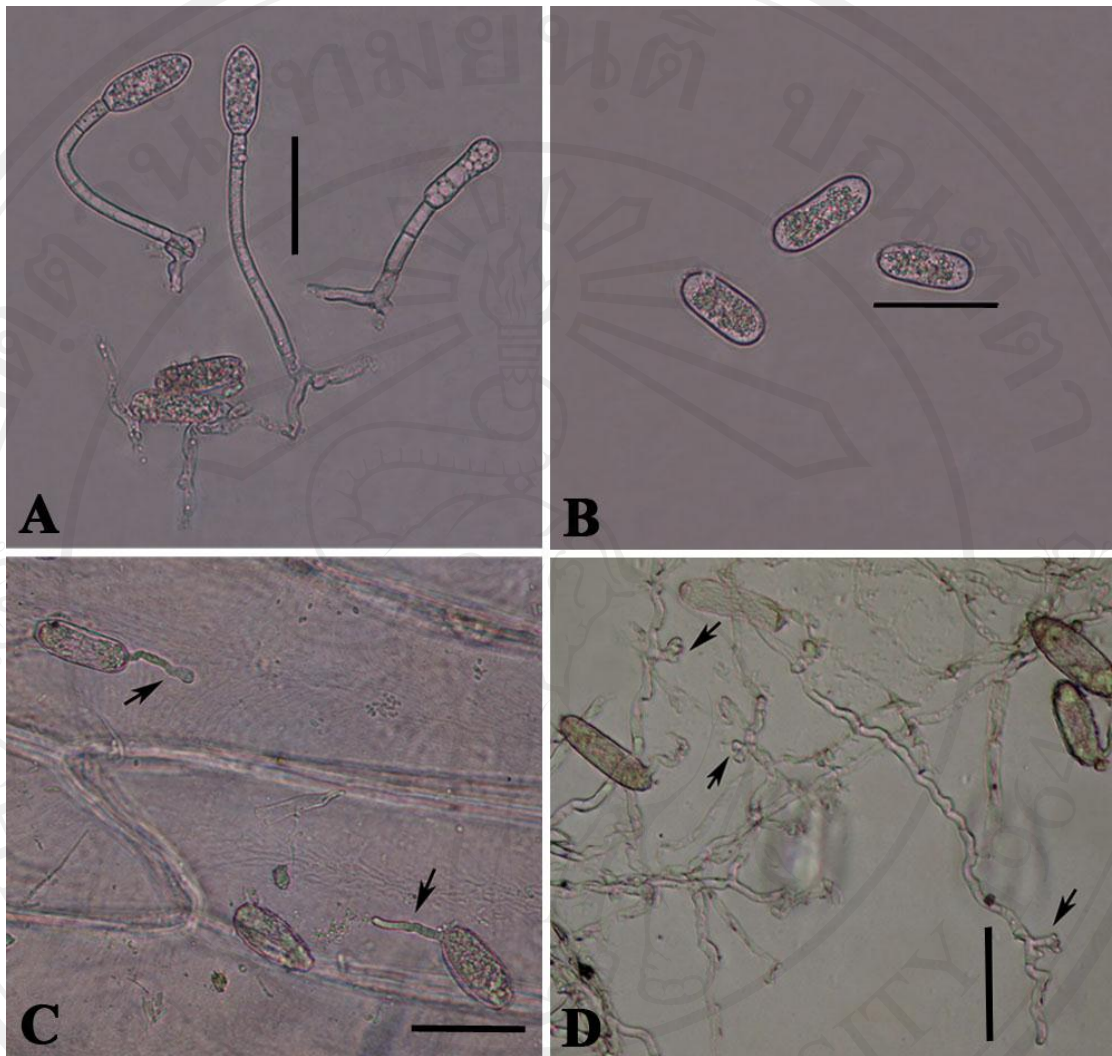


Figure 59 *Ovulariopsis* anamorph of *Phyllactinia cassiae-fistulae*; (A) conidiophores and conidia (B) conidia (C) conidial germination on onion epidermal cell and (D) mycelia with appressorium. (Bar 30 µm)

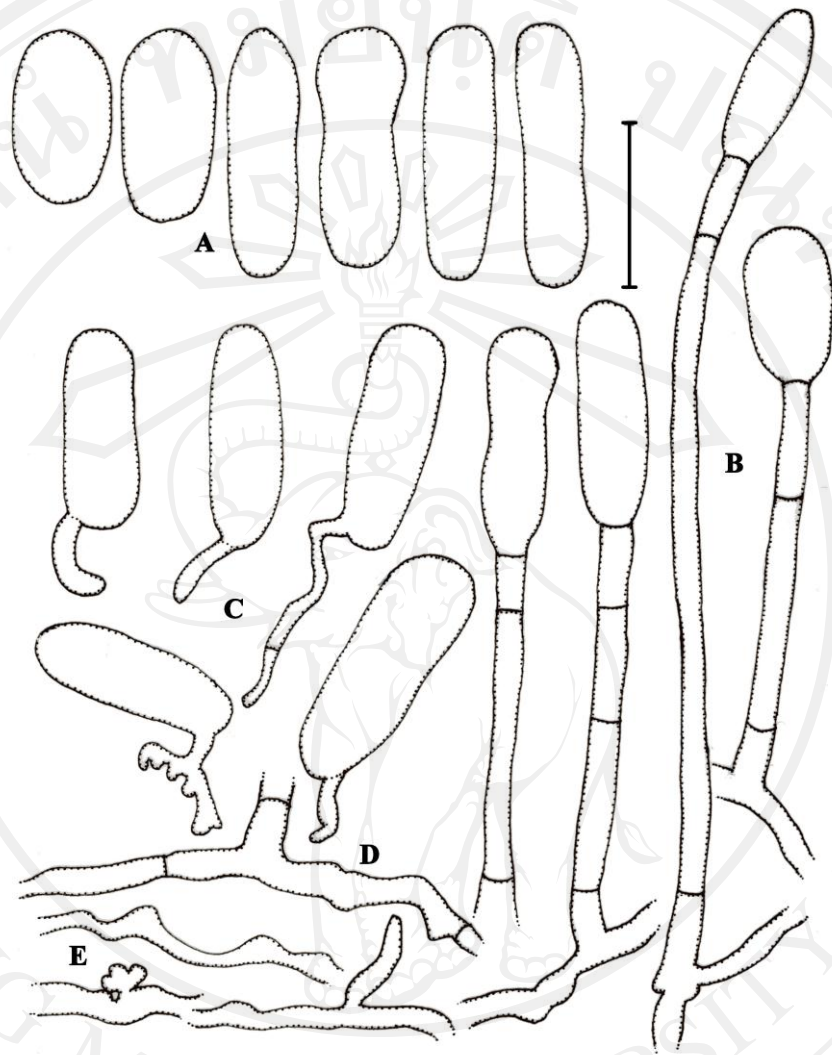


Figure 60 Illustration of *Ovulariopsis* anamorph of *Phyllactinia cassiae-fistulae* on *Cassia fistula*; (A) conidia (B) conidiophores and conidia (C) conidia with germ tubes of *Ovulariopsis* type (D) mother cell leading to conidiophore and (E) mycelia with appressorium. (Bar 30 μm)

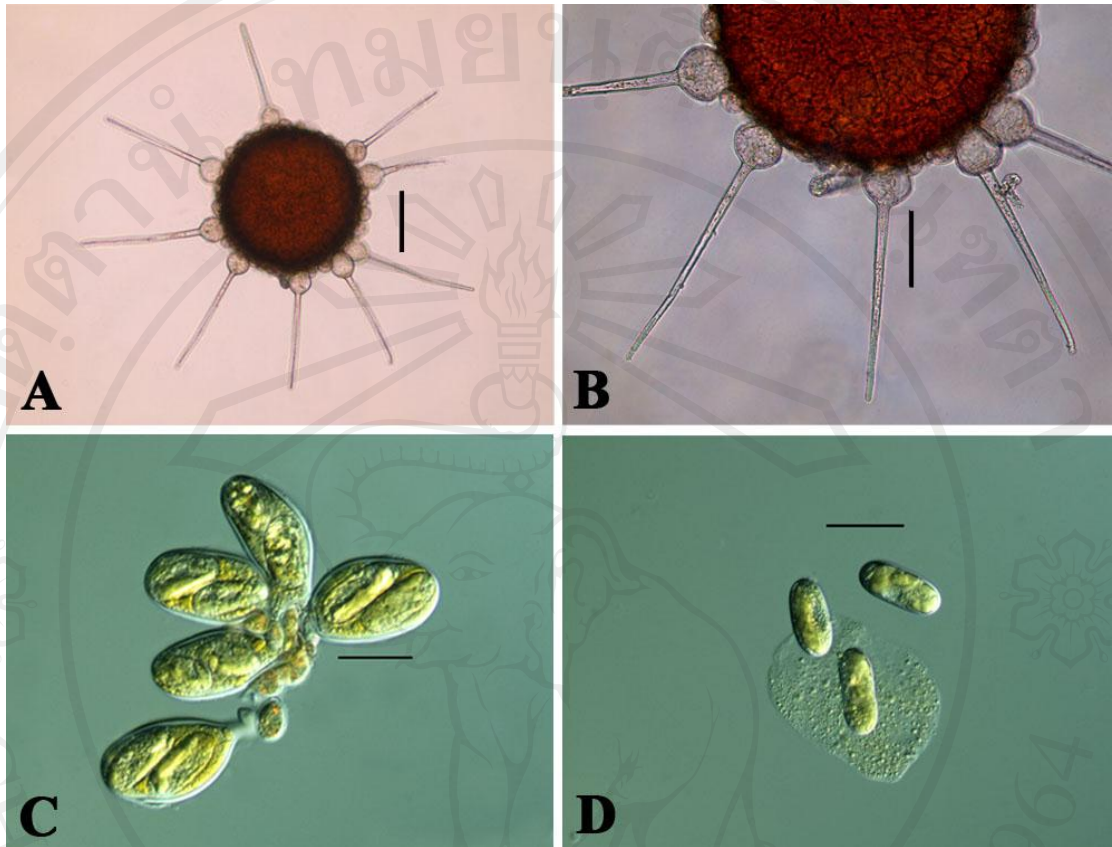


Figure 61 *Phyllactinia cassiae-fistulae* on leaves of *Cassia fistula*; (A) chasmothecium (B) acicular with bulbous basal swelling appendages (C) asci and ascospores (2 ascospores/ascus) and (D) ascospore. (Bar 50 μm in A, Bar 30 μm in B and Bar 25 μm in C & D)

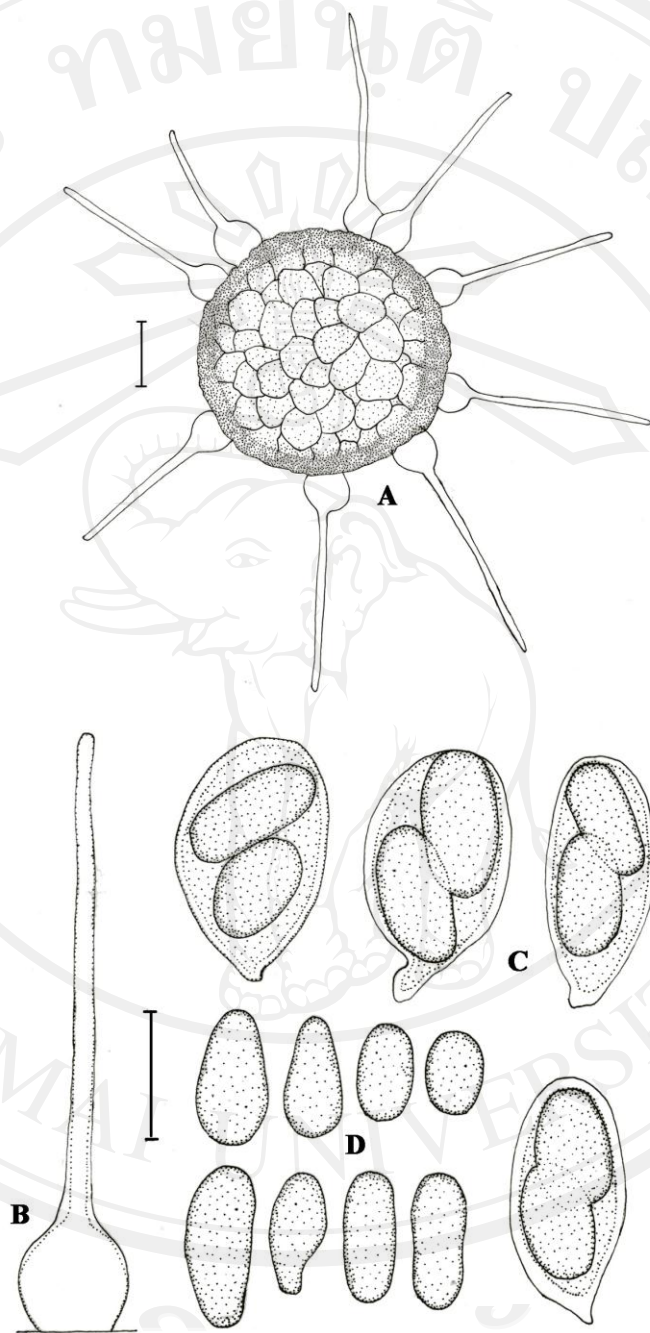


Figure 62 Illustration of *Phyllactinia cassiae-fistulae* on leaves of *Cassia fistula*; (A) chasmothecium (B) acicular appendage with bulbous base (C) asci (D) ascospores. (Bar 50 μm in A and Bar 30 μm in B-D)

2.5 *Ovulariopsis* sp. on *Dalbergia cana*, Caesalpiniaceae

Mycelium hypophyllous, white, thin to dense, hyaline; *appressoria* nipple-shaped, rarely lobed to elongated; *conidiophores* arising from ectophytic hyphae, on upper surface of mother cells, position not central, rarely central, long, (175.68–)180.56–280.6(–303.78) × 7.32–19.52 μm, basal septum (2.44–)4.88–14.64(–21.96) μm displaced from the branching point of the mycelium; *mother cells* forming conidia singly, (30.5–)46.36–74.42(–100.04) × 3.66–6.1 μm; *foot-cells* sinuous to twisted, with a basal septum near branching point of mycelium up to away from it, (43.92–)58.56–170.8(–195.2) × 4.88–6.1 μm; *conidia* variable, dimorphic, *primary conidia*, lanceolate, attenuated towards the apex, (62.22–)68.32–80.52(–82.96) × (13.42–)15.86–20.74(–21.96) μm, *secondary conidia* clavate, (58.56–)63.44–78.08(–82.96) × (15.86–)17.08–21.96(–24.4) μm, hyaline without conspicuous fibrosin-bodies and *conidial germination* produced germ tubes on the apically side or at the end of spore, lobed appressorium, formed *Ovulariopsis* type.

Chasmothecia scattered to subgregarious, (145–)150–182.5(–185) μm diameter, brown-blackish and yellowish in young chasmothecia; *appendages* 4–12 in number, acicular with bulbous basal swelling, (57.34–)107.36–226.92(–273.28) × (23.18–)24.4–32.94(–39.04) μm, apex subobtuse, hyaline; *Chasmothecia* proposed in immature stage; *asci* and *ascospores* can not observed.

Specimens examined: on leaves of *Dalbergia cana* CMU-BG9

Note: This is first report of powdery mildew fungi on *Dalbergia cana* in Thailand and in the world. Based on teleomorphic features mentioned above, this fungus can be identified as genus *Phyllactinia* sp. which having acicular appendage with bulbous swelling at the base as a typical character for *Phyllactinia* teleomorph (Braun, 1987; Takamatsu *et al.*, 2008; Braun and Cook, 2012). The present anamorph of *Phyllactinia* sp. on *Dalbergia cana* differed from the general features by having twisted at the base of foot-cells; dimorphic conidia. As the description, *Phyllactinia* sp. on *Dalbergia cana* is morphologically most similar to *Phyllactinia dalbergiae*. However, molecular analysis should be used for identification in this species.

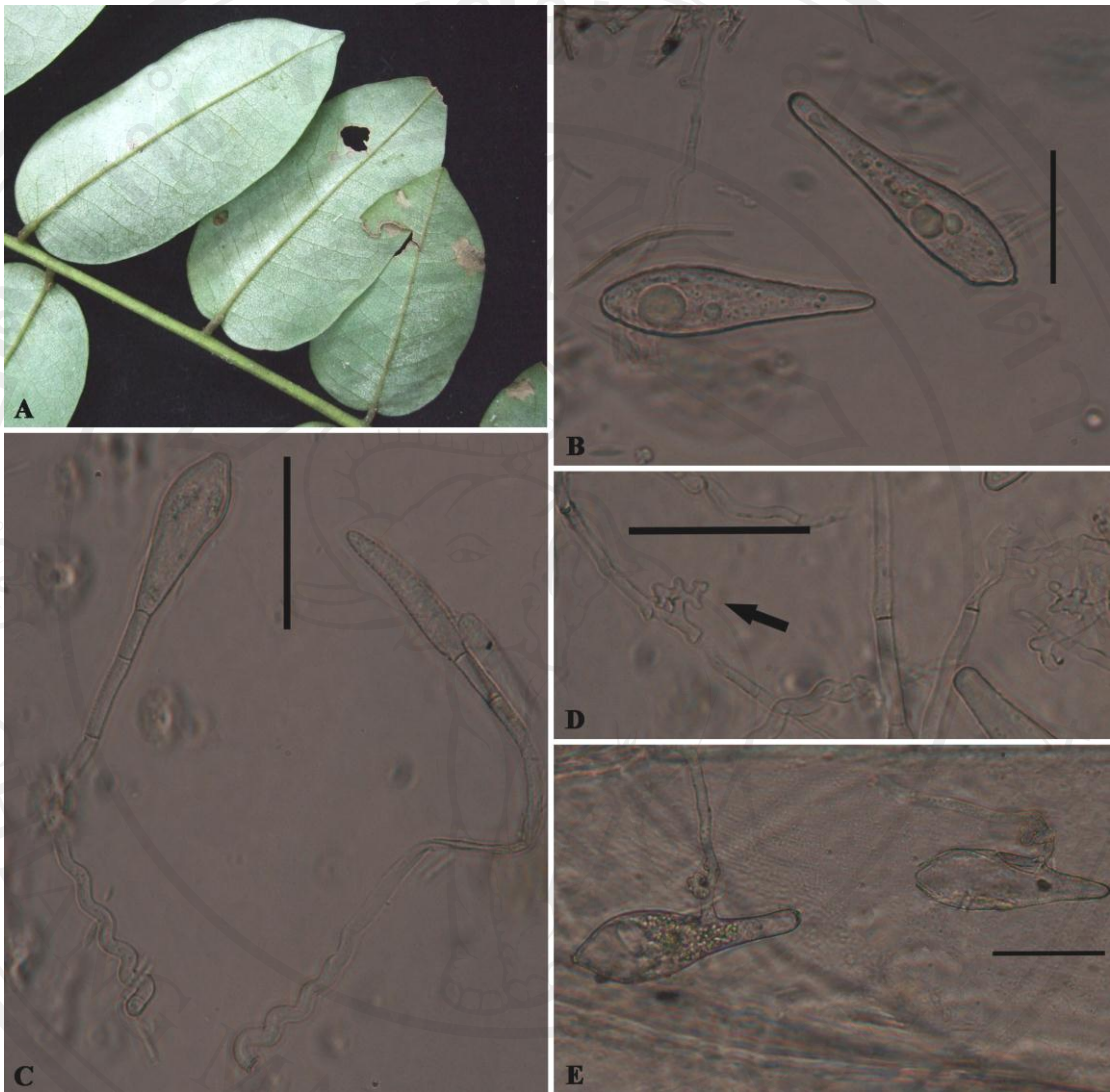


Figure 63 *Ovulariopsis* sp. on leaves of *Dalbergia cana*; (A) mycelia colonized on lower side of leaves (B) conidia (C) conidiophores and conidia (D) mycelia with appressoria (E) conidial germination. (Bar 30 μ m)

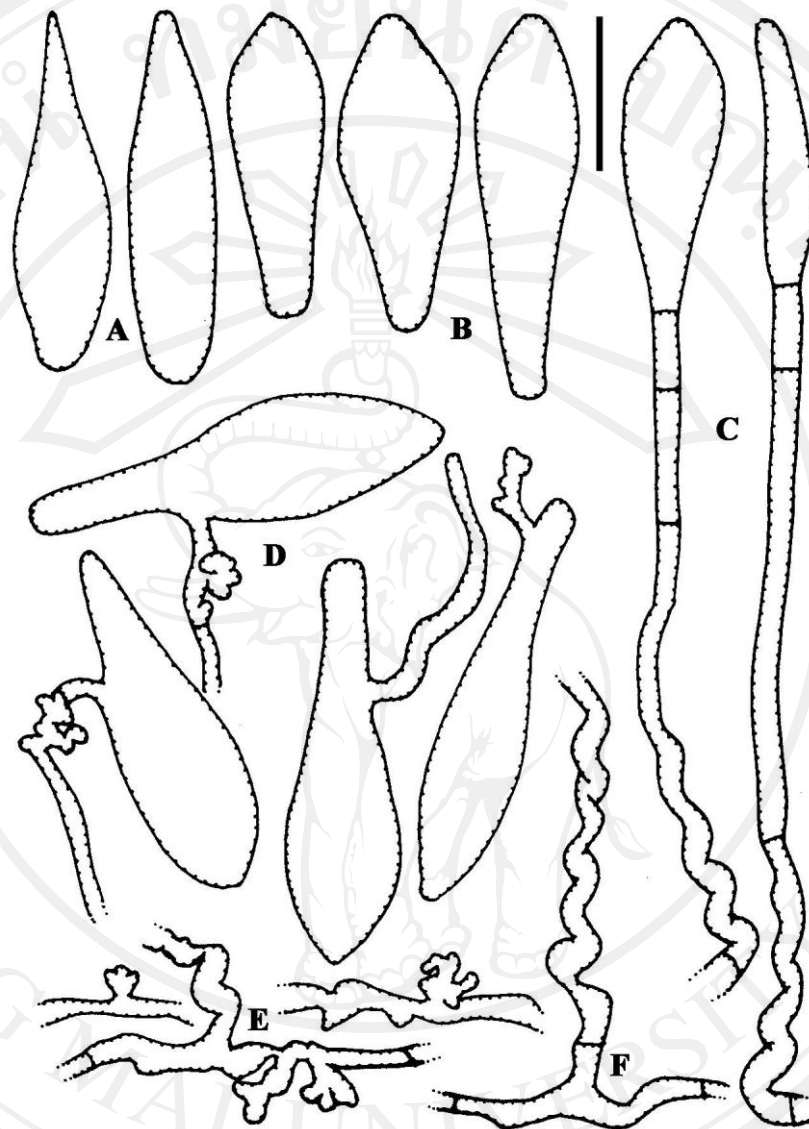


Figure 64 Illustration of *Ovulariopsis* sp. on leaves of *Dalbergia cana*; (A) primary conidia (B) secondary conidia (C) conidiophores and conidia (D) conidia with germ tubes of *Ovulariopsis* pattern (E) mycelia with appressoria and (F) mother cell which leading conidiophore. (Bar 30 μ m)



Figure 65 *Phyllactinia* sp. on leaves of *Dalbergia cana*; (A) symptoms on *Dalbergia cana* leaves (B) closed-up of chasmothecium under stereo microscope (C) chasmothecium and (D) acicular with bulbous basal swelling appendages. (Bar 50 μm in C and Bar 30 μm in D)

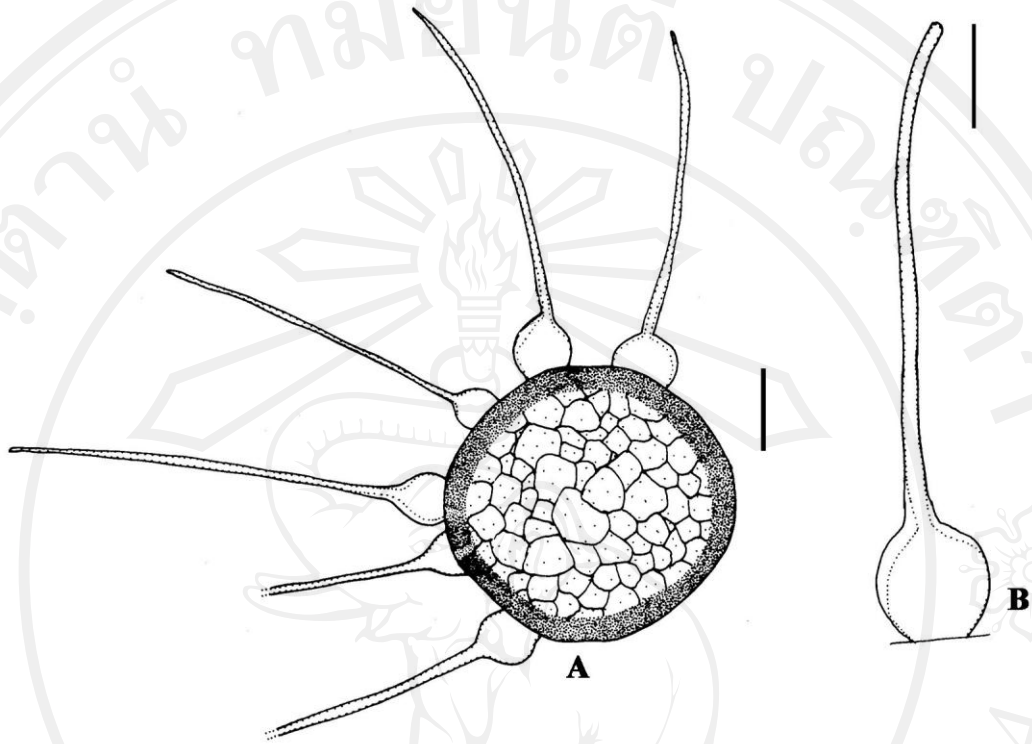


Figure 66 Illustration of *Phyllactinia* sp. on leaves of *Dalbergia cana*; (A) chasmothecium with appendages and (B) appendages. (Bar 50 μm in A and Bar 30 μm in B)

2.6 *Ovulariopsis* sp. on *Dalbergia lanceolaria*, Caesalpiniaceae

Mycelium hypophyllous, white, thin to dense, hyaline; *apressoria* nipple-shaped, rarely lobed to elongated; *conidiophores* arising from ectophytic hyphae, on upper surface of mother cells, position not central, rarely central, erect or slightly bent, long and slender, (173–)208–313(–330) × (5–)6–12(–22) µm; basal septum (3–)4–9(–12) µm displaced from the branching point of the mycelium; *mother cells* forming conidia singly, (52–)65–76(–89) × (3–)4–5(–5.4) µm; *foot-cells* sinuous to twisted, with a basal septum near branching point of mycelium up to away from it, (83–)97–213(–260) × (3–)4–5(–6) µm; *conidia* lanceolate or clavate, (35–)67–81(–89) × (12–)13–19(–24) µm, hyaline without conspicuous fibrosin bodies, conidia formed singly (solitary) and *conidial germination* produced at the end of spore, moderately long, sometime rarely lobed, formed *Ovulariopsis* type.

Chasmothecia scattered to subgregarious, (173–)198–215(–254) µm in diameter, brown-blackish and yellowish in young chasmothecia; *appendages* 5–9 in number, acicular with bulbous basal swelling, (133–)173–282(–307) × (29–)32–40(–44) µm, apex subobtuse, hyaline; *penicillate cells* in the upper part; *asci* numerous, sessile, (48–)54–72(–82) × (26–)29–38(–42) µm, 2-spored; *ascospores* ellipsoid-ovoid, rarely subglobose, (28–)33–36(–46) × (14–)17–22(–26) µm.

Specimens examined: on leaves of *Dalbergia lanceolaria*, MUMH5087

Note: *Dalbergia* spp., a genus of woody plant has been reported the powdery mildew disease caused by *Phyllactinia dalbergiae* in India and Pakistan (Pawar and Patil, 2011; Sharma and Khare, 1995; Shah *et al.*, 2010). *Phyllactinia dalbergiae* has been reported in Indian mycologist for the first time according to Pirozynski in 1965. The host plant, *Derbergia sissoo* is infected by this fungus (Braun, 1987; Paul and Thakur, 2006; Pirozynski, 1965). Furthermore, Braun (1987) has been reported that *P. dalbergiae* also caused powdery mildew disease on *Dalbergia lanceolaria*. Recently, Braun and Cook (2012) reported *Phyllactinia dalbergiae* on *Dalbergia* spp. including *Dalbergia lanceolaria*. The present study, morphological features mentioned above has identical with powdery mildew on *Dalbergia lanceolaria* in previous study. Anamorphic stage of *P. dalbergiae* has the unique conidiophore foot-cells that having sinuous to twisted formed as a typical of conidiophore foot-cells in genus *Streptopodium*. Furthermore, molecular analysis was performed to clarify taxonomy of *Phyllactinia dalbergiae*. The result indicated that *P. dalbergiae* formed an independent clade at the basal part of *Phyllactinia/Leveillula* clade with bootstrap support of 100%. Therefore, molecular phylogenetic analysis supported the unique anamorphic morphology of *P. dalbergiae*.



Figure 67 *Phyllactinia dalbergiae* on *Dalbergia lanceolaria* leaves; (A) symptoms appeared on the lower surface of leaves and (B) close-up of chasmothecia scattered on the lower surface of leaves.



Figure 68 *Ovulariopsis* anamorph of *Phyllactinia dalbergiae*; (A) conidiophores with foot-cell twisted and conidia (B) conidia (C) mycelia with appressoria and (D) conidial germination. (Bar 50 μm in A, Bar 27 μm in B-D)

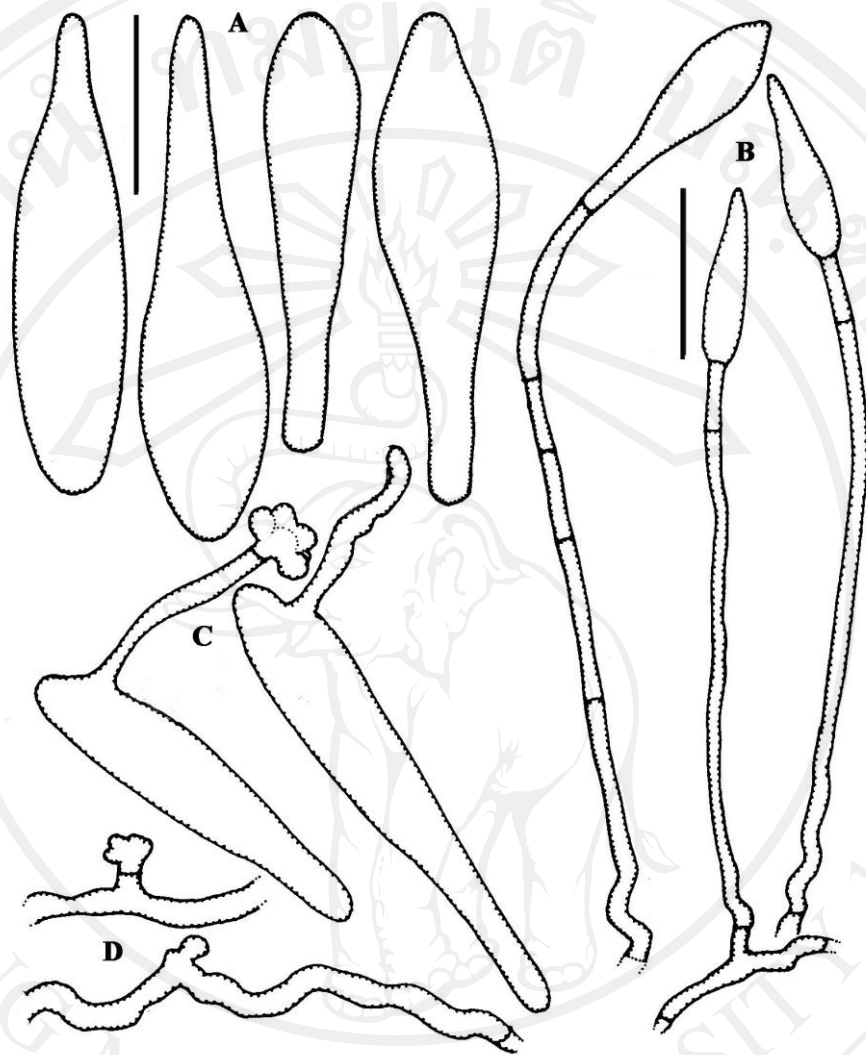


Figure 69 Illustration of *Ovulariopsis* anamorph of *Phyllactinia dalbergiae*; (A) conidia (B) conidiophores and conidia (C) conidia with germ tubes of the *Ovulariopsis* type and (D) mycelia with appressoria. (Bar 27 μm in A, C-D, Bar 50 μm in B)

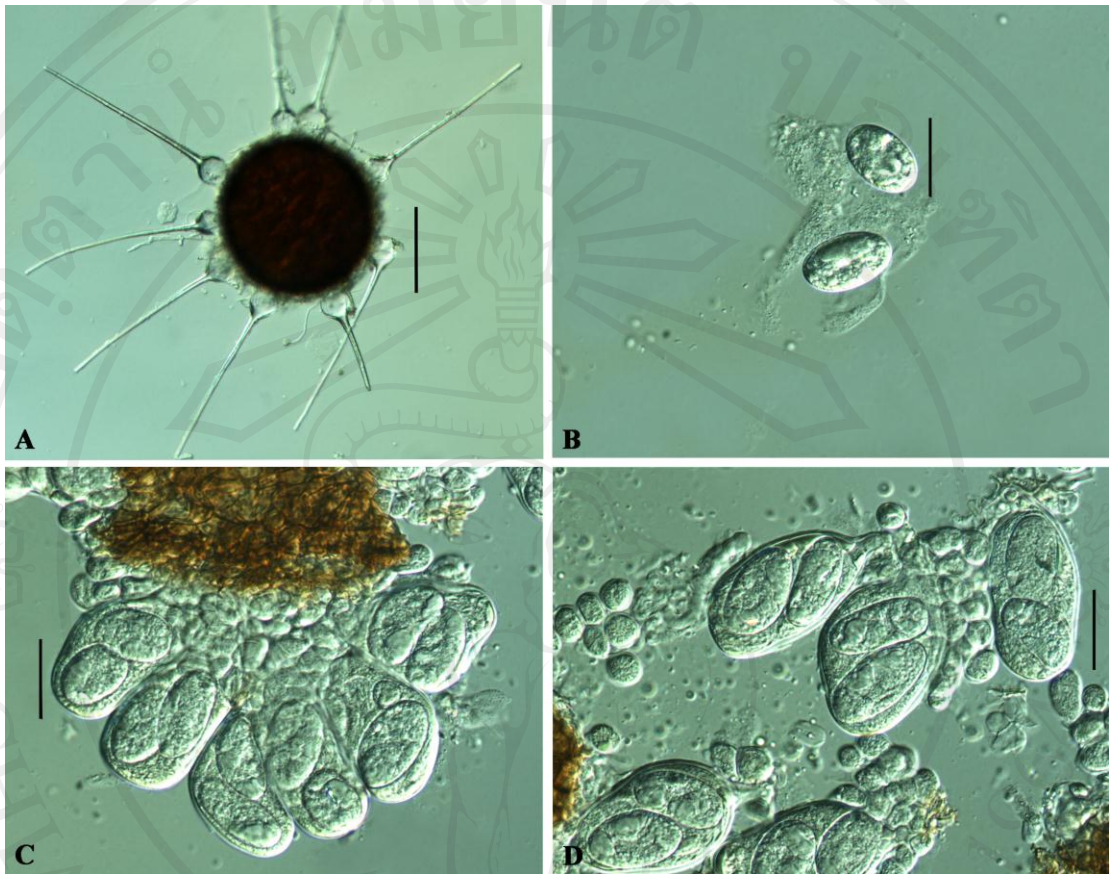


Figure 70 *Phyllactinia dalbergiae* on leaves of *Dalbergia lanceolaria*; (A) chasmothecium (B) ascospores (C) numerous asci per chasmothecium and (D) ascus with 2 ascospores. (Bar 111 μm in A, Bar 27 μm in B-D)

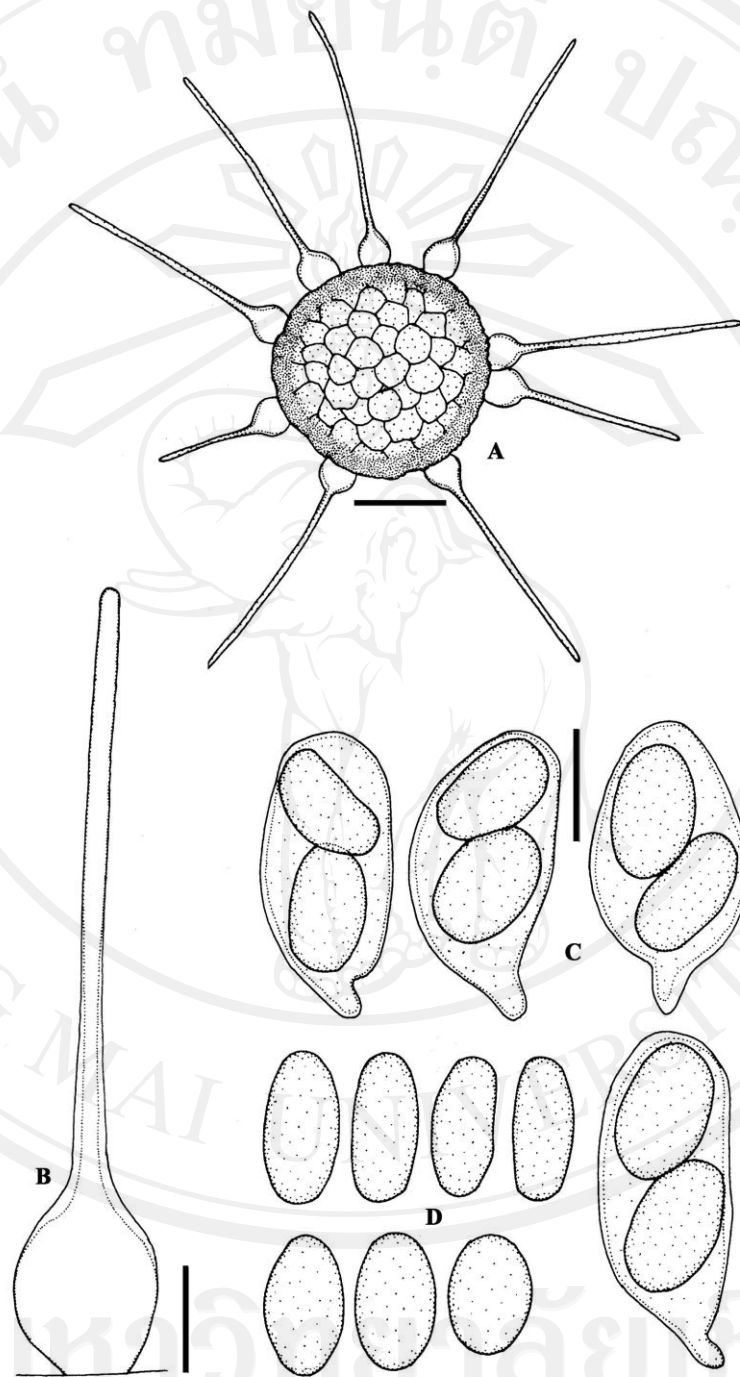


Figure 71 Illustration of *Phyllactinia dalbergiae* on leaves of *Dalbergia lanceolaria*; (A) chasmothecium (B) acicular appendage with bulbous base (C) asci and (D) ascospores. (Bar 111 μm in A, Bar 27 μm in B-D)

2.7 *Ovulariopsis* sp. on *Ehretia laevis*, Boraginaceae

Mycelium hypophyllus, white, thin to dense patches, hyaline; *appressoria* lobed or occasionally lobed-opposite; *conidiophores* arising from upper part of ectophytic hyphae, erect or slightly bent, long, (139.08–)195.2–247.66(–301.34) × (7.32–)8.54–21.96(–26.84) μm; *mother cell* forming conidia singly, (53.68–)65.88–89.06(–129.32) × 3.66–4.88(–7.32) μm; straight in *foot-cells*, (81.74–)100.04–173.24(–195.2) × 4.88–7.32 μm, with a basal septum at 12.2–25.62(–29.28) μm away from the branching point of mycelium; *conidia* clavate, non-papillate, (56.12–)63.44–81.74(–85.4) × (21.96–)23.18–28.06(–31.72) μm, hyaline without conspicuous fibrosin-bodies and *conidial germination* formed *Ovulariopsis* type. The teleomorphic state can not be found.

Specimens examined: on leaves of *Ehretia laevis* MUMH5095

Note: Braun and Cook (2012) have been reported *Phyllactinia ehretiae* on *Ehretia corylifolia*. But, this study has been found only *Ovulariopsis* anamorph of *Phyllactinia* on *Ehretia laevis*. However, molecular analysis was performed to clarify taxonomy of *Ovulariopsis* anamorph on *Ehretia laevis*. The result showed this fungus formed an independent *Phyllactinia* clade. This is the first report of *Ovulariopsis* anamorph which linked to *Phyllactinia* on *Ehretia laevis* in Thailand and in the world.

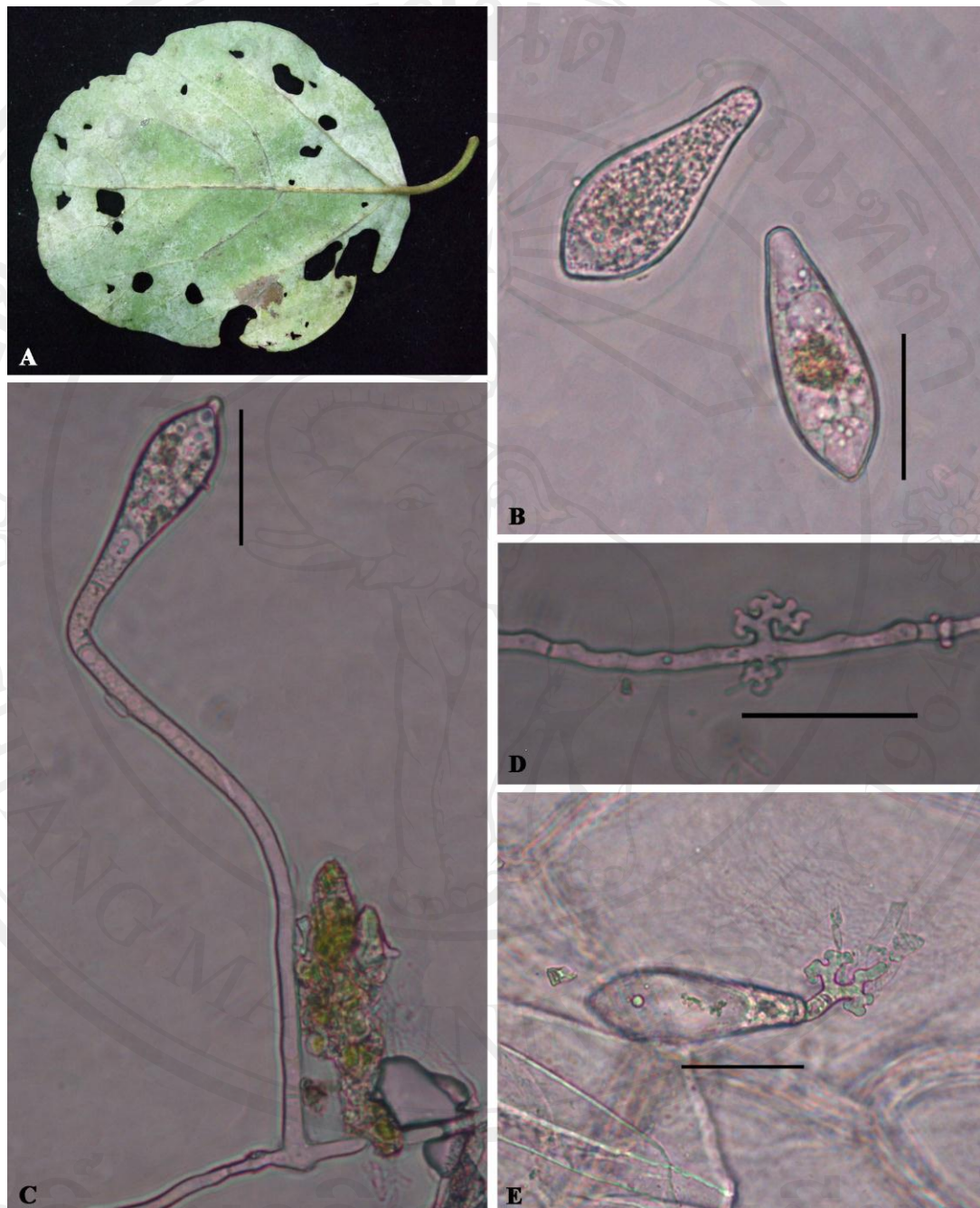


Figure 72 *Ovulariopsis* sp. on leaves of *Ehretia laevis*; (A) mycelia colonized on lower side of leaf (B) conidia (C) conidiophores and conidia (D) mycelium with appressoria and (E) conidial germination. (Bar 30 μ m)

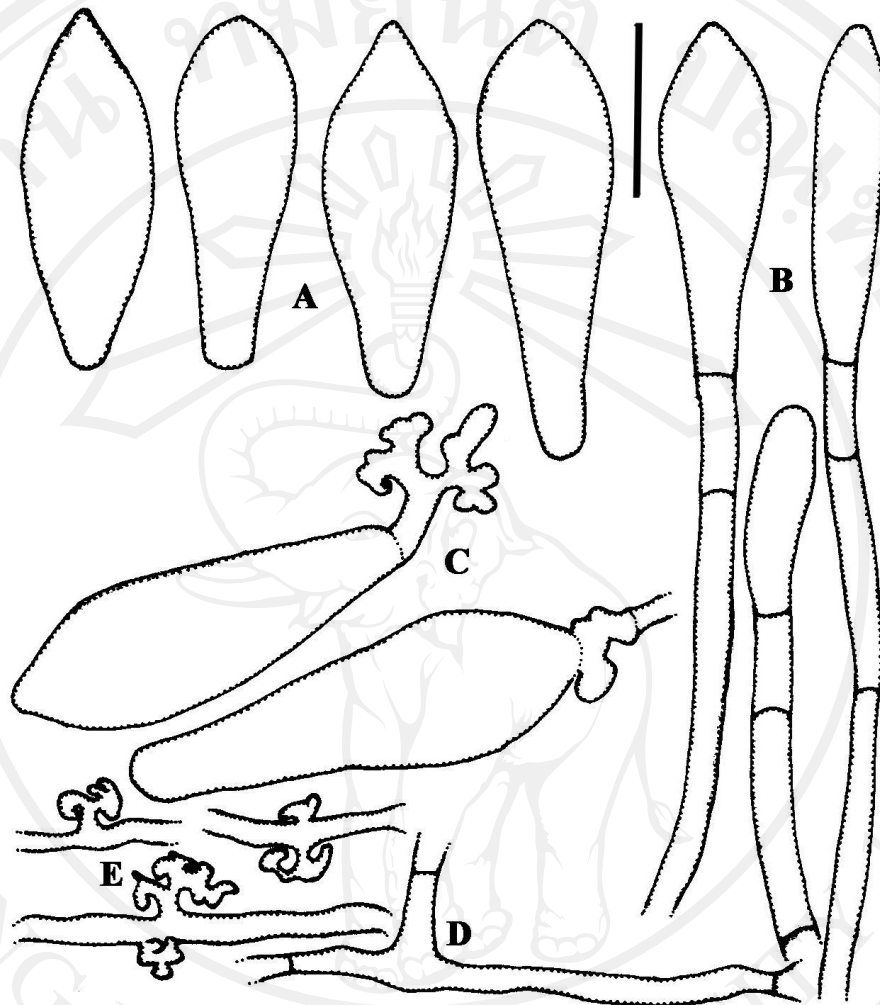


Figure 73 Illustration of *Ovulariopsis* sp. on leaves of *Ehretia laevis*, illustrated using a line drawing under a light microscope. (A) conidia (B) conidiophores and conidia (C) conidia with germ tubes of the *Ovulariopsis* type (D) mother cell leading to conidiophore and (E) mycelia with appressorium. (Bar 30 μ m)

2.8 *Ovulariopsis* sp. on *Euphorbia heterophylla*, Euphorbiaceae

Mycelium white, thin to thick patches, amphigenous, hyaline; *appressoria* variable in morphology, nipple to elongate shaped, rarely lobed; *conidiophores* arising from upper part of ectophytic hyphae, erect or slightly bent, long, (112.24–)150.06–353.8(–424.56) \times (7.32–)9.76–13.42(–19.52) μm , position non-central; *mother cell* forming conidia singly, (43.92–)51.24–97.6(–117.12) \times 3.66–6.1 μm ; straight in *foot-cells*, (56.12–)58.56–139.08(–180.56) \times 4.88–6.1 μm , with a basal septum at (1.22–)2.44–7.32(–10.98) μm away from the branching point of mycelium; *conidia* clavate, non-papillate, (46.36–)50.02–62.22(–70.76) \times (13.42–)14.64–18.3 μm , hyaline without conspicuous fibrosin-bodies and *conidial germination* produced germ tubes on the apically side or at the end of spore, lobed appressorium, formed *Ovulariopsis* type. The teleomorphic state can not be found.

Specimens examined: on leaves of *Euphorbia heterophylla* CMU38

Note: Interestingly, powdery mildew fungus in tribe Phyllactinieae on *Euphorbia heterophylla* have been recorded only *Oidiopsis* sp. in previously time (Braun, 1987; Shin, 2000; Braun and Cook, 2012). This is the first report of *Ovulariopsis* sp. on *Euphorbia heterophylla* in Thailand and in the world. However, molecular analysis should be used for identification in this species.



Figure 74 *Ovulariopsis* sp. on leaves of *Euphorbia heterophylla*; (A) mycelia colonized on both side of leaves (B) conidia (C) conidiophores and conidia (D) mycelium with appressoria and (E) conidial germination. (Bar 30 μm)

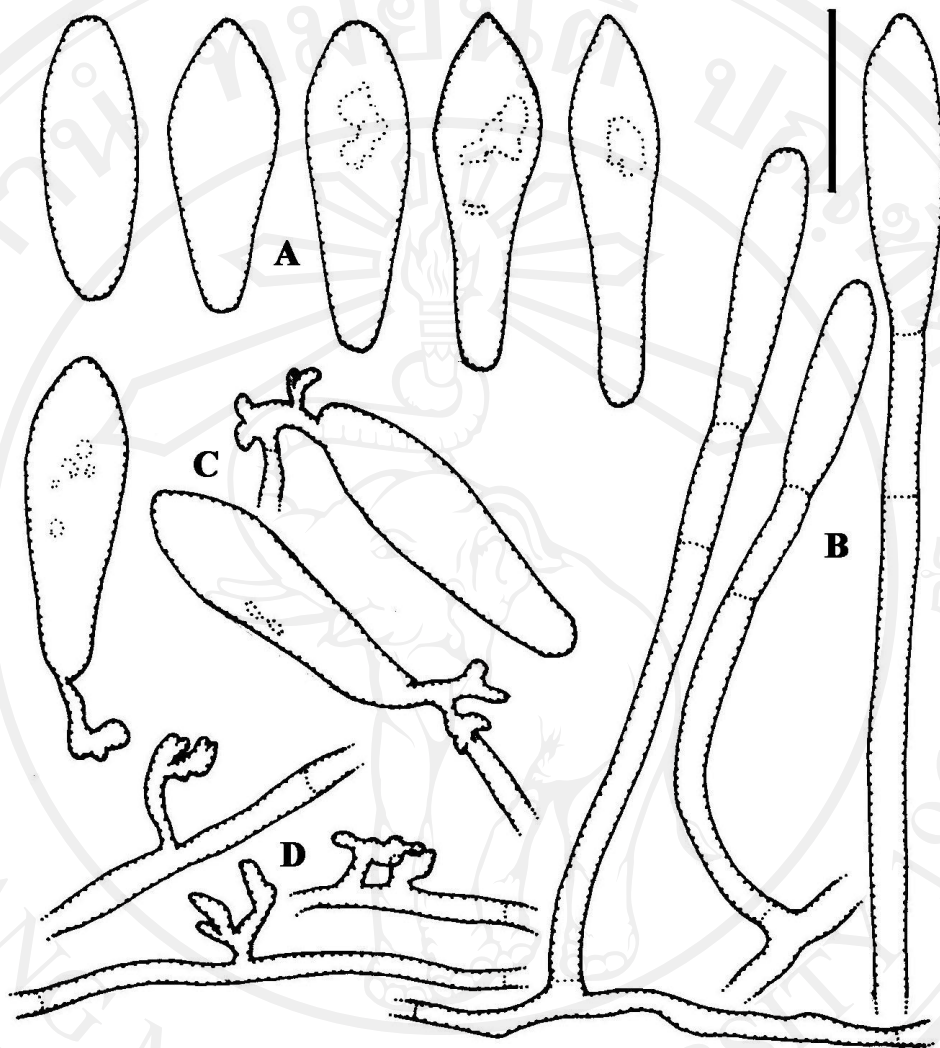


Figure 75 Illustration of *Ovulariopsis* sp. on leaves of *Euphorbia heterophylla*; (A) conidia (B) conidiophores and conidia (C) conidia with germ tubes of the *Ovulariopsis* pattern and (D) mycelia with appressoria. (Bar 30 μm)

2.9 *Ovulariopsis* sp. on *Gmelina arborea*, Verbenaceae

Mycelium hypophyllus, white, thin to thick patches, hyaline; *appressoria* variable in morphology, nipple to elongate shaped, rarely lobed; *conidiophores* arising from upper part of ectophytic hyphae, erect or slightly bent, long, (97.6–)129.32–163.48(–309.88) × (14.64–)20.74–29.4(–31.56) µm, composed of 2–5 cells of variable length, position non-central; *mother cell* forming conidia singly, (29.28–)34.16–46.36 × (2.44–)3.66–6.1 µm; straight in *foot-cells*, (14.64–)36.6–63.44(–124.44) × 2.44–4.88(–7.32) µm, with a basal septum at 7.32–9.76(–14.64) µm away from the branching point of mycelium; *conidia* clavate, non-papillate, (26.84–)45.14–63.44(–69.54) × (12.2–)21.96–29.28(–31.72) µm, hyaline without conspicuous fibrosin-bodies and *conidial germination* produced germ tubes on the apically side or at the end of spore, lobed appressorium, formed *Ovulariopsis* type.

Chasmothecia scattered to gregarious, (264.53–)272.72–332.65(–361.52) µm in diameter, brown-blackish; *appendages* 4–10 in number, acicular with bulbous basal swelling, (146.29–)299.1–456.2(–526.27) × (38.99–)45.87–59.93(–68.97) µm, apex subacute or subobtuse, hyaline; *penicillate cells* in the upper part; *asci* numerous, sessile, (47.94–)71.3–85.67(–93.38) × (29.06–)33.78–39.46(–42.47) µm, 2-spored; *ascospores* ellipsoid-ovoid, rarely subglobose, (18.42–)22.11–29.87(–31.63) × (17.55–)19.41–24.44(–24.89) µm.

Specimens examined: on leaves of *Gmelina arborea* MUMH5117

Note: Braun and Cook (2012) reported *Phyllactinia gmelinae* on *Gmelina arborea* in Asia (India, Andhra Pradesh, Maharashtra, Tamil Nadu). Base on the features mentioned above in the present study showed the characteristic both of teleomorphic and anamorphic state are closely similar to the reported of Braun and Cook (2012) including based on host plant. Therefore, the powdery mildew on *Gmelina arborea* in this study can be identified as *Phyllactinia gmelinae*. Furthermore, molecular analysis was performed to clarify taxonomy of this fungus. This is the first report of *Phyllactinia gmelinae* on *Gmelina arborea* in Thailand.

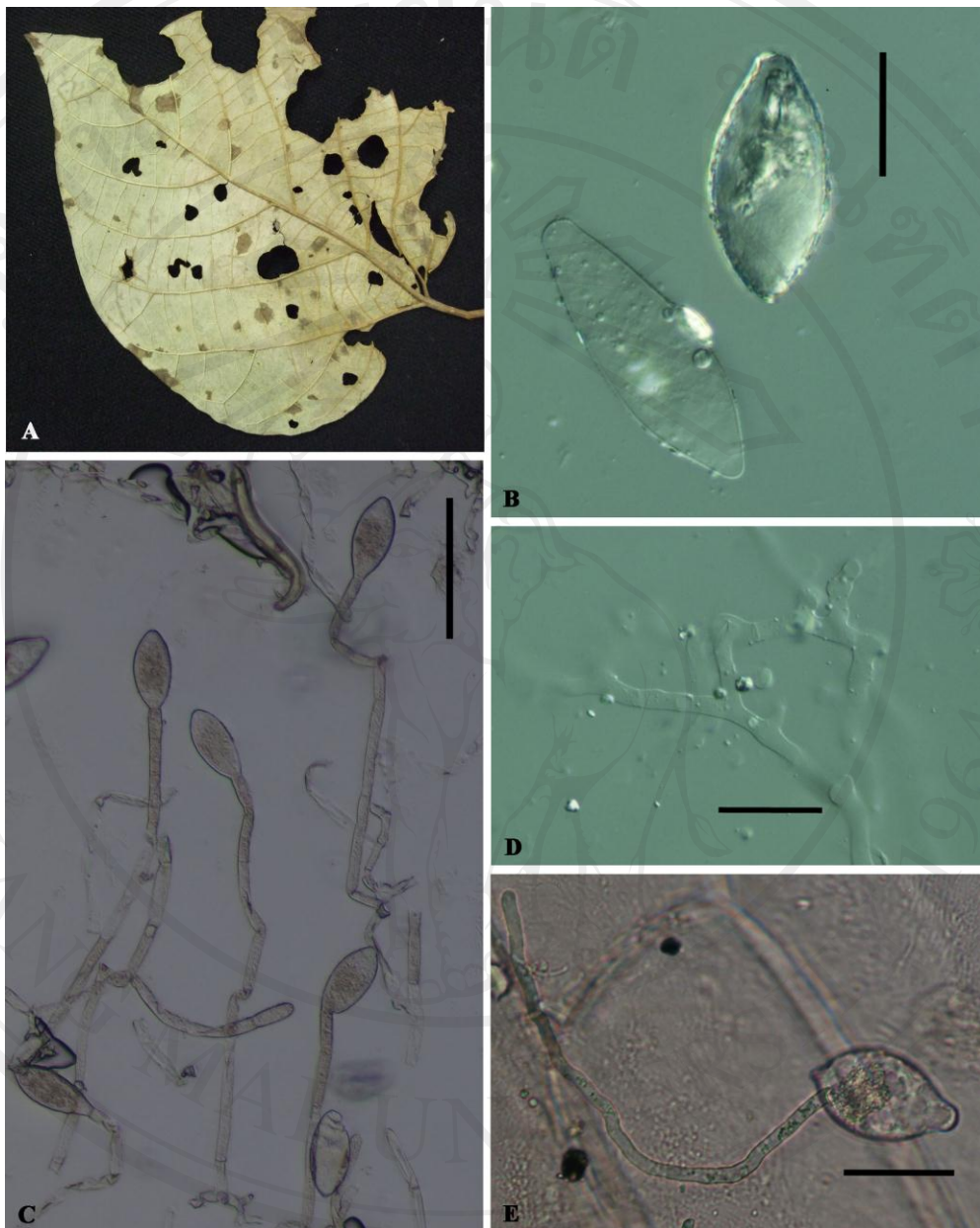


Figure 76 *Ovulariopsis* sp. on leaves of *Gmelina arborea*; (A) mycelia colonized on lower side of leaf (B) conidia (C) conidiophores and conidia (D) mycelia and (E) conidial germination. (Bar 50 μm in C, Bar 25 μm in B and D-E)

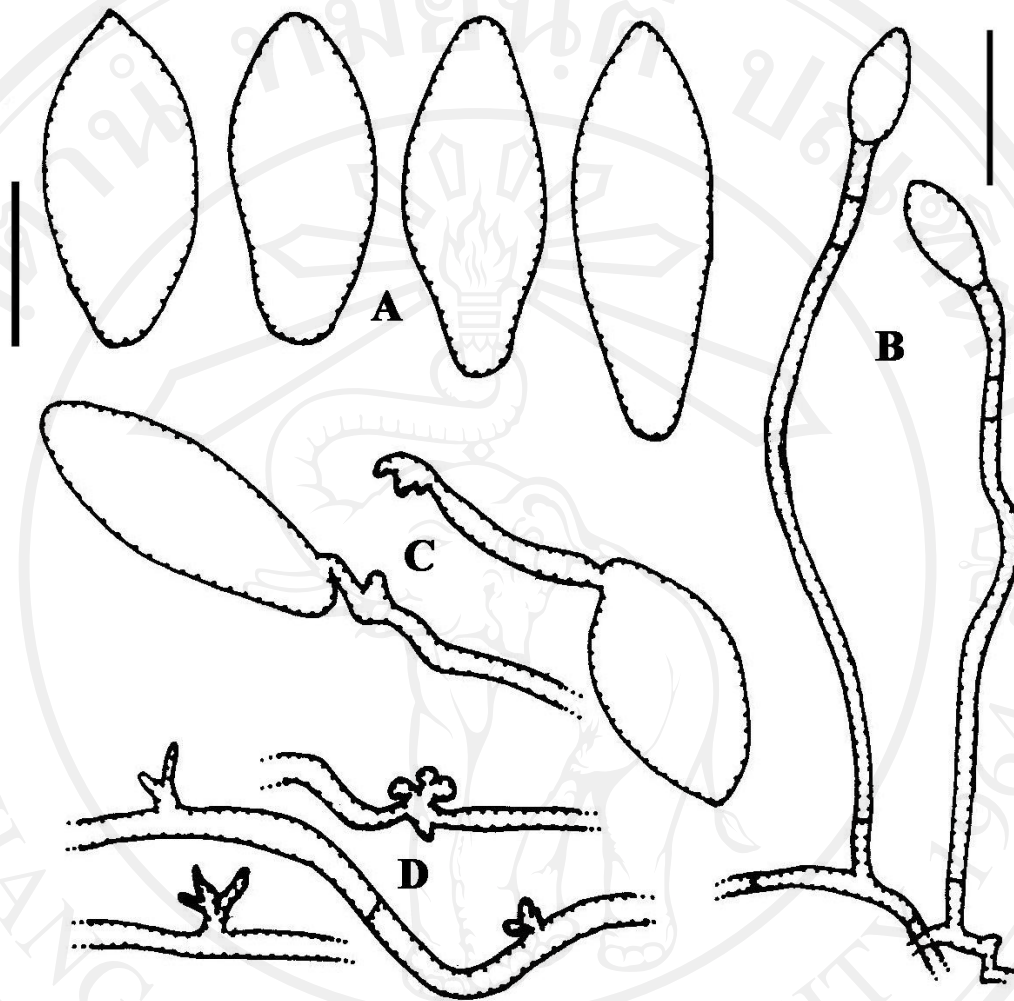


Figure 77 Illustration of *Ovulariopsis* sp. on leaves of *Gmelina arborea*; (A) conidia (B) conidiophores and conidia (C) conidia with germ tubes of the *Ovulariopsis* pattern and (D) mycelia with appressoria. (Bar 27 μm in A, C-D and Bar 50 μm in B)



Figure 78 *Phyllactinia* sp. on leaves of *Gmelina arborea*; (A) chasmothecium (B) acicular with bulbous basal swelling appendages (C) asci and (D) ascus with 2 ascospores. (Bar 105 μm in A and B, Bar 27 μm in C and D)

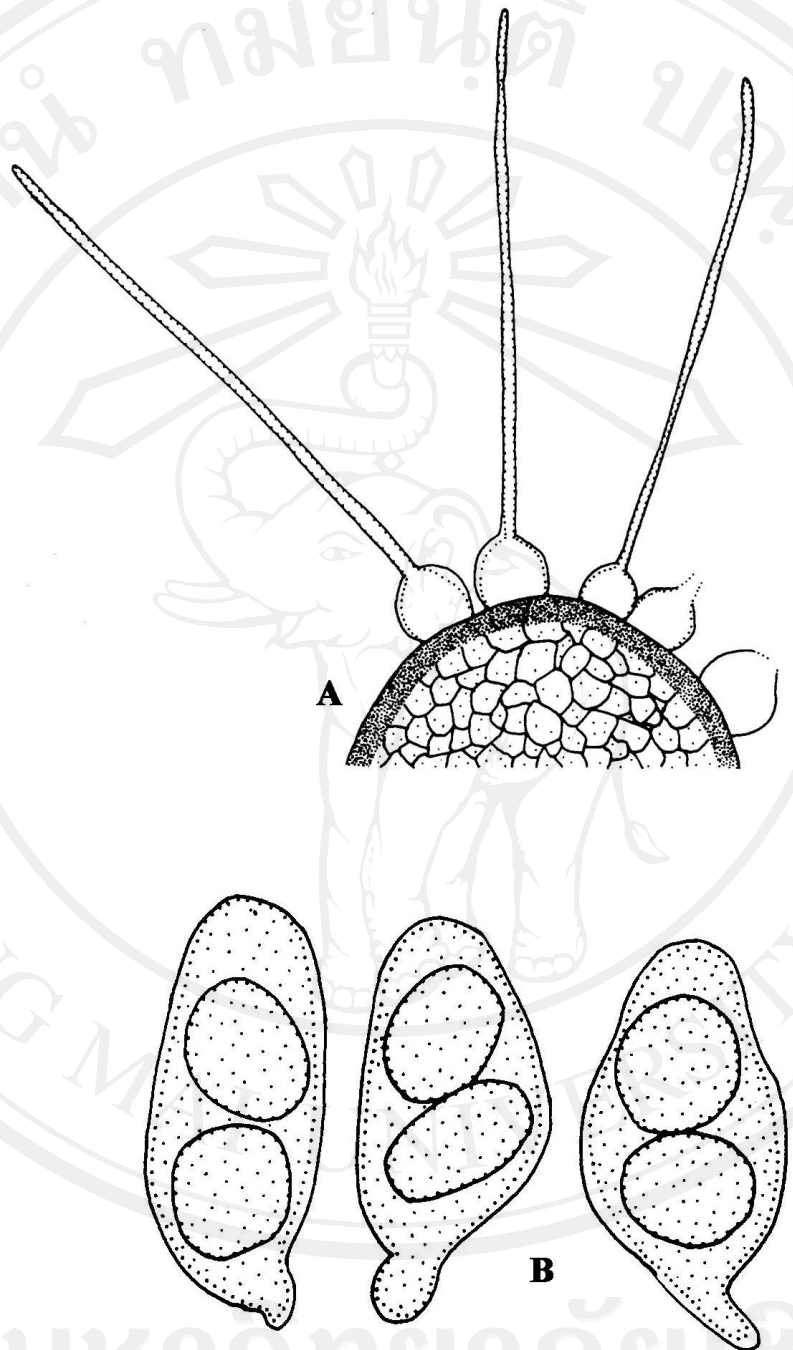


Figure 79 Illustration of *Phyllactinia* sp. on leaves of *Gmelina arborea*, illustrated using a line drawing under a light microscope; (A) chasmothecium with appendages (100X) and (B) asci with ascospores. (Bar 114 μm in A and Bar 27 μm in B)

2.10 *Ovulariopsis* sp. on *Lagerstroma macrocarpa*, Lythraceae

Mycelium hypophyllus, white, thin to thick patches, hyaline; *appressoria* variable in morphology, nipple to elongate shaped, rarely lobed; *conidiophores* arising from upper part of ectophytic hyphae, erect or slightly bent, long, (104.92–)178.12–234.24(–247.66) × 8.54–14.64(–15.86) μm, composed of 2–5 cells of variable length, position non-central; *mother cell* forming conidia singly, (36.6–)51.24–78.08(–85.4) × (3.66–)4.88–7.32 μm; *foot-cells*, long, spirally twisted, (50.02–)63.44–146.4(–158.6) × 4.88–6.1 μm, with a basal septum at (3.66–)4.88–14.64(–19.52) μm away from the branching point of mycelium; *conidia* variable, dimorphic, *primary conidia*, lanceolate, attenuated towards the apex, (65.88–)69.54–78.08(–84.18) × (14.64–)15.86–17.08(–19.52) μm, *secondary conidia* clavate, (56.12–)59.78–75.64(–108.58) × (13.42–)15.86–18.3(–20.74) μm, hyaline without conspicuous fibrosin-bodies and *conidial germination* produced germ tubes at the apical or at the end of spore, lobed appressorium, formed *Ovulariopsis* type.

Specimens examined: on leaves of *Lagerstroma macrocarpa* MUMH335, 5116

Note: This is the first report powdery mildew on *Lagerstroma macrocarpa* in Thailand and in the world. Based on anamorphic features mentioned above, this fungus has anamorphic features similar to *Pleochaeta* by having dimorphic conidia and twisted at the base of foot-cells. (Braun, 1987; Braun and Cook, 2012). Moreover, this fungus has been identified by using phylogenetic analysis based on ITS and 28S rDNA. The result revealed that this fungus formed an independent clade at the basal part of *Phyllactinia/Leveillula* clade with bootstrap support of 97%. Therefore, molecular phylogenetic analysis supported the unique anamorphic morphology of *P. dalbergiae*. As the result, this powdery mildew on *Lagerstroma macrocarpa* can be classified as a new species.

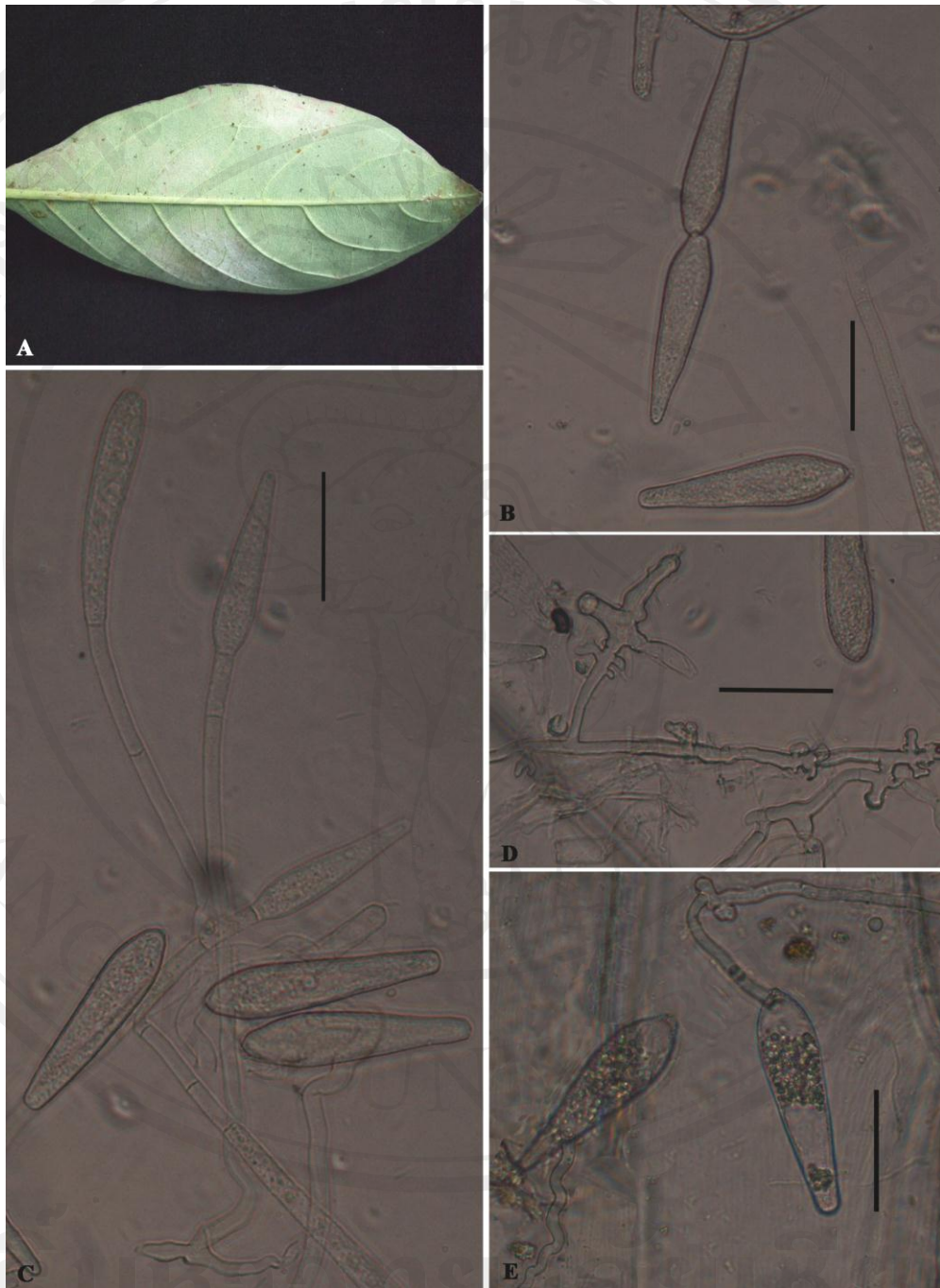


Figure 80 *Ovulariopsis* sp. on leaves of *Lagerstroma macrocarpa*; (A) mycelia colonized on lower side of leaves (B) conidia (C) conidiophores and conidia (D) mycelium with appressoria (E) conidial germination. (Bar 30 μm)

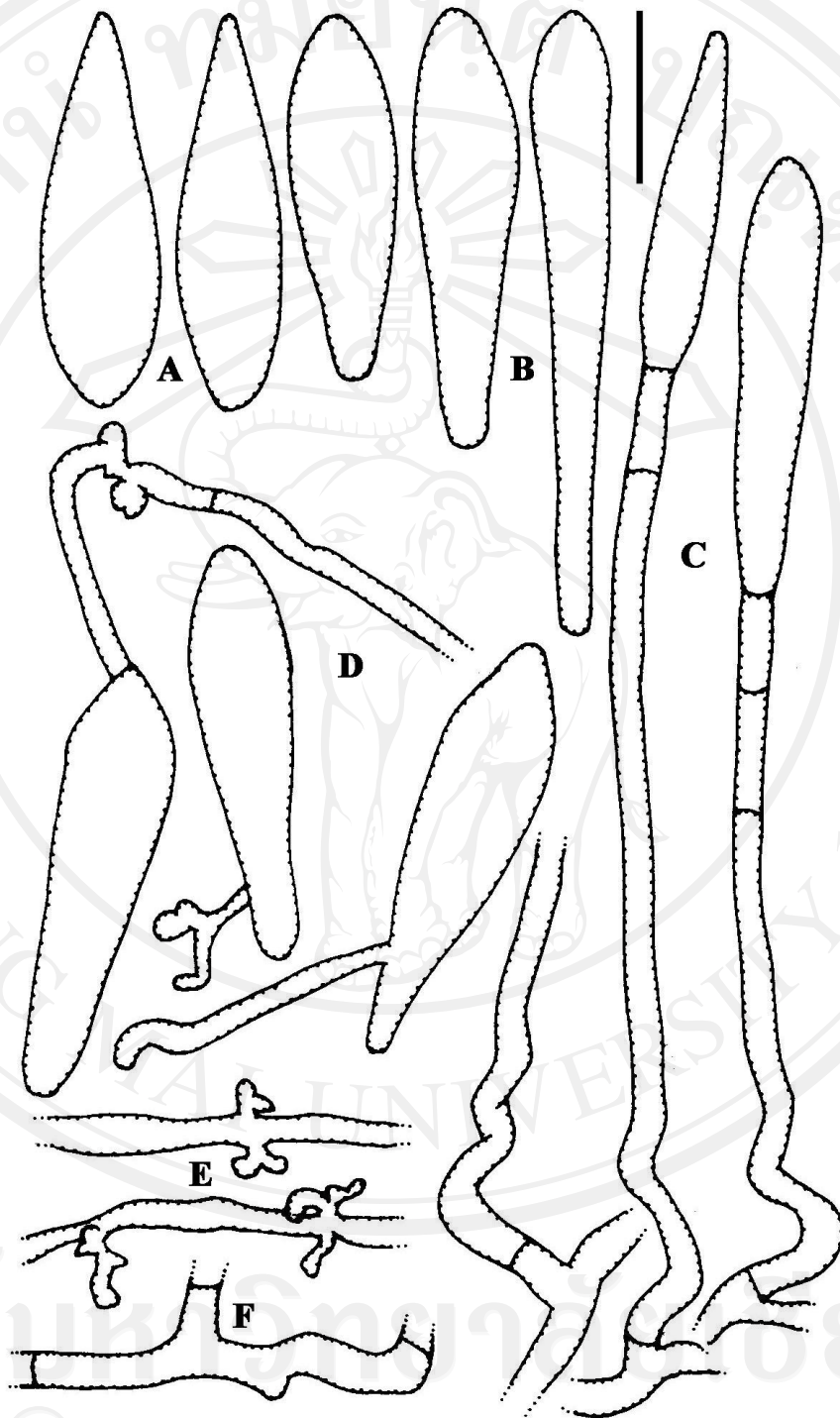


Figure 81 Illustration of *Ovulariopsis* sp. on leaves of *Lagerstroma macrocarpa*; (A) primary conidia (B) secondary conidia (C) conidiophores and conidia (D) conidia with germ tubes of the *Ovulariopsis* pattern (E) mycelia with appressoria and (F) mother cell. (Bar 30 μ m)

2.11 *Ovulariopsis* sp. on *Morus alba*, Moraceae

Mycelium hypophyllus, white, thin or occasionally thick patches, hyaline; *appressoria* variable in morphology, nipple to elongate shaped, rarely lobed; *conidiophores* arising from upper part of ectophytic hyphae, erect or slightly bent, long, (104–)151–276(–344) × (9.7–)12–22(–25.6) μm, composed of 2–5 cells of variable length, position non-central; *mother cell* forming conidia singly, (56–)61–111(–121) × (3.6–)5–6 μm; straight in *foot-cells*, (48.8–)51.24–114.68(–129.32) × 4.88–6.1 μm, with a basal septum at 2.4–12(–17) μm away from the branching point of mycelium; *conidia* clavate, non-papillate, (55–)66–82(–86.6) × (17–)20–24(–30.5) μm, hyaline without conspicuous fibrosin-bodies and *conidial germination* produced germ tubes on the apically side or at the end of spore, lobed appressorium, formed *Ovulariopsis* type.

Chasmothecia hypophyllous, scattered, sometimes subgregarious, (140–)150–180(–185) μm; *appendages* (65–)95–240(–245) × (20–)25–35 μm in diam, acicular with bulbous basal swelling, apex obtuse, hyaline; *penicillate cells* present; *asci* numerous, stalked to sessile, yellowish in immature stage; *ascospores* not found.

Specimens examined: on leaves of *Morus alba* MUMH5089, 5090, 5098, 5099, 5103, 5105, 5111, 5115

Note: *Phyllactinia moricola* and *Phyllactinia suffulta* have been reported as a powdery mildew disease on *Morus alba* in Asia (Amino, 1986). In this study, the fungus has been identified by using phylogenetic analysis based on ITS and 28S rDNA. The result indicated that both anamorphic and teleomorphic state on *Morus alba* form a clade with *Phyllactinia guttata* on *Morus* spp. Therefore, powdery mildew on *Morus alba* in Thailand based on morphological and molecular analysis should be identified as *Phyllactinia guttata*.

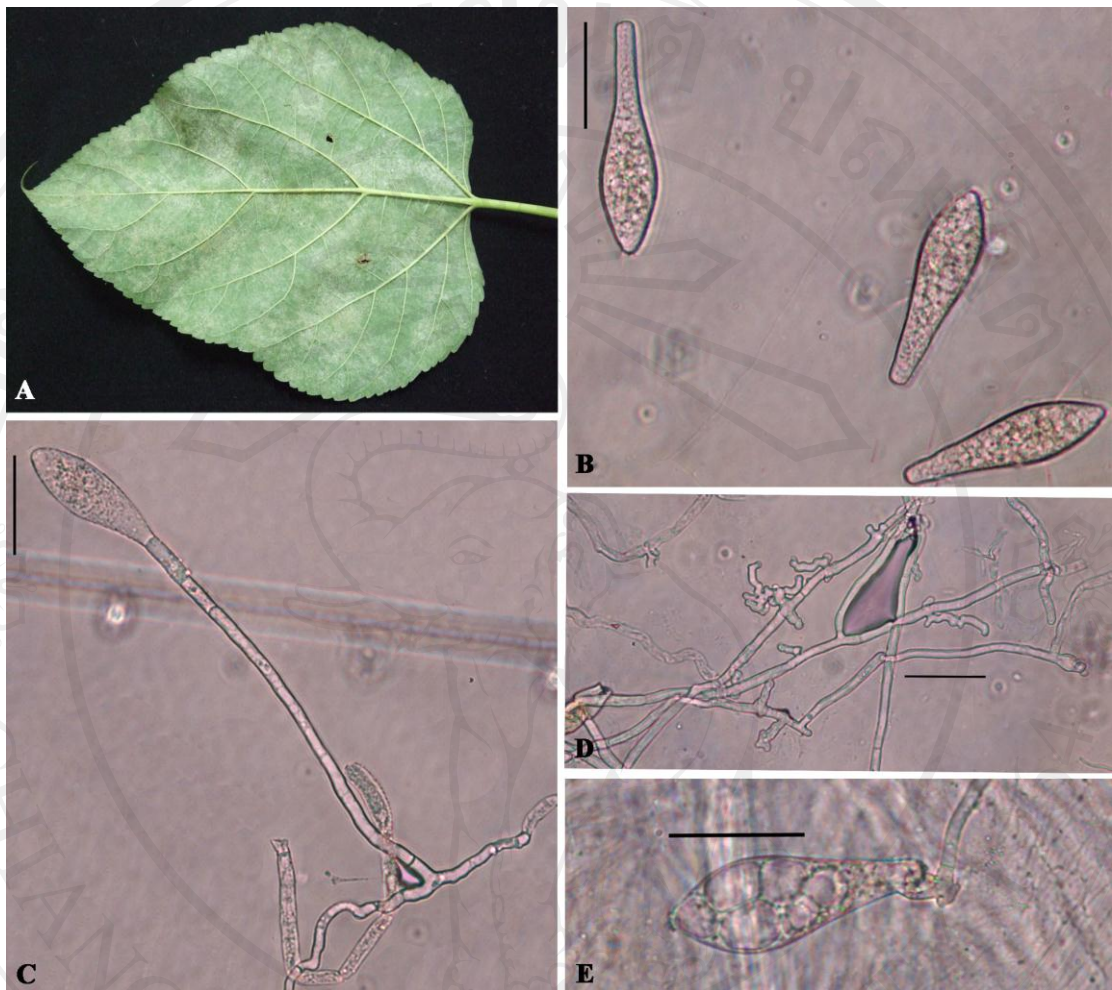


Figure 82 *Ovulariopsis* sp. on leaves of *Morus alba*; (A) mycelia colonized on lower side of leaf (B) conidia (C) conidiophores and conidia (D) mycelium with appressoria and (E) conidial germination. (Bar 30 μm)

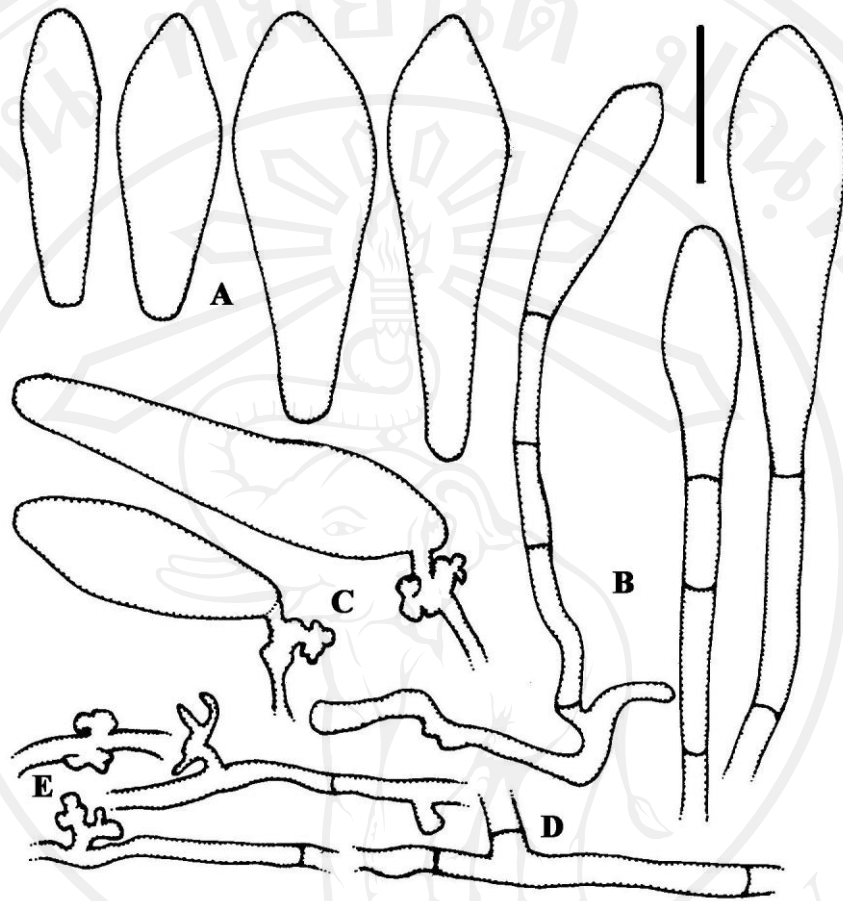


Figure 83 Illustration of *Ovulariopsis* sp. on leaves of *Morus alba*, illustrated morphological characteristics; (A) conidia (B) conidiophores and conidia (C) conidia with germ tubes of the *Ovulariopsis* type (D) mother cell that leading originated conidiophore and (E) mycelia with appressoria. (Bar 30 μm)

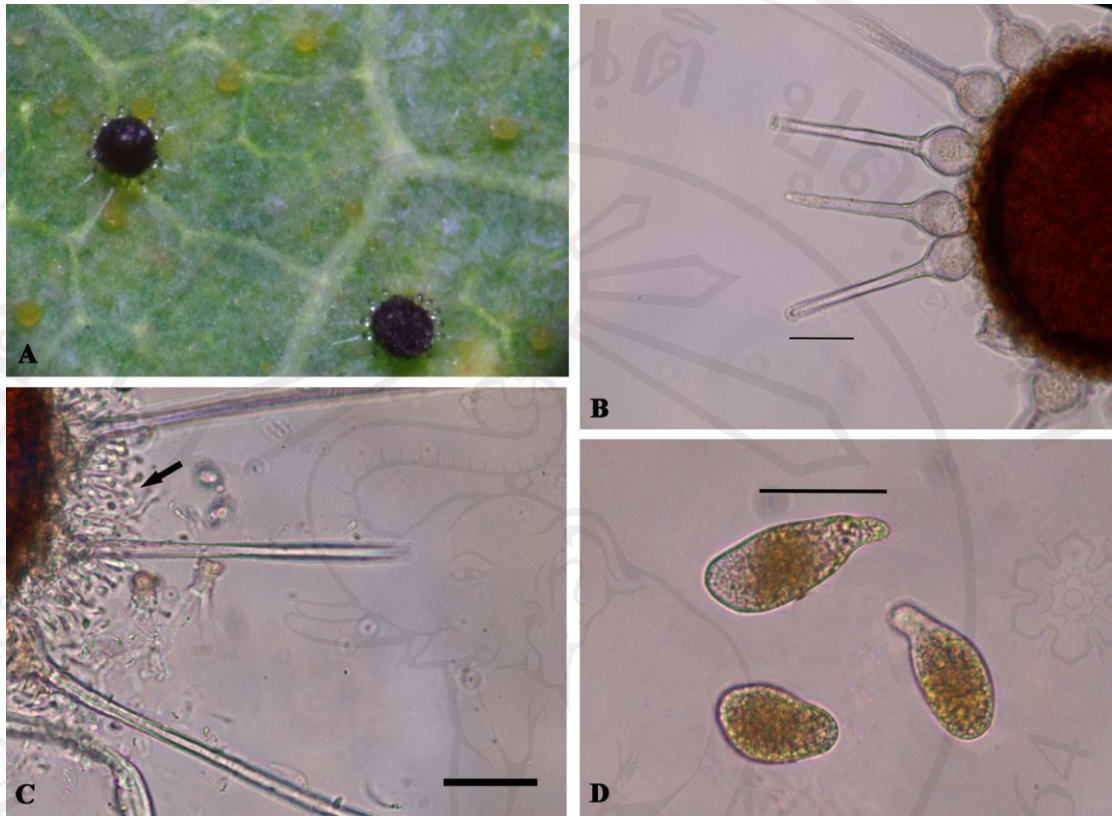


Figure 84 *Phyllactinia guttata* on leaves of *Morus alba*; (A) chasmothecium (B) appendages with bulbous base (C) penicillate cells and (D) immatured asci. (Bar 30 μm)

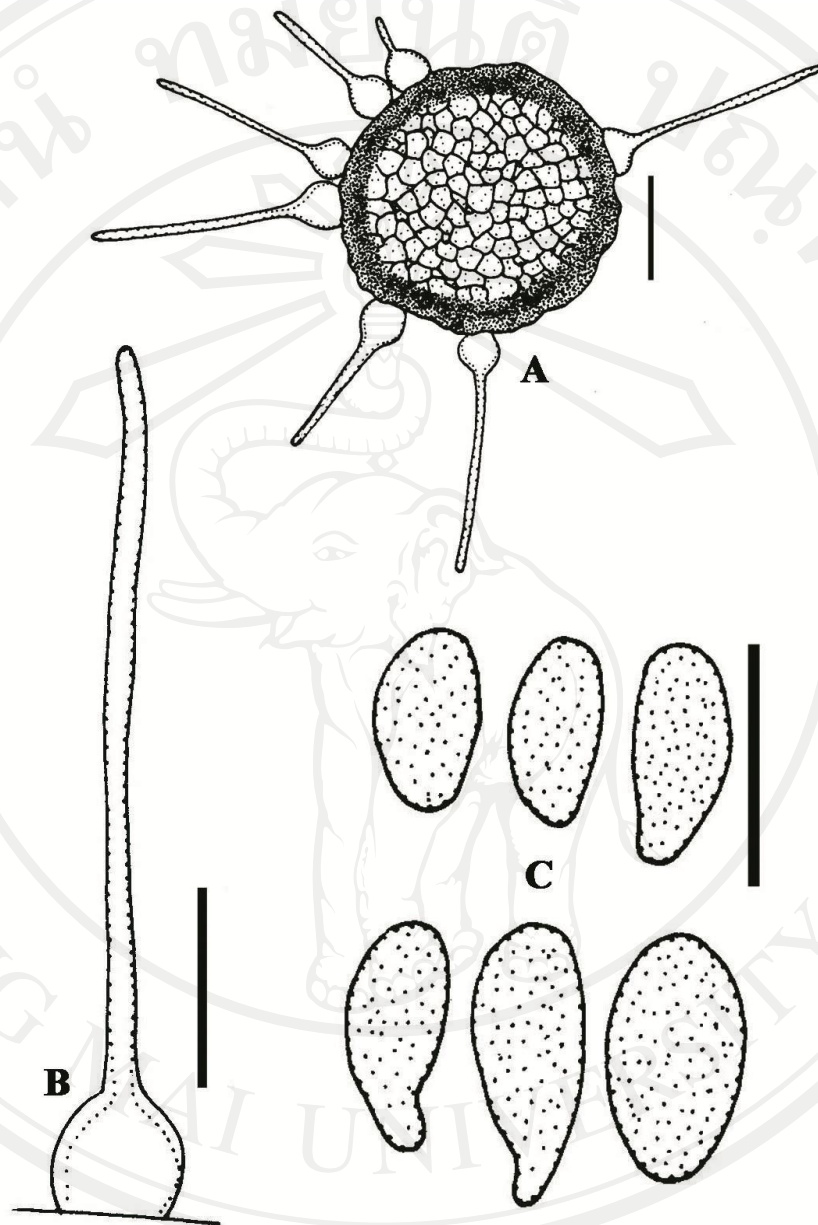


Figure 85 Illustration of *Phyllactinia guttata* on leaves of *Morus alba* illustrated using a line drawing; (A) chasmothecium (B) acicular appendage with bulbous base and (C) immature asci. (Bar 50 μm in A, Bar 30 μm in B and C)

2.12 *Ovulariopsis* sp. on *Pyrus pyrifolia*, Rosaceae

Mycelium hypophyllus, white, thin to dense patches, hyaline; *appressoria* nipple to collar-liked; *conidiophores* arising from upper part of ectophytic hyphae, erect or slightly bent, long, $(85.4-87.84-268.4(-445.3)) \times 7.32-10.98(-19.52)$ μm ; *mother cell* forming conidia singly, $(48.8-53.68-73.2(-112.24)) \times 4.88-7.32$ μm ; straight in *foot-cells*, $(31.72-41.48-65.88(-139.08)) \times 6.1-7.32(-8.54)$ μm , with a basal septum at $(0-1.22-9.76(-10.98))$ μm away from the branching point of mycelium; *conidia* clavate, non-papillate, $(58.56-8.32-90.28(-103.7)) \times (15.86-17.08-21.96(-24.4))$ μm , hyaline without conspicuous fibrosin-bodies and *conidial germination* formed *Ovulariopsis* type. The teleomorphic state can not be found.

Specimens examined: on leaves of *Pyrus pyrifolia* MUMH5109

Note: Previously, the powdery mildew on *Pyrus* spp. has been reported as caused by *Phyllactinia guttata* (Amino, 1986; Shin, 2000; Paul and Thakur, 2006). After that, Braun (1987) proposed new species of *Phyllactinia* on *Pyrus* as *P. mali*. Based on the results mentioned above in this study, the characteristics of the fungus similar to those of the anamorph of *P. mali* that were reported in previous study (Shin, 2000; Braun and Cook, 2012). In addition, the fungus has been identified by using phylogenetic analysis based on ITS and 28s rDNA. The result indicated that both of *Ovulariopsis* sp. on *Pyrus pyrifolia* form a clade with *Phyllactinia mali* on *Pyrus pyrifolia* var. *culta* which the specimen is collected in Japan (Takamatsu *et al.*, 2008), with strongly bootstrap support. Therefore, powdery mildew on *Pyrus pyrifolia* in Thailand based on morphological and molecular analysis should be identified as *Phyllactinia mali*. This is the first report of *Phyllactinia mali* on *Pyrus pyrifolia* in Thailand.

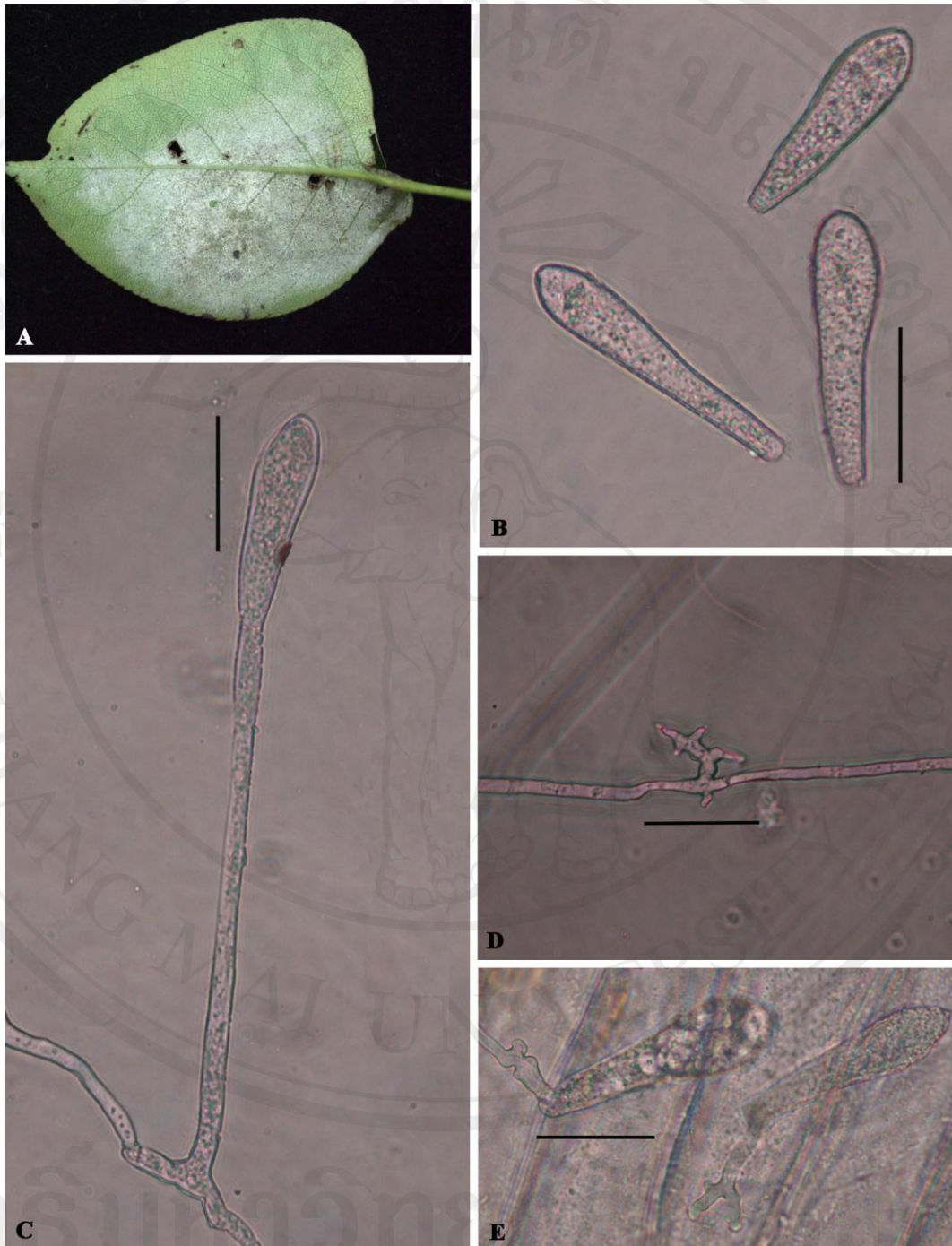


Figure 86 *Ovulariopsis* sp. on leaves of *Pyrus pyrifolia*; (A) mycelia colonized on lower side of leaf (B) conidia (C) conidiophores and conidia (D) mycelium with appressoria and (E) conidial germination. (Bar 30 μm)

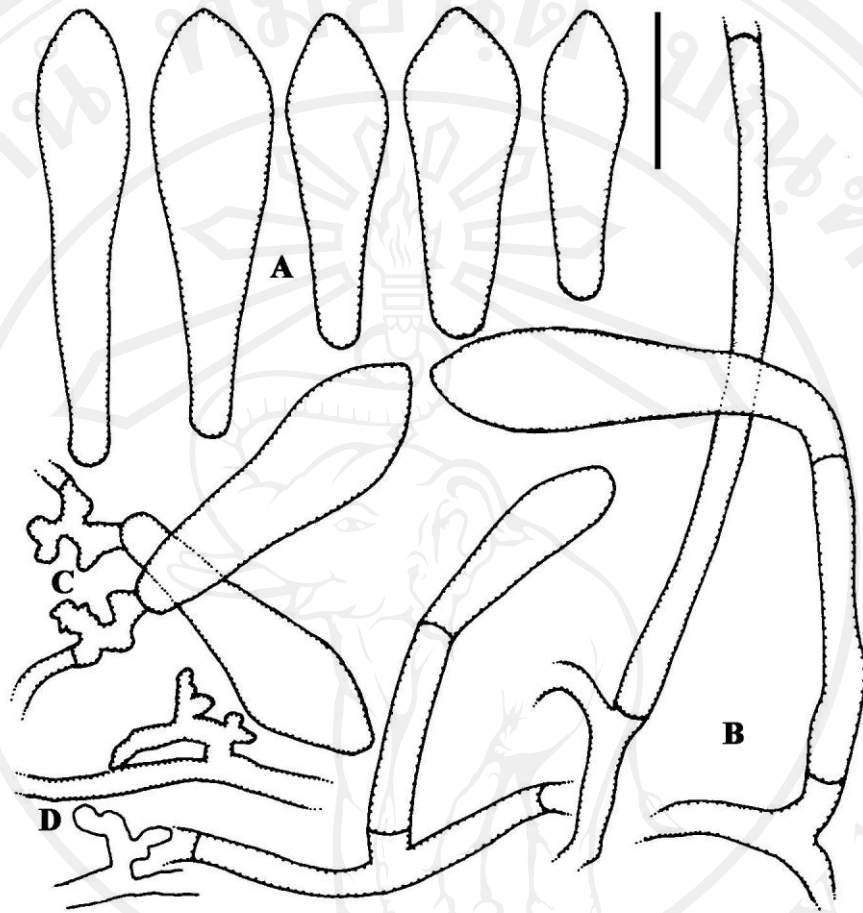


Figure 87 Illustration of *Ovulariopsis* sp. on leaves of *Pyrus pyrifolia*; (A) conidia (B) conidiophores and conidia (C) conidia with germ tubes of the *Ovulariopsis* pattern and (D) mycelia with appressoria. (Bar 30 μm)

2.13 *Ovulariopsis* sp. on *Senna siamea*, Caesalpiniaceae

Mycelium hypophyllous, white, thin to dense patches, hyaline; *hyphal appressoria* nipple-shaped, rarely lobed to elongated; *conidiophores* arising from ectophytic hyphae, on upper surface of mother cells, position not central, rarely central, erect, straight or slightly bent, $(32.22-65.77-128.47(-148.41) \times (6.6-7.41-14.43(-16.18) \mu\text{m}$; basal septum displaced from the branching point of the mycelium, $(2.95-6.93-16.24(-18.38) \mu\text{m}$; *mother cells* forming conidia singly, $(38.35-51.9-74.94(-85.36) \times (4.05-4.34-5.06(-5.42) \mu\text{m}$; *foot-cells* straight with a basal septum near branching point of mycelium up to away from it, $(12.29-24.29-78.01(-98.91) \times (4.51-5.01-6.15(-6.8) \mu\text{m}$; *conidia* cylindrical-ellipsoid, $(31.53-36.71-49.92(-54.06) \times (9.55-11.65-15.94(-18.45) \mu\text{m}$, hyaline without conspicuous fibrosin-bodies, produced solitary on conidiophores; *conidial germination* germinate at the ends, long branch, sometime rarely lobed, formed *Ovulariopsis* type.

Specimens examined: on leaves of *Senna siamea* MUMH3331

Note: This is the first report of powdery mildew on *Senna siamea* in Thailand and in the world. Anamorph of this fungus has a unique characteristic that is conspicuously distinct from all other species of *Phyllactinia*. Morphological observations showed conidiophore shorter than other *Ovulariopsis* species anamorph of *Phyllactinia* and showed production of cylindrical-ellipsoid conidia. This anamorphic feature is consistent with typical characteristic of *Oidium*, not *Ovulariopsis*. The present study, morphological features mentioned above has mostly similar to *Phyllactinia cassiae-fistulae* on *Cassia fistula* (Braun, 1987; Braun and Cook, 2012). In this study, molecular analysis combined with morphological analysis was performed to clarify taxonomy of this fungus. The result indicated that *Ovulariopsis* sequences on *Senna siamea* formed a clade with *Phyllactinia cassiae-fistulae* sequences at the basal part of *Phyllactinia/Leveillula* clade with bootstrap support of 100%. Therefore, molecular phylogenetic analysis supported the unique anamorphic morphology of this fungus. The nucleotide sequence of this fungus has highest similar with *Phyllactinia cassiae-fistulae* on *Cassia fistula* with only one nucleotide difference. Hence, this fungus should be identified as new species.

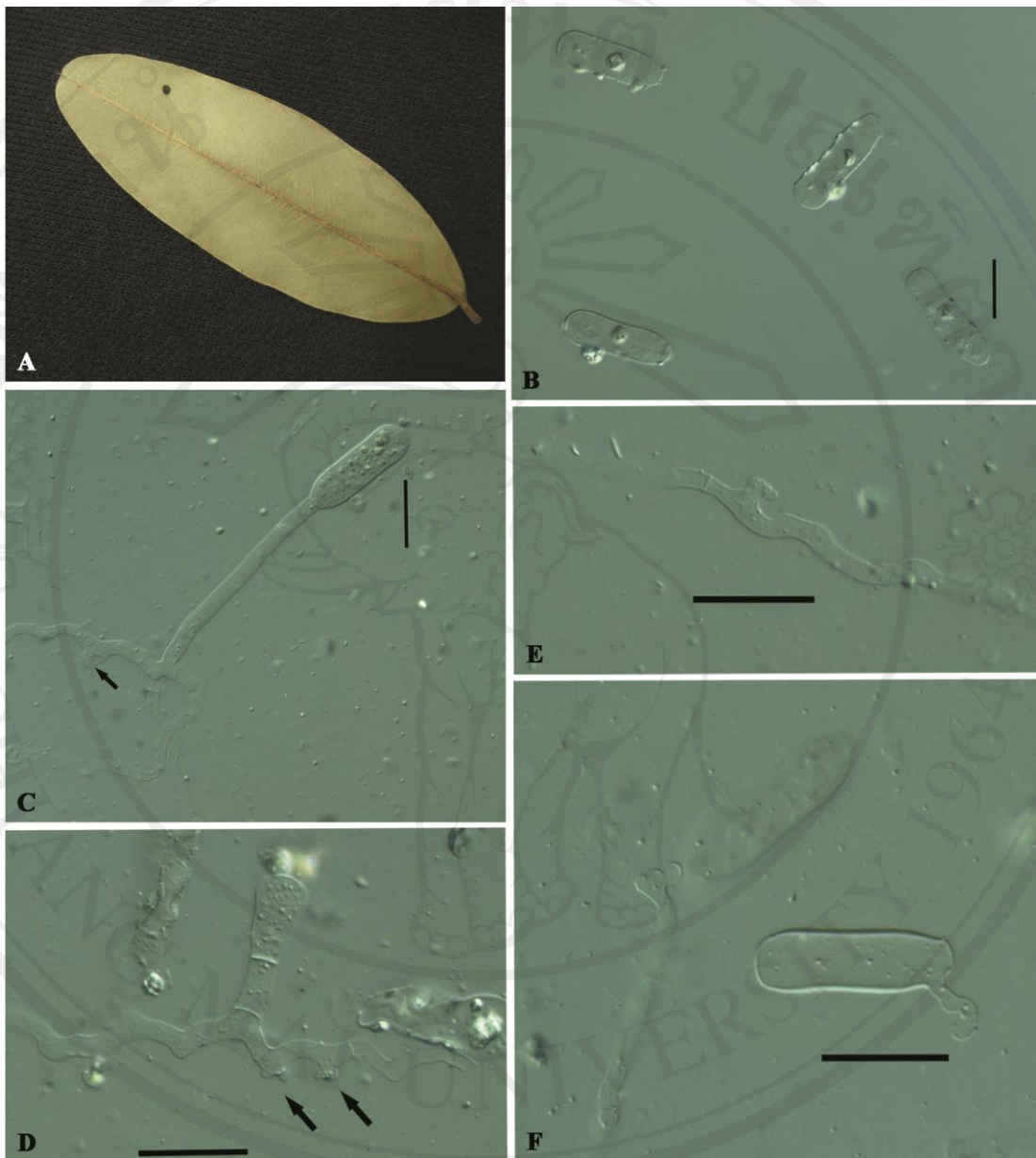


Figure 88 *Ovulariopsis* sp. on leaves of *Senna siamea*; (A) mycelia colonized on lower side of leaves (B) conidia (C) conidiophores and conidia and (D) conidiophores with appressoria (E) mycelium with appressoria and (F) conidial germination. (Bar 25 μ m)

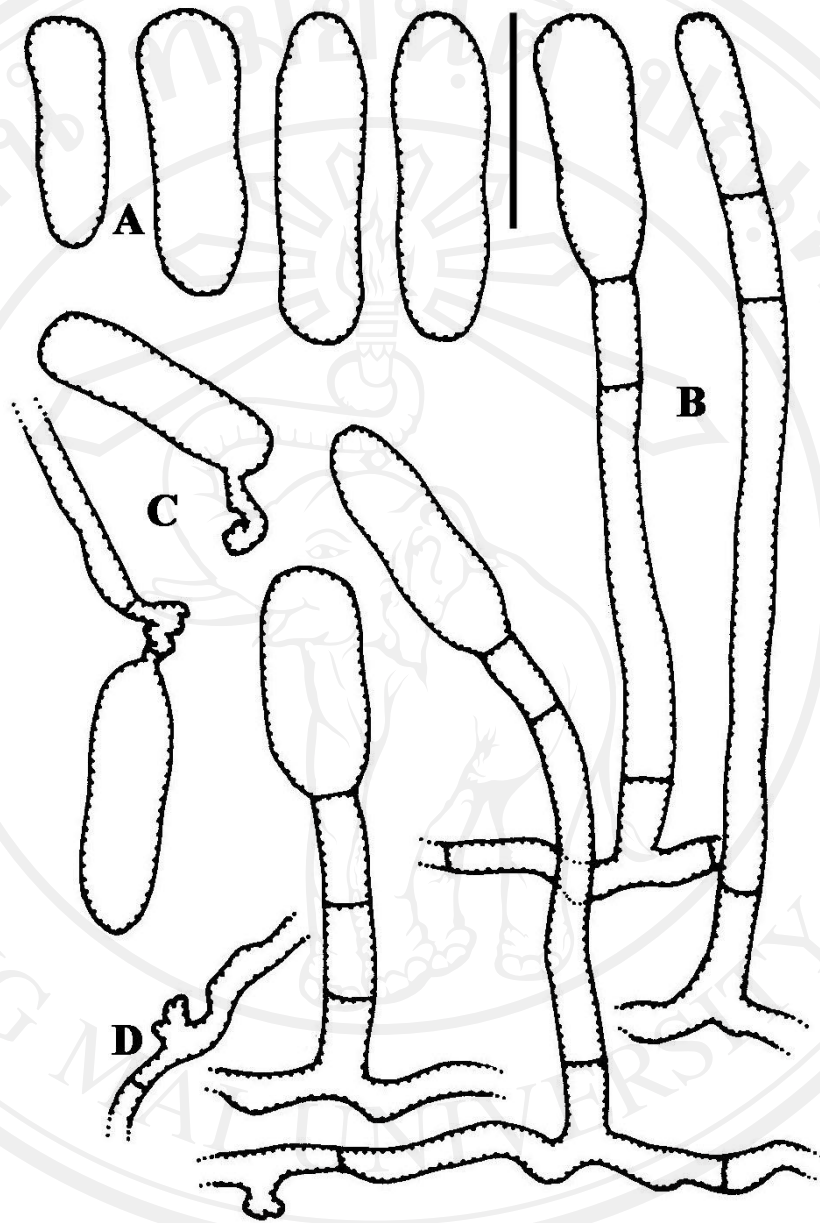


Figure 89 Illustration of *Ovulariopsis* sp. on leaves of *Senna siamea*; (A) conidia (B) conidiophores and conidia (C) conidia with germ tubes of the *Ovulariopsis* pattern and (D) mycelia with appressoria. (Bar 30 μ m)

2.14 *Ovulariopsis* sp. on *Terminalia bellirica*, Combretaceae

Mycelium hypophyllous, white, thin to dense, hyaline; *appressoria* nipple-shaped, occasionally lobed; *conidiophore* arising from ectophytic hyphae, on upper surface of mother cells, position not central, rarely central, (154.94–)175.68–248.88(–287.92) × (7.32–)14.64–19.52(–21.96) μm; basal septum (0–)2.44–14.64(–19.52) μm displaced from the branching point of the mycelium; *mother cells* forming conidia singly, (46.36–)51.24–64.66(–80.52) × 4.88–6.1(–7.32) μm; *foot-cells* sinuous to twisted, with a basal septum near branching point of mycelium up to away from it, (39.04–)51.24–90.28(–114.68) × 4.88–7.32(–8.54) μm; *conidia* clavate, (68.32–)71.98–90.28(–92.72) × (15.86–)19.52–24.4(–26.84) μm, hyaline without conspicuous fibrosin-bodies and *conidial germination* formed *Ovulariopsis* type.

Chasmothecia scattered to subgregarious, (143.96–)153.72–183(–195.2) μm diameter, black and yellowish in young chasmothecia; appendages 6–12 in number, acicular with bulbous basal swelling, (117.12–)141.52–231.8(–258.64) × 29.28–34.16(–36.6) μm, apex subobtuse, hyaline; *penicillate cells* found; *asci* and *ascospore* not produced.

Specimens examined: on leaves of *Terminalia bellirica* MUMH3337

Note: Braun (1987) reported *Phyllactinia guttata* on *Terminalia* spp. Paul and Thakur (2006) described powdery mildew on *Terminalia bellirica* to new species as *P. belliricae*. The present study, the description of this fungus that mentioned above has identical with *P. belliricae* on *Terminalia bellirica* and also reported the same host species. Anamorphic stage of *P. belliricae* has the unique conidiophore foot-cells that having sinuous to twisted formed as a typical of conidiophore foot-cells in genus *Streptopodium*. Furthermore, molecular analysis was performed to clarify taxonomy of *P. belliricae*. The result indicated that *P. belliricae* formed an independent clade at the basal part of *Phyllactinia/Leveillula*. Therefore, molecular phylogenetic analysis supported the unique anamorphic morphology of *P. belliricae*. This fungus can be identified as *Phyllactinia belliricae*.

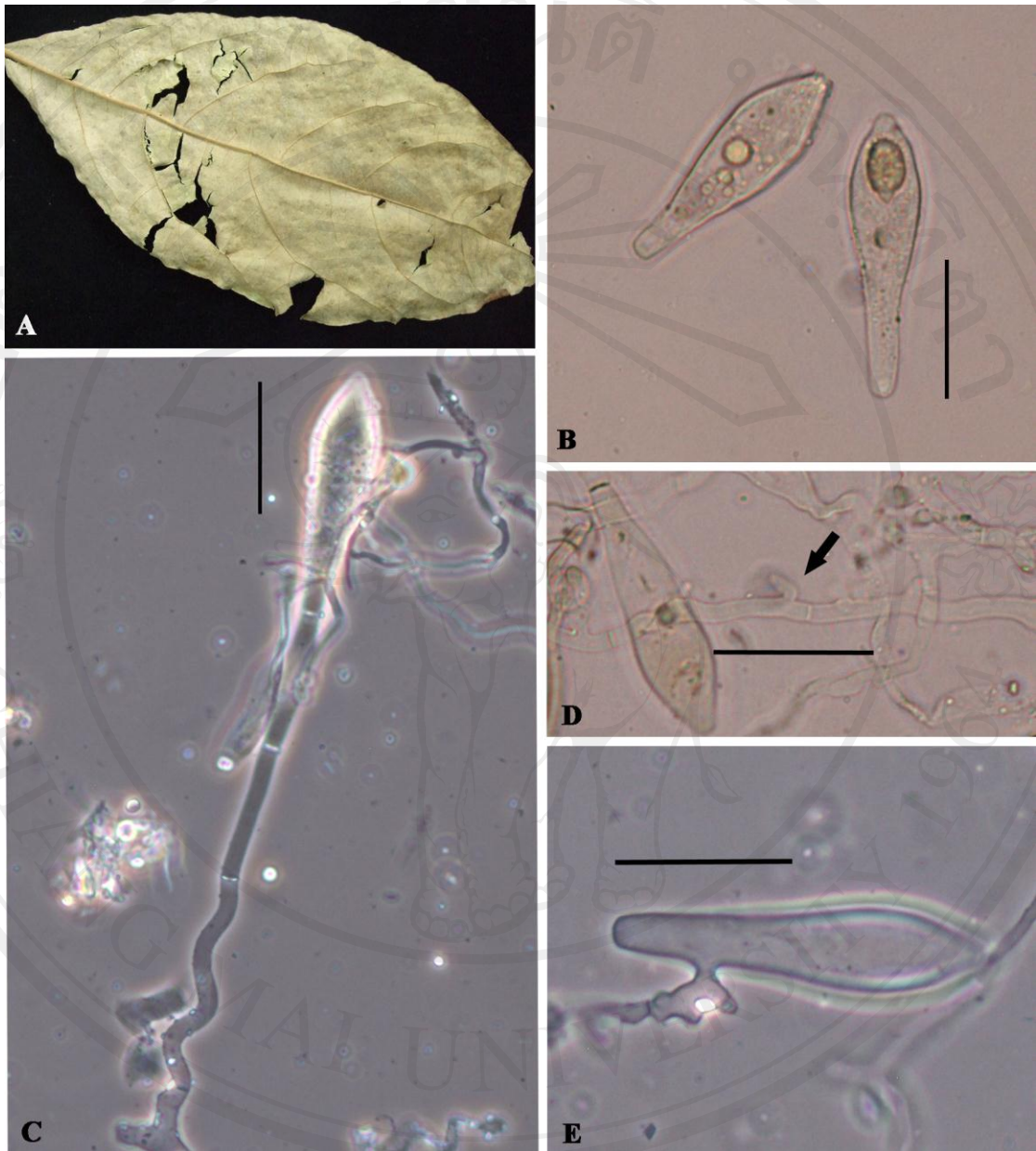


Figure 90 *Ovulariopsis* sp. on leaves of *Terminalia bellirica*; (A) mycelia colonized on lower side of leaf (B) conidia (C) conidiophores and conidia (D) mycelium with appressoria and (E) conidial germination. (Bar 30 μ m)

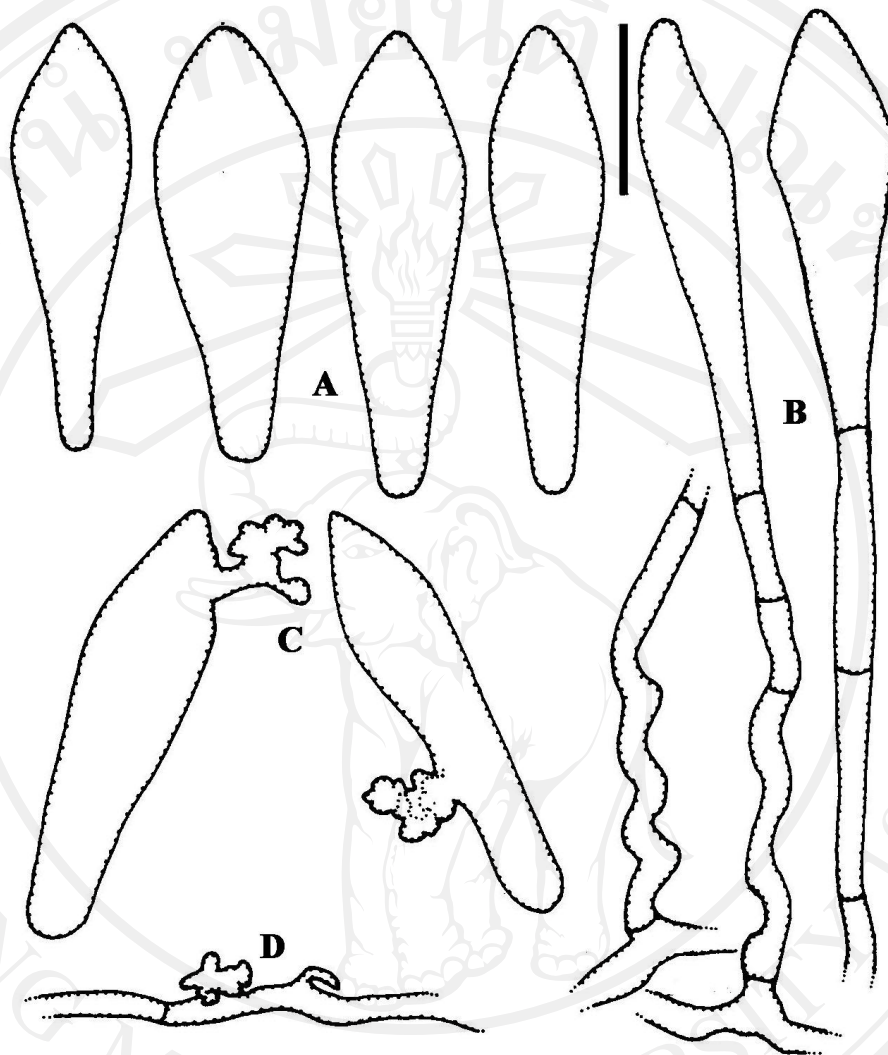


Figure 91 Illustration of *Ovulariopsis* sp. on leaves of *Terminalia bellirica*, (A) conidia (B) conidiophores with twisted foot cells and conidia (C) conidia with germ tubes of the *Ovulariopsis* type and (D) mycelia with appressorium. (Bar 30 μm)

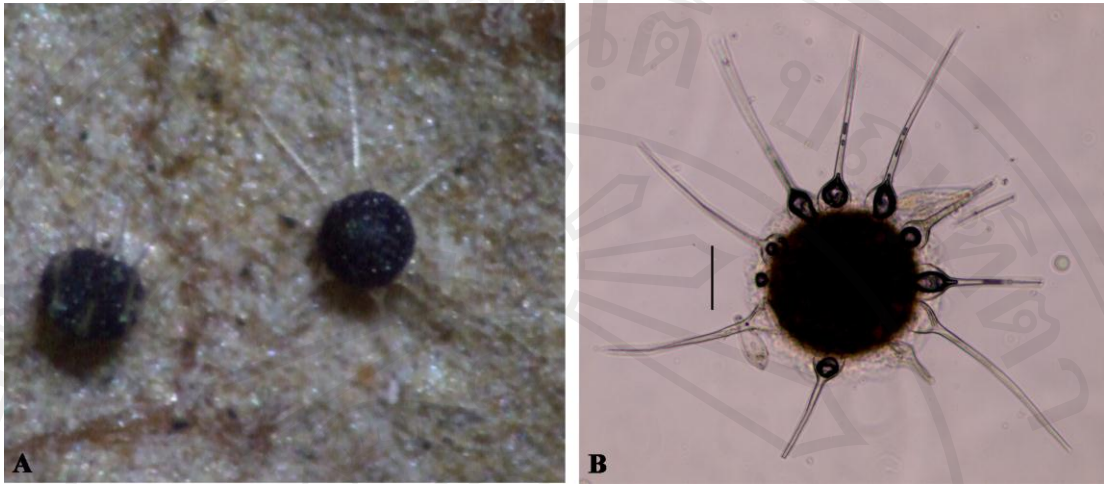


Figure 92 *Phyllactinia belliricae* on leaves of *Terminalia bellirica*; (A) close-up of chasmothecia scattered on the lower surface of leaves and (B) chasmothecium forming appendages with bulbous base. (Bar 50 μm)

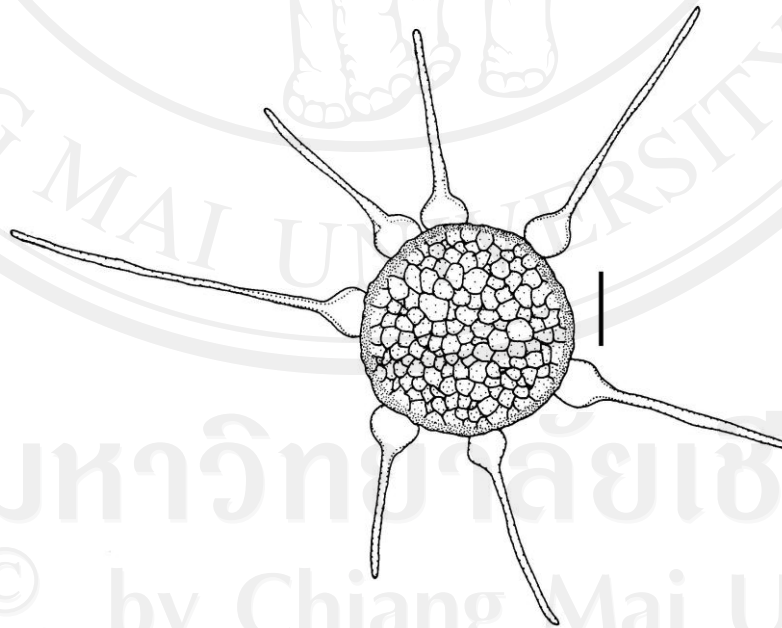


Figure 93 Illustration of *Phyllactinia belliricae* on leaves of *Terminalia bellirica*. (Bar 50 μm)

3. Molecular phylogenetic analysis

Currently, the ambiguous taxonomic characters or inadequate morphological characters have been resolved and clarify the problem by providing the useful DNA techniques that involve PCR and DNA sequencing for identification (Glen, 2006).

3.1 Phylogenetic study of powdery mildew in tribe Phyllactinieae in Thailand

Phylogenetic analyses were investigated based on a combined data set of the ITS and 28S rDNA sequences. A total of 68 nucleotide sequences, consisting of 27 sequences from *Leveillula*, 39 from *Phyllactinia* and 2 from *Pleochaeta*, were used for the analyses. *Pleochaeta indica* and *Pleochaeta shiraiana* were used as an outgroup taxa. The dataset of multiple alignments consisted of 892 characters, of which 44 characters were variable and 128 characters were phylogenetically informative for parsimony analysis. A total of 193 equally most parsimonious trees with 342 steps (CI = 0.6696, RI = 0.9172, RC = 0.6141, HI = 0.3304) were constructed by parsimony ratchet analysis. A tree with the highest likelihood value among the 193 tree is shown in Figure 94.

As the result of phylogenetic placement of tribe Phyllactinieae (Fig. 94), *Phyllactinia* grouped with *Leveillula* to form a clade with strongly bootstrap support (BS) by 100% value. *Phyllactinia* was paraphyletic to *Leveillula*. *Pleochaeta* was the sister group of *Phyllactinia/Leveillula* clade. The phylogenetic analysis within tribe Phyllactinieae of this study was divided into 6 groups and 4 subgroups with strongly bootstrap support.

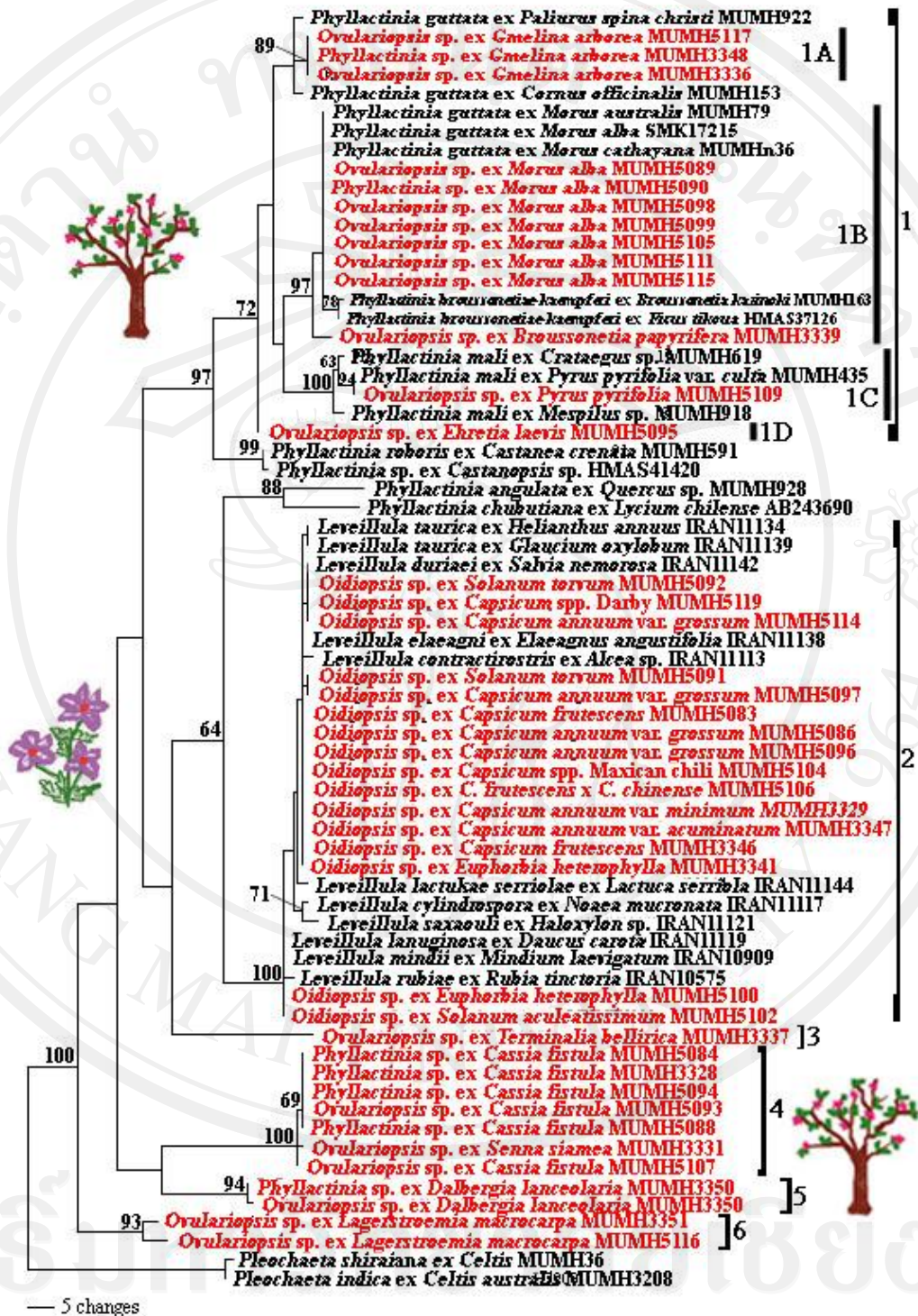


Figure 94 A Parsimony ratchet tree which combined dataset of ITS and 28S rDNA was found using a heuristic search employing a parsimony ratchet algorithm. Value above branching nodes indicate bootstrap support obtain from bootstrap analysis with 1000 replicates. (CI = 0.6696, RI = 0.9172, RC = 0.6141)

Group 1 consisted of 23 specimens from host families, i.e. Boraginaceae, Moraceae, Rosaceae, Verbenaceae (BS = 72%). A tree with the highest likelihood value is shown in Figure 95. Group 1 was further subdivided into 4 subgroups. Each subgroup belongs to host-specific group: Verbenaceae in subgroup 1A, Moraceae in subgroup 1B, Rosaceae in subgroup 1C and Boraginaceae in subgroup 1D and supported with strongly bootstrap value (BS = 89% in subgroup 1A, BS = 97% in subgroup 1B, BS = 94% in subgroup 1C). This group has 2 *Phyllactinia* species; *P. gmelinae* in group 1A on *Gmelina arborea* and *P. mali* in 1C on *Pyrus pyrifolia*. This group is parasitic fungus on trees or shrubs.

Group 2 and 3 This parsimony tree comprised of *Leveillula* and *Ovualtriopsis* sp. on *Terminalia bellirica*. These groups consist of a total of 28 sequences, 27 from group 2 and 1 from group 3. A tree with the highest likelihood value is shown in Figure 96. Group 2 consisted of 27 specimens from host families, i.e. Euphorbiaceae, Solanaceae (BS = 64%). This group was from the specimens of *Leveillula taurica* on *Capsicum* spp., *Euphorbia heterophylla*, *Solanum aculeatissimum* and *S. torvum*. The results indicated that *Leveillula* sp. is parasitic fungus on herbaceous plants. Group 3 included only a single specimen from Combretaceae found on *Terminalia bellirica* which identified as *Phyllactinia belliricae*. This group is parasitic fungus on tree.



Figure 95 Maximum parsimony tree estimated under the highest likelihood value for 23 specimens belonging to group 1 of *Phyllactinia*.

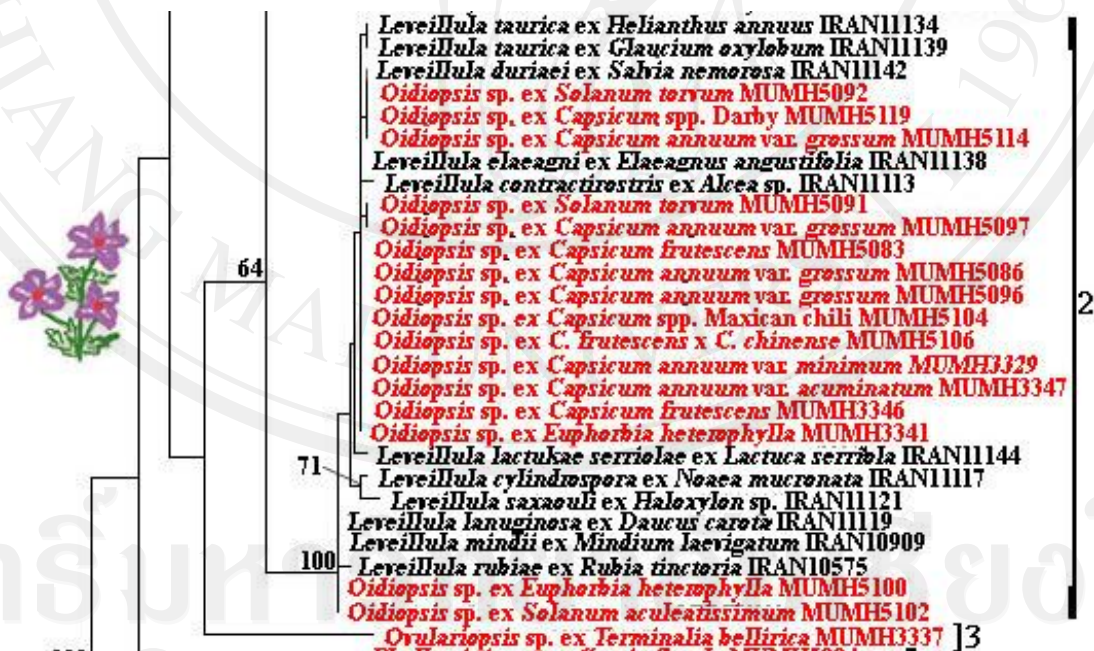


Figure 96 Maximum parsimony tree estimated under the highest likelihood value for 28 specimens belonging to group 2 and 3 of *Leveillula* and *Phyllactinia*, respectively.

Group 4, 5 and 6 consist of 11 specimens from host families, i.e. Caesalpiniaceae, Lythraceae (BS = 100%). A total of 13 nucleotide sequences were used for analyse, of which 11 from *Phyllactinia* and 2 from *Pleochaeta* species used as an outgroup. A tree with the highest likelihood value is shown in Figure 97. The result showed these groups (group 4, 5 and 6) distinctly formed an independent clade at the basal part of *Phyllactinia/Leveillula* clade with bootstrap support of 100% which supported the unique morphological characteristics of anamorphic state. Group 4 consisted of a total of 7 specimens from Caesalpiniaceae, 6 from *Cassia fistula*, and 1 from *Senna siamea* which identified as *Phyllactinia cassiae-fistulae*. The anamorphic characteristics of this group are quite distinct from other known *Phyllactinia* species by having cylindrical-ellipsoid conidia. Group 5 comprised of 2 specimens from Caesalpiniaceae on *Dalbergia lanceolaria* which having the unique anamorphic characteristics as found in group 6 and were identified as *Phyllactinia dalbergiae*. These groups are parasitic fungus on tree or woody plants. Group 6 comprised of 2 specimens from Lythraceae on *Lagerstroma macrocarpa*. The anamorphic characteristics of *Phyllactinia* sp. on *Lagerstroma macrocarpa* have dimorphic conidia and sinuous to twisted foot-cells.



Figure 97 Maximum parsimony tree estimated under the highest likelihood value for 11 specimens belonging to group 4, 5 and 6 of *Phyllactinia*.

3.2 Phylogenetic study of selected powdery mildew fungi in tribe Phyllactinieae

3.2.1 Powdery mildew on chilli plants

The five rDNA sequences data on ITS region were aligned with 21 *Leveillula* sequences retrieved from GenBank. The alignment data matrix consists of 26 taxa and 621 characters were used in the analysis. The dataset of multiple alignments consisted of 621 characters, of which 45 characters were variable and 42 characters were phylogenetically informative for parsimony analysis. A total of 201 most parsimonious trees with 120 steps (CI = 0.8333, RI = 0.8450, HI = 0.1667, RC = 0.7041) were constructed by parsimony ratchet analysis. A tree with the highest likelihood value showed in Fig 98.

The phylogenetic analysis represented by MP tree indicated that the five *Oidiopsis* specimens on chilli plants are located in a clade of *Leveillula* causing powdery mildew on chilli under the accession numbers of AB000940 and MUMH3830 which confirms an anamorph-teleomorph connection of this fungus with *Leveillula*. *Leveillula* on *Acroptilon*, *Artemisia* and *Chondrilla* were used as the outer group based on Khodaparast *et al.* (2001).

The present phylogenetic result supported the morphological examination that showed no significant differences among five *Oidiopsis* found on *Capsicum* spp. (Braun, 1987 and Palti, 1988). Conidial germination type is *pseudoidium*-type (syn. *polygoni*-type) cited by Cook and Braun (2009). Thus, the morphological and phylogenetic analyses suggested strongly that the powdery mildew on *Capsicum* spp. is infected by *O. sicula* (teleomorph *L. taurica*) which agrees with the report of Goldberg (2004). Cunnington *et al.* (2003) revealed that *L. taurica* is a causal agent of powdery mildew disease on *C. annuum* in Australia. As a result, molecular analysis of rDNA ITS region is a strong tool to clarify taxonomy for species level in the genus. Species identification is an important information for accurate controlling this disease. In addition, this is the first report of taxonomy of powdery mildew on chilli plants by using morphological characteristics associated with molecular approach in Thailand.

This fungus attacks broadly range of plants (Glawe *et al.* 2005; Khodaparast *et al.* 2001). Future work such as pathogenicity test is necessary in order to determine pathogenicity of this fungus on different varieties of chilli plants including other plants.

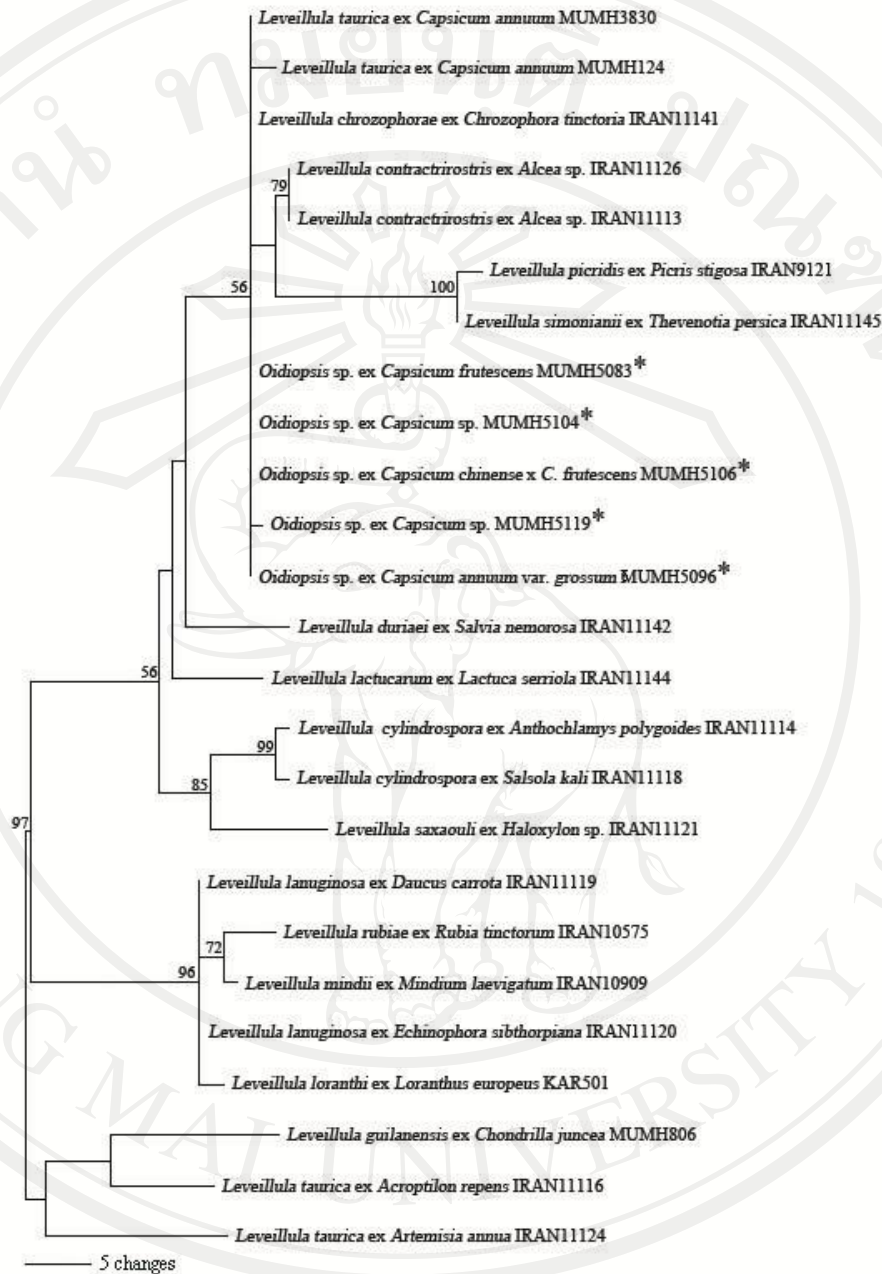


Figure 98 The Maximum parsimony phylogenetic tree of *Leveillula* sp. based on fungal ITS gene sequences. Numbers above or below branches indicate bootstrap values (>50%) from 1,000 replicates. Asterisk is represented as *Oidiopsis* that cause powdery mildew on chilli plants were used in this study.

3.2.2 Powdery mildew on *Cassia fistula*, *Dalbergia lanceolaria* and *Senna siamea*

The 28S rDNA combined with ITS including 5.8S rDNA consists of 29 alignment data matrix were constructed the phylogenetic tree. A total of 29 nucleotide sequences, of which 24 sequences from *Phyllactinia*, 4 sequences from *Leveillula taurica* and one sequence from *Pleochaeta shiraiana* that used an outgroup taxon based on Takamatsu *et al.* (2008). All 880 total characters were used in this analysis, 720 of all characters were constant, 50 characters were variable (uninformative) and 110 characters were informative for parsimony analysis. A total of 201 equally parsimonious trees (CI = 0.6438, RI = 0.8078, RC = 0.5200) with 320 steps were constructed by the parsimony ratchet analysis. A tree with the highest likelihood value among 201 trees is shown in Fig 99.

Phyllactinia dalbergiae under the accession number AB724092–AB724094 distinctly formed an independent clade at the basal part of *Phyllactinia/Leveillula* clade with bootstrap support of 97%, which support a unique characteristic of conidiophore foot-cells. In this phylogenetic analysis revealed that *Phyllactinia dalbergiae* on *Dalbergia lanceolaria* were split from other *Phyllactinia* at early stage of evolution. However, *Phyllactinia cassiae-fistula* clade further clustered also at the basal position. The sequences of *Phyllactinia dalbergiae* that obtained from either developmental states (conidia and chasmothecia) were identical with grouping together in the clade.

Phyllactinia cassiae-fistulae sequences that deposited in DDBJ under the accession number AB691226 and AB691227 including *Ovulariopsis* anamorph on *S. siamea* AB691228 distinctly formed an independent clade at the basal part of *Phyllactinia/Leveillula* clade with bootstrap support (BS) of 100%. There was one base nucleotides substitution between isolates on *C. fistula* and *S. siamea* that suggest closely related to each other. However, specimens on *C. fistula* formed small clade from *S. siamea* which supported by 62% BP value.

We also determined the rDNA ITS sequences for five samples of *P. cassiae-fistulae* on *C. fistula* and conducted FASTA search at the EMBL DNA database (<http://www.ebi.ac.uk/embl/>) using the sequences as queries. The highest similarities were obtained with *P. angulata* AB080566 (76.9%) and next with *P. chabutiana* AB243690 (75.8%). This result indicates that *P. cassiae-fistulae* is genetically isolated among *Phyllactinia* species. Because we could not obtain unambiguous alignment of *P. cassiae-fistulae* with other *Phyllactinia* species in ITS sequences, we did not conduct phylogenetic analysis of ITS sequences.

The present study is the first report of phylogenetic analysis of *P. cassiae-fistulae*. The result indicated that the sequences data from three *P. cassiae-fistulae* isolates on *C. fistula* and *S. siamea* formed an independent clade at the basal part of *Phyllactinia/Leveillula* clade with bootstrap support of 100%, and are sister group to all other *Phyllactinia* and *Leveillula* sequences.

A recent molecular phylogenetic study of the genera in the subtribe Cassiinae (Acharya *et al.*, 2011) demonstrated that *Cassia fistula* and *Senna siamea* are classified into *Cassia sensu lato*. The present study shows that both *Cassia fistula* and *Senna siamea* are commonly infected by *P. cassiae-fistulae* and this supports the close relationship of the host plants.

This result may indicate that *Phyllactinia* is paraphyletic group as described by Takamatsu *et al.* (2008). Additionally, this phylogenetic clade showed the closest relationship between *P. cassiae-fistulae* on *C. fistula* and *S. siamea*. Therefore, molecular phylogenetic analysis based on the 28S rDNA sequences supported the unique anamorphic morphology of *P. cassiae-fistulae*. The isolated phylogenetic placement of *P. cassiae-fistulae* was also supported by the ITS sequence analysis.

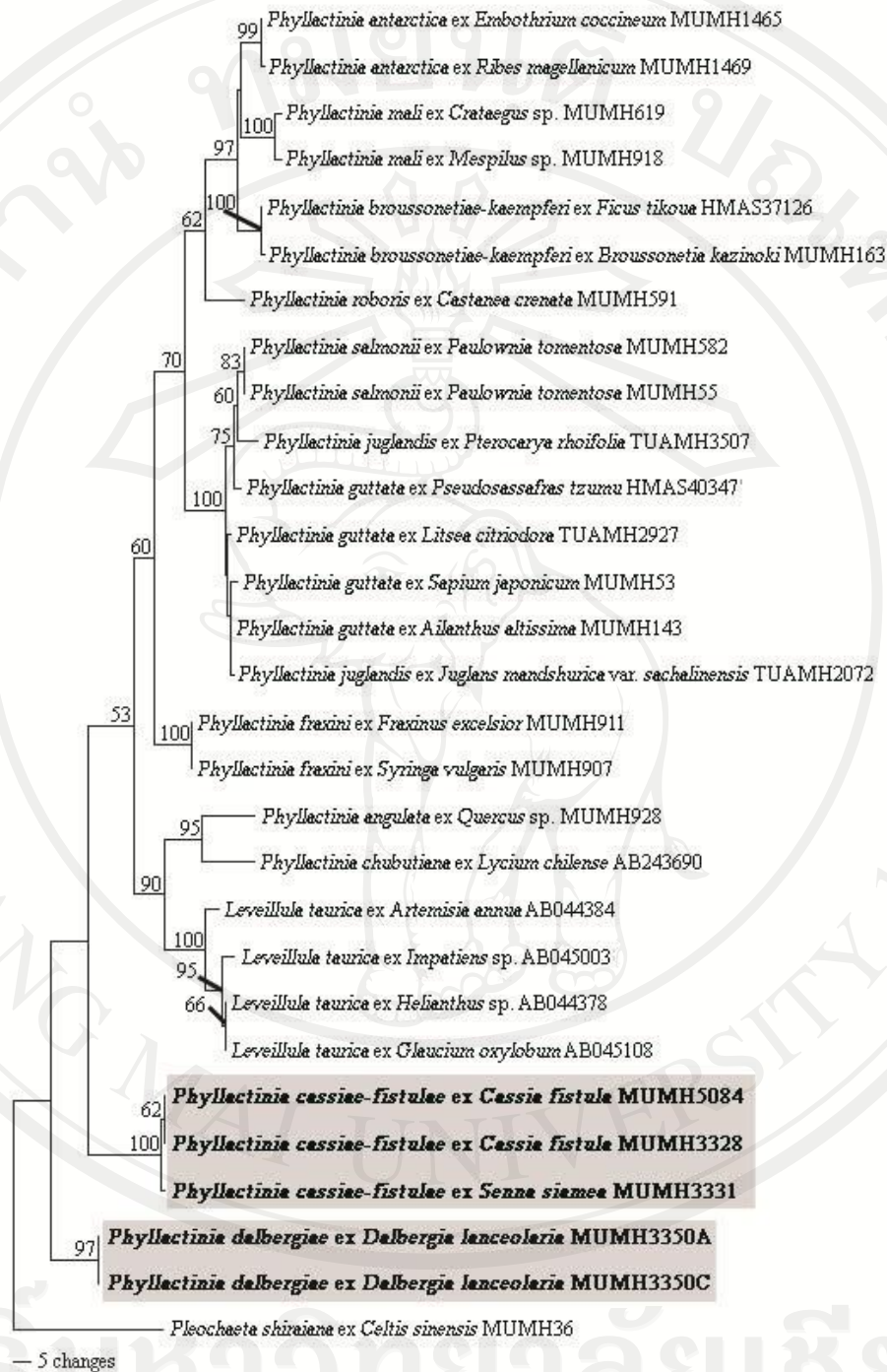


Figure 99 Phylogenetic relationship between *Phyllactinia dalbergiae* on *Dalbergia lanceolaria*, *P. cassiae-fistulae* on *Cassia fistula*, *Senna siamea*, *Phyllactinia* species and *Leveillula taurica*, inferred by parsimony ratchet method using the combined dataset of the rDNA ITS regions and the divergent domains D1 and D2 sequences of the 28S rDNA. Bootstrap value ($\geq 50\%$) was shown above branches.